



UNIVERSITÄT  
LEIPZIG

# **Analysis of consciousness for complete locked-in syndrome patients**

Der Fakultät für Mathematik und Informatik  
der Universität Leipzig  
angenommene

**D I S S E R T A T I O N**

zur Erlangung des akademischen Grades

**DOKTOR-INGENIEURIN**  
(Dr.-Ing.)

im Fachgebiet Informatik

vorgelegt von

**M.Sc. Shang-Ju Wu**

geboren am 17. Mai 1985 in Taipeh/Taiwan

Die Annahme der Dissertation wurde empfohlen von:

1. Prof. Dr. Martin Bogdan (Universität Leipzig)
2. Prof. Dr. Po-Lei Lee (National Central University, Taiwan)

Die Verleihung des akademischen Grades erfolgt mit Bestehen  
der Verteidigung am 30. März 2022 mit dem Gesamtprädikat *magna cum laude*.



*“The key to growth is the introduction of higher dimensions of consciousness into our awareness.”*

**– Lao Tzu**

*“For a research worker the unforgotten moments of his life are those rare ones which come after years of plodding work, when the veil over nature's secret seems suddenly to lift & when what was dark & chaotic appears in a clear & beautiful light & pattern.”*

**– Gerty Cori (1896-1957)**



# Zusammenfassung

In dieser Dissertation werden Methoden zur Feststellung des Bewusstseins bei Patienten mit vollständigem Locked-in-Syndrom (CLIS) vorgestellt. CLIS-Patienten können nicht sprechen und haben jegliche Muskelbewegung verloren. Äußerlich ist die innere Hirnaktivität solcher Patienten nicht leicht wahrzunehmen, aber CLIS-Patienten gelten als noch bei Bewusstsein und kognitiv aktiv. Die Feststellung des aktuellen Bewusstseinszustandes von CLIS-Patienten ist nicht trivial, und es ist schwierig festzustellen, ob CLIS-Patienten bei Bewusstsein sind oder nicht. Daher ist es von entscheidender Bedeutung, alternative Wege zu entwickeln, um die Kommunikation mit diesen Patienten während der Bewusstseinsperioden wiederherzustellen, und eine mögliche Plattform sind Gehirn-Computer-Schnittstellen (BCI).

Da für den korrekten Einsatz von BCI das Bewusstsein erforderlich ist, schlägt diese Studie einen Modus Operandi vor, um nicht nur Signale der intrakranielle Elektrokortikographie (ECoG) mit größerem Signal-Rausch-Verhältnis (SRV) und höherer Signalamplitude, sondern auch Signale der nicht-invasive Elektroenzephalographie (EEG) zu analysieren. Durch die Anwendung von drei verschiedenen Zeitbereich-Ansätze, der Sample-Entropie, der Permutation Entropie und dem Poincaré-Plot als Feature-Extraktion soll vermieden werden, dass krankheitsbedingte Reduktionen der Frequenzbänder in den Gehirnwellen der CLIS-Patienten auftreten. Ebenfalls wird Cross-validiert, um zur Verbesserung der Wahrscheinlichkeit der korrekten Erkennung der bewussten Zuständen von CLIS-Patienten zu kommen. Aufgrund des Fehlens einer "Grundwahrheit", die als Lehreingabe zur Korrektur der Ergebnisse verwendet werden könnte, wurden k-Means und DBSCAN als unüberwachte Lernmethoden verwendet, um das Vorhandensein verschiedener Bewusstseinsstufen für die individuelle Teilnahme am Experiment zunächst bei Locked-in-State (LIS) Patienten mit einem ALSFRS-R-Score von 0 aufzudecken.

Die Ergebnisse dieser verschiedenen Methoden stimmen in Bezug auf die spezifischen Bewusstseinsperioden von CLIS/LIS-Patienten überein, die mit dem Zeitraum übereinstimmen, in dem CLIS/LIS-Patienten die Kommunikation mit einem Experimentator aufgezeichnet haben. Um die methodische Durchführbarkeit zu prüfen, wurden die Methoden auch bei Patienten mit Bewusstseinsstörungen angewandt. Die Ergebnisse deuten darauf hin, dass die Verwendung der Sample-Entropie hilfreich sein könnte, um Bewusstsein nicht nur bei CLIS/LIS-Patienten, sondern auch bei Patienten mit dem minimal bewussten

Zustand (MCS) und dem Syndrom reaktionsloser Wachheit (SRW) zu erkennen, und zeigten eine gute Auflösung sowohl für ECoG-Signale bis zu 24 Stunden am Tag als auch für EEG-Signale, die zum Zeitpunkt des Experiments auf eine oder zwei Stunden beschränkt waren. Diese Arbeit konzentriert sich auf konsistente Ergebnisse über mehrere Kanäle, um kompensatorische Effekte von Hirnverletzungen zu vermeiden.

Im Gegensatz zu den meisten Techniken, welche den Klinikern helfen sollen, den langfristigen Krankheitsverlauf von Patienten zu diagnostizieren und zu verstehen oder zwischen verschiedenen Krankheitstypen auf der klinischen Skala des Bewusstseins zu unterscheiden. Das Ziel dieser Untersuchung ist die Entwicklung einer zuverlässigen, auf einer Gehirn-Computer-Schnittstelle basierenden Kommunikationshilfe, um letztendlich den Familienmitgliedern eine Methode für die kurzfristige Kommunikation mit CLIS-Patienten im Alltag an die Hand zu geben und gleichzeitig soll dadurch das Gehirn der Patienten aktiv gehalten werden, um die Lebensbereitschaft der Patienten zu erhöhen und ihre Lebensqualität zu verbessern.

## Abstract

This thesis presents methods for detecting consciousness in patients with complete locked-in syndrome (CLIS). CLIS patients are unable to speak and have lost all muscle movement. Externally, the internal brain activity of such patients cannot be easily perceived, but CLIS patients are considered to be still conscious and cognitively active. Detecting the current state of consciousness of CLIS patients is non-trivial, and it is difficult to ascertain whether CLIS patients are conscious or not. Thus, it is vital to develop alternative ways to re-establish communication with these patients during periods of awareness, and a possible platform is through brain-computer interface (BCI).

Since consciousness is required to use BCI correctly, this study proposes a modus operandi to analyze not only in intracranial electrocorticography (ECoG) signals with greater signal-to-noise ratio (SNR) and higher signal amplitude, but also in non-invasive electroencephalography (EEG) signals. By applying three different time-domain analysis approaches sample entropy, permutation entropy, and Poincaré plot as feature extraction to prevent disease-related reductions of brainwave frequency bands in CLIS patients, and cross-validated to improve the probability of correctly detecting the conscious states of CLIS patients. Due to the lack a of "ground truth" that could be used as teaching input to correct the outcomes, k-Means and DBSCAN these unsupervised learning methods were used to reveal the presence of different levels of consciousness for individual participation in the experiment first in locked-in state (LIS) patients with ALSFRS-R score of 0.

The results of these different methods converge on the specific periods of consciousness of CLIS/LIS patients, coinciding with the period during which CLIS/LIS patients recorded communication with an experimenter. To determine methodological feasibility, the methods were also applied to patients with disorders of consciousness (DOC). The results indicate that the use of sample entropy might be helpful to detect awareness not only in CLIS/LIS patients but also in minimally conscious state (MCS)/unresponsive wakefulness syndrome (UWS) patients, and showed good resolution for both ECoG signals up to 24 hours a day and EEG signals focused on one or two hours at the time of the experiment. This thesis focus on consistent results across multiple channels to avoid compensatory effects of brain injury.

Unlike most techniques designed to help clinicians diagnose and understand patients' long-term disease progression or distinguish between different disease types on the clinical scales of consciousness. The aim of this investigation is to develop a reliable brain-computer

interface-based communication aid eventually to provide family members with a method for short-term communication with CLIS patients in daily life, and at the same time, this will keep patients' brains active to increase patients' willingness to live and improve their quality of life (QOL).



## Acknowledgements

Foremost, I am highly grateful to the National Chung-Shan Institute of Science & Technology (NCSIST) for granting me a doctoral scholarship that allows me to be able to concentrate on my research. This thesis could not have been performed without this scholarship.

I offer my sincere gratitude to my supervisor, Prof. Dr. Martin Bogdan, whose patient guidance and encouragement enabled me to gradually develop my own ideas and opinions, which led to the generation of the entire thesis. Thank you for his valuable comments that improved the quality of this thesis. I also gratefully acknowledge Dr. Nicoletta Nicolaou, from University of Nicosia Medical School, who guided me with her knowledge throughout this work. I am greatly indebted to them for their constructive guidance and advice during the preparation of this thesis.

Special thanks go to Prof. Dr. h. c. mult. Niels Birbaumer and Dr. Ujwal Chaudhary from the Institute for Medical Psychology and Behavioural Neurobiology, University of Tübingen, who kindly provided the data of CLIS patients. I am also very grateful to Prof. Dr. Manuel Schabus and Dr. Malgorzata Wilowska from the Centre for Cognitive Neuroscience Salzburg (CCNS), University of Salzburg, Austria, for providing the dataset of DOC patients, without which the following data analysis would never have been possible.

I thank my colleagues for their feedbacks and suggestions to improve my work. Many thanks to Thomas for his advice on machine learning, who is also a good listener and always encourages me when I felt frustrated, and to Sophie who transferred her enthusiasm and effort for her work to me. Furthermore, I appreciate the NCSIST staff who helped me during my studies and did their best to give me the time I needed to work on my dissertation.

During my studies I met many nice people, Molly, Lani and all my friends who came to Leipzig from Taiwan. Thank you all for making me a part of your lives. Each gathering and every pleasant moment when we get together is the greatest and warmest support for a student studying abroad. And also to all the friends I have made in Leipzig. The time I spend with you guys helps me relieve stress and balance my work and leisure life!

Last but not least, I would like to express my deepest gratefulness and appreciation to my parents and sister for always supporting, advising and inspiring me when I have encountered difficulties in my life, and for being my spiritual pillars that give me the mental strength to keep striving forward!

# Contents

Zusammenfassung.....	I
Abstract.....	III
Acknowledgements .....	V
Contents .....	VI
List of Figures.....	VIII
List of Tables .....	XII
Abbreviations .....	XIII
Chapter 1 Introduction and Overview.....	1
1.1 Motivation of Current Work .....	1
1.2 Aim and Organization of Thesis.....	3
Chapter 2 Basics.....	5
2.1 Clinical scales of consciousness.....	5
2.2 Brain-Computer Interface .....	8
2.3 Sample Entropy.....	12
2.4 Permutation Entropy.....	14
2.5 Poincaré plot.....	15
2.6 Multiscacle Approach.....	16
2.7 k-Means.....	17
2.8 Elbow method.....	19
2.9 DBSCAN .....	20
2.10 K-distance graph.....	21
Chapter 3 State of the art.....	23
3.1 CLIS .....	23
3.2 Time Domain vs. Frequency Domain Analyses.....	26
3.3 Auditory vs. Motor imagery vs. Visual paradigms.....	27
3.4 Summary.....	29
Chapter 4 Modus Operandi .....	30
4.1 Pre-Processing .....	32
4.2 Feature Extraction .....	32
4.3 Machine Learning .....	33

<b>Chapter 5 Datasets</b> .....	<b>35</b>
<b>5.1 ECoG recordings of a CLIS patient</b> .....	<b>35</b>
<b>5.2 EEG recordings of CLIS patients</b> .....	<b>37</b>
<b>5.3 EEG recordings of LIS patients</b> .....	<b>40</b>
<b>5.4 EEG recordings of DOC patients</b> .....	<b>43</b>
<b>5.5 Discussion of datasets</b> .....	<b>44</b>
<b>Chapter 6 Results</b> .....	<b>46</b>
<b>6.1 Feature Extraction part</b> .....	<b>47</b>
6.1.1 Multiscale Approach result.....	47
6.1.2 Multiscale Sample Entropy result.....	48
6.1.3 Multiscale Permutation Entropy result .....	49
6.1.4 Multiscale Poincaré plot result .....	50
6.1.5 Discussion of ECoG signal results.....	52
6.1.6 Poincaré plot results from CLIS patients.....	56
6.1.7 Sample Entropy results from CLIS patients .....	60
6.1.8 Sample Entropy results from LIS patients.....	65
6.1.9 Sample Entropy results from DOC patients .....	70
6.1.10 Discussion of EEG signal results.....	78
<b>6.2 Machine learning part</b> .....	<b>80</b>
6.2.1 k-Means results .....	81
6.2.2 DBSCAN results.....	90
6.2.3 Discussion of machine learning results .....	100
<b>Chapter 7 Discussion &amp; Conclusions</b> .....	<b>102</b>
<b>7.1 Discussion</b> .....	<b>102</b>
<b>7.2 Conclusions &amp; Future work</b> .....	<b>105</b>
<b>Appendix A Supplemental Material</b> .....	<b>107</b>
<b>Appendix B Sample entropy results</b> .....	<b>109</b>
<b>Appendix C Poincaré plot results</b> .....	<b>114</b>
<b>Bibliography</b> .....	<b>119</b>
<b>Bibliographic Details</b> .....	<b>130</b>
<b>Selbständigkeitserklärung</b> .....	<b>131</b>

## List of Figures

Figure 2.1: Clinical scales of consciousness.....	6
Figure 2.2: Schematic of a brain–computer interface (BCI) system.....	9
Figure 2.3: A diagram where each point represents one data point in time domain to explain the operation of sample entropy depending on the row of occurrence over time.....	13
Figure 2.4: Example of Permutation Entropy estimation.. .....	14
Figure 2.5: The Poincaré plot (time delay = 1), standard deviation perpendicular to the diagonal line (SD1) and standard deviation along the diagonal line (SD2) describing the fitted ellipse of the ECoG voltage dispersion along the minor and major axis. ....	16
Figure 2.6: The coarse-graining procedure for scale 4. ....	17
Figure 2.7: The schematic illustration of the k-Means algorithm cluster model (k = 3). ....	18
Figure 2.8: The elbow method for determining number of clusters, where the x-axis represents the number of clusters and the y-axis represents the cost.....	19
Figure 2.9: An illustration of the DBSCAN for minPts parameter is 4, and the radius $\epsilon$ is indicated by the circles.....	20
Figure 2.10: Plot of the k-distance graph, where the x-axis represents the points sorted by distance and the y-axis represents the epsilon ( $\epsilon$ ) value. ....	22
Figure 4.1: The data processing flow chart of Modus Operandi. ....	31
Figure 4.2: The data processing flow chart of ECoG signals. ....	32
Figure 4.3: The data processing flow chart of EEG signals.....	33
Figure 5.1: Channel locations of the electrocorticography (ECoG) electrode array in a CLIS patient.....	36
Figure 5.2: Channel positions of CLIS patients.....	38
Figure 5.3: Channel positions of LIS patients.....	41
Figure 5.4: The channel positions of electroencephalography (EEG) for DOC patients.....	43
Figure 6.1: The result of Sample Entropy for 24 h. ....	48
Figure 6.2: The results of multiscale sample entropy (MSE) (scale = 4) for 24 h.....	49
Figure 6.3: The results of multiscale permutation entropy (MPE) (scale = 4) for 24 h.....	50
Figure 6.4: The Poincaré plot. Left: 30 seconds during experiment. Right: other 30 seconds during non-experiment.....	51

Figure 6.5: The SD1 of the multiscale Poincaré (MSP) plots (scale = 4) for 24 h.....	51
Figure 6.6: The SD2 of multiscale Poincaré (MSP) plots (Scale=4) for 24 h. ....	52
Figure 6.7: The result of the majority decision of three methods is indicated by the dark red block.....	53
Figure 6.8: The statistical results (Z-test) for (a) MSE, (b) MPE, and (c) MSP over 24 h..	55
Figure 6.9: The SD1 result of Poincaré plot for CLIS patient B on day 1. ....	57
Figure 6.10: The SD1 result of Poincaré plot for CLIS patient B on day 2. ....	58
Figure 6.11: The SD1 result of Poincaré plot for CLIS patient F on day 1.....	59
Figure 6.12: The SD1 result of Poincaré plot for CLIS patient F on day 2.....	60
Figure 6.13: The sample entropy result for CLIS patient G on day 1. ....	61
Figure 6.14: The sample entropy result for CLIS patient G on day 2. ....	62
Figure 6.15: The sample entropy result for CLIS patient W on day 1. ....	63
Figure 6.16: The sample entropy result for CLIS patient W on day 2. ....	64
Figure 6.17: The sample entropy result for LIS patient 11 (ALSFRS-R=0) on day 1. ....	66
Figure 6.18: The sample entropy result for LIS patient 11 (ALSFRS-R=0) on day 2. ....	67
Figure 6.19: The sample entropy result for LIS patient 13 (ALSFRS-R=0) on day 1. ....	69
Figure 6.20: The sample entropy result for LIS patient 13 (ALSFRS-R=0) on day 2. ....	70
Figure 6.21: The channel F3 result of sample entropy for Patient MCS1.....	71
Figure 6.22: The channel P4 result of sample entropy for Patient MCS2.....	72
Figure 6.23: The channel C4 result of sample entropy for Patient UWS1. ....	73
Figure 6.24: The channel F8 result of sample entropy for Patient UWS2.....	74
Figure 6.25: The channel C4 result of sample entropy for Patient UWS3 (PSG1). ....	75
Figure 6.26: The channel C4 result of sample entropy for Patient UWS3 (PSG2). ....	76
Figure 6.27: The channel C4 result of sample entropy for Patient UWS3 (PSG3). ....	76
Figure 6.28: The channel C4 result of sample entropy for Patient UWS4. ....	77
Figure 6.29: The k-Means results for LIS patient 11 (ALSFRS-R=0) on day 1, where the x-axis and y-axis show the sample entropy values after mean normalization and feature scaling at different time points (t=1 vs. t=2).....	82
Figure 6.30: Cost of k-Means for LIS patient 11 on day 1, where the x-axis represents the number of clusters and the y-axis represents the cost.....	83

Figure 6.31: The k-Means results for LIS patient 11 (ALSFRS-R=0) on day 2, where the x-axis and y-axis show the sample entropy values after mean normalization and feature scaling at different time points (t=1 vs. t=2).....	84
Figure 6.32: Cost of k-Means for LIS patient 11 on day 2, where the x-axis represents the number of clusters and the y-axis represents the cost.....	84
Figure 6.33: The k-Means results for LIS patient 13 (ALSFRS-R=0) on day 1, where the x-axis and y-axis show the sample entropy values after mean normalization and feature scaling at different time points (t=1 vs. t=2).....	86
Figure 6.34: Cost of k-Means for LIS patient 13 on day 1, where the x-axis represents the number of clusters and the y-axis represents the cost.....	86
Figure 6.35: The k-Means results for LIS patient 13 (ALSFRS-R=0) on day 2, where the x-axis and y-axis show the sample entropy values after mean normalization and feature scaling at different time points (t=1 vs. t=2).....	87
Figure 6.36: Cost of k-Means for LIS patient 13 on day 2, where the x-axis represents the number of clusters and the y-axis represents the cost.....	88
Figure 6.37: The k-Means results for LIS patient 11 &13 (ALSFRS-R=0) on day 2, where the x-axis and y-axis show the sample entropy values after mean normalization and feature scaling at different time points (t=1 vs. t=2).....	89
Figure 6.38: Cost of k-Means for LIS patient 11 & 13 on day 2, where the x-axis represents the number of clusters and the y-axis represents the cost.....	90
Figure 6.39: The k-distance graph for LIS patient 11 on day 1, where the x-axis represents the points sorted by distance and the y-axis represents the epsilon ( $\epsilon$ ) values. ....	92
Figure 6.40: The DBSCAN results for LIS patient 11 (ALSFRS-R=0) on day 1, where the x-axis and y-axis show the sample entropy values after mean normalization and feature scaling at different time points (t=1 vs. t=2).....	92
Figure 6.41: The k-distance graph for LIS patient 11 on day 2, where the x-axis represents the points sorted by distance and the y-axis represents the epsilon ( $\epsilon$ ) values. ....	93
Figure 6.42: The DBSCAN results for LIS patient 11 (ALSFRS-R=0) on day 2, where the x-axis and y-axis show the sample entropy values after mean normalization and feature scaling at different time points (t=1 vs. t=2).....	94
Figure 6.43: The k-distance graph for LIS patient 13 on day 1, where the x-axis represents the points sorted by distance and the y-axis represents the epsilon ( $\epsilon$ ) values.. ....	95

Figure 6.44: The DBSCAN results for LIS patient 13 (ALSFRS-R=0) on day 1, where the x-axis and y-axis show the sample entropy values after mean normalization and feature scaling at different time points (t=1 vs. t=2).....	96
Figure 6.45: The k-distance graph for LIS patient 13 on day 2, where the x-axis represents the points sorted by distance and the y-axis represents the epsilon ( $\epsilon$ ) values. ....	97
Figure 6.46: The DBSCAN results for LIS patient 13 (ALSFRS-R=0) on day 2, where the x-axis and y-axis show the sample entropy values after mean normalization and feature scaling at different time points (t=1 vs. t=2).....	97
Figure 6.47: The k-distance graph for LIS patient 11 & 13 on day 2, where the x-axis represents the points sorted by distance and the y-axis represents the epsilon ( $\epsilon$ ) values. ....	99
Figure 6.48: The DBSCAN results for LIS patient 11 & 13 (ALSFRS-R=0) on day 2, where the x-axis and y-axis show the sample entropy values after mean normalization and feature scaling at different time points (t=1 vs. t=2). ....	99
Figure 7.1: The average value of sample entropy for 24 h at the time of experiment for 6 patients versus the number of months between experiment and death.....	104
Figure B.1: The sample entropy result for CLIS patient B on day 1.....	109
Figure B.2: The sample entropy result for CLIS patient B on day 2.....	110
Figure B.3: The sample entropy result for CLIS patient F on day 1. ....	111
Figure B.4: The sample entropy result for CLIS patient F on day 2. ....	112
Figure C.1: The SD1 result of Poincaré plot for CLIS patient G on day 1.....	115
Figure C.2: The SD1 result of Poincaré plot for CLIS patient G on day 2.....	116
Figure C.3: The SD1 result of Poincaré plot for CLIS patient W on day 1.....	116
Figure C.4: The SD1 result of Poincaré plot for CLIS patient W on day 2.....	117

## List of Tables

Table 2.1: Advantages and disadvantages of signal acquisition for different BCI/BMI modalities.....	10
Table 3.1: Typical frequency bands of brain waves in healthy adult individuals.....	26
Table 5.1: Electrodes and sampling rates recording the EEG signals of the four CLIS patients on different days. ....	38
Table 5.2: Electrodes recording the EEG signals of the two LIS patients on different days. ....	41
Table 5.3: Demographic information of all DOC patients. The analyzed patient sample consisted of two MCS and four UWS patients. ....	44
Table 6.1: The event notes for Patient UWS1. ....	73
Table 6.2: The event notes for Patient UWS2. ....	74
Table 6.3: The event notes for Patient UWS3 (PSG1). ....	75
Table 6.4: The event notes for Patient UWS3 (PSG2). ....	76
Table 6.5: The event notes for Patient UWS4. ....	77



## Abbreviations

AAC	Augmentative and Alternative Communication
ALS	Amyotrophic Lateral Sclerosis
ALSFRS-R	ALS Functional Rating Scale-Revised
APF	Alpha Peak Frequency
BCI	Brain-Computer Interface
BMI	Brain–Machine Interface
CLIS	Complete Locked-In Syndrome
CRS-R	Coma Recovery Scale-Revised
DBSCAN	Density-Based Spatial Clustering of Applications with Noise
DOC	Disorders of Consciousness
ECG	ElectroCardioGram
ECoG	ElectroCorticoGraphy
EEG	ElectroEncephaloGraphy
EMG	ElectroMyoGram
EOG	ElectroOculoGraphy
ERD	Event-Related Desynchronization
ERP	Event-Related Potential
ERS	Event-Related Synchronization
fMRI	functional Magnetic Resonance Imaging
fNIRS	functional Near-Infrared Spectroscopy
GCS	Glasgow coma scale
LFP	Local Field Potential
LIS	Locked-In Syndrome
LOC	Loss of Consciousness
MCN	Modified Combinatorial Nomenclature
MCS	Minimally Conscious State
MEG	MagnetoEncephaloGraphy
MI	Motor Imagery
MND	Motor Neuron Disease
MPE	Multiscale Permutation Entropy
MSE	Multiscale Sample Entropy
MSP	Multiscale Poincaré

NIRS	Near-Infrared Spectroscopy
PET	Positron Emission Tomography
PSG	PolySomnoGraphic
PVS	Persistent Vegetative State/Permanent Vegetative State
QOL	Quality of Life
REM	Rapid Eye Movement
ROC	Recovery of Consciousness
SNR	Signal-to-noise ratio
SSVEP	Steady-State Visually Evoked Potential
SWS	Slow Wave Sleep
SVM	Support Vector Machine
TBI	Traumatic Brain Injury
TLS	Totally Locked-in State
TMS	Transcranial Magnetic Stimulation
UWS	Unresponsive Wakefulness Syndrome
VS	Vegetative State

# Chapter 1

## Introduction and Overview

*"The Human being lives according to its capacity to communicate, losing communication means losing life."*

*– Ludwig Hohl (1904-1980)*

### 1.1 Motivation of Current Work

Amyotrophic Lateral Sclerosis (ALS) is the most common type of motor neuron disease (MND) and the third most common neurodegenerative disease after Alzheimer's disease and Parkinson's disease (Renton et al. 2014). The renowned British theoretical physicist and astrophysicist Stephen Hawking, who passed away in 2018, was diagnosed with ALS in 1963, suffered from this disease and shared his thoughts through augmentative and alternative communication (AAC) (Beukelman and Light 2020) and wrote the widely known book *A Brief History of Time*, which also gives us the opportunity to glimpse into the secrets of his brain. The "Ice Bucket Challenge" was launched by the ALS Association (ALSA) in 2014. In this challenge, those who accept the challenge can either film themselves pouring a bucket of ice water over their head and upload the video to the Internet, donate to research and the fight against ALS, or do both. The campaign has promoted worldwide public attention to the disease due to the response of many celebrities.

Amyotrophic Lateral Sclerosis (ALS) is considered a rare disease, although it occurs worldwide. The annual incidence is 1.9 per 100,000 and the prevalence (the number of people with the disease at any given time) is 4.5 per 100,000 (Chiò et al. 2013). The number of new cases per year is about 2.6 people per 100,000 in Europe (Hardiman, Al-Chalabi,

Brayne et al. 2017), and about 0.8 people per 100,000 in east Asia (Hardiman, Al-Chalabi, Chio et al. 2017). ALS occurs in a gender ratio of approximately 1.5:1 and is more common in men than in women. ALS is a well-known disease that may cause locked-in state (LIS) and then could be lead to completely locked-in syndrome (CLIS).

The typical characteristic of locked-in state (LIS) patients is nearly complete paralysis while retaining full cognition. Some traumatic, systemic or progressive neurological diseases with different neuropathological and etiological features, such as Traumatic brain injury (TBI), pontine stroke, amyotrophic lateral sclerosis (ALS), end-stage Parkinson disease, are some examples of conditions that could lead to a LIS state. Patients in a LIS state are often misdiagnosed as suffering from a disorder of consciousness. One such example is a patient who was regarded as being in an unresponsive wakefulness syndrome (UWS) state until 20 years later, when the patient woke up (Vanhaudenhuyse et al. 2018). LIS patients can communicate with the outside world by moving their eye muscles or eyebrows. However, when the patients slip into the completely locked-in syndrome (CLIS), they eventually lose control of these last few remaining muscles, such as the anal sphincter and eye movements or eyebrows (Hayashi and Oppenheimer 2003; Ramos-Murguialday et al. 2011), but their cognition is assumed to remain intact.

Despite constantly evolving technology, the ground truth of the level of consciousness of CLIS patients is still missing (Kübler and Birbaumer 2008). Some researchers attempted to communicate with CLIS patients using near-infrared spectroscopy (NIRS) (Gallegos-Ayala et al. 2014; Chaudhary et al. 2017), leading to many controversies (Spüler 2019) and finally to the retraction of (The PLOS Biology Editors 2019) by the editors (due to doubts on the selection within the used data sets and not the applied algorithms; the authors are currently contesting this decision). The main problem is to objectively identify the existence of a consciousness level in CLIS patients, who cannot themselves make this known to the outside world through self-expression. In contrast to other studies that attempt to seek methods of classifying between different clinically defined states of consciousness, such as LIS, minimally conscious state (MCS) and vegetative state (VS) (Owen et al. 2006; Casali et al. 2013), our aim is to identify patterns that are most likely indicative of a minimum level of consciousness that will allow successful communication with ALS patients in CLIS.

This thesis proposes to apply sample entropy, permutation entropy and Poincaré plots as feature extraction to analyze continuously recorded intracranial electrocorticography (ECoG) and non-invasive electroencephalography (EEG) signals from the patients of different clinical scales of consciousness in an attempt to uncover whether the patient is

experiencing periods of consciousness. Such "ground truth" was first obtained from one CLIS patient who successfully communicated and answered patient-specific questions asked by an investigator using a brain-computer interface system. To the best of my knowledge, there is no other such dataset in existence. The sample entropy and Poincaré plots methods were then extended to other CLIS and LIS patients and cross-validated to improve the probability of correctly detecting the conscious states of CLIS patients. Finally, k-Means and DBSCAN were used as unsupervised learning methods to estimate the threshold of consciousness for individual participation in the experiment in locked-in state (LIS) patients with ALSFRS-R score of 0. The results of these different methods converge on the specific periods of consciousness of CLIS patients, coinciding with the period during which CLIS patients recorded communication with the experimenter. To determine methodological feasibility, the methods were also applied to patients with disorders of consciousness (DOC). The results indicate that the use of sample entropy might be helpful to detect awareness not only in CLIS/LIS patients but also in minimally conscious state (MCS)/unresponsive wakefulness syndrome (UWS) patients.

Final aim of the investigation is to develop a reliable brain-computer interface-based communication tool that will eventually provide family members with a method of communicating with CLIS patients and further enhance their brain stimulation in order to increase patients' willingness to live and significantly improve their quality of life (QOL) (Kögel et al. 2020). Relatively speaking, while the patient is stuck immobile in his or her body, he or she is still unable to communicate and interact with the social environment through our modus operandi. This modus operandi can help physicians estimate the patient's cognitive status, which is of great help to the treating physicians in deciding whether to turn off life-sustaining equipment and can also reduce the patient's suffering and the burden on the family.

## **1.2 Aim and Organization of Thesis**

The chapters of this thesis are organized as follows: Chapter 2 first describes the clinical scale of consciousness to understand the brainstem and cortico-thalamic network in CLIS patients. Then, the brain-computer interface is introduced to know how to extract EEG and ECoG signals from the human brain. Methodologies such as sample entropy, permutation entropy, Poincaré plots, multiscale approach, k-Means and DBSCAN are then presented, which are all applicable to many different fields, but in the case of microvolts in the brainwave range, all parameters must be changed to fit into this time scale. In Chapter 3,

a demonstration of the current state of the art in this field is given. In order to understand the entire concept of system architecture, information about the modus operandi is presented in Chapter 4. The details about the data set of EEG and ECoG signals are presented in Chapter 5. In addition to using the data set with "ground truth", sleep data sets from the other researchers (Blume et al. 2015; Wielek et al. 2018) are also included to demonstrate the feasibility of the methods. Chapter 6 presents the results and discusses the possible influencing factors. Finally, future developments are considered.

# Chapter 2

## Basics

*“The increase of disorder or entropy is what distinguishes the past from the future, giving a direction to time.”*

*– Stephen Hawking (1942-2018)*

### 2.1 Clinical scales of consciousness

Until now, there are only few researches on detecting the consciousness of the CLIS patients with non-invasive EEG and intracranial ECoG signals. Therefore other consciousness-related fields such as anesthesia, Minimally-Conscious-State (MCS), unresponsive wakefulness syndrome (UWS) were referenced to detect consciousness, so Disorders of consciousness (DOC) patients datasets are also included in this thesis to cross-validate whether the approaches are useful for CLIS patients.

After Plum and Posner (Plum and Posner 1982) defined consciousness in neurology. Luaute´ et al. (Laureys et al. 2004; Laureys 2005; Luaute´ et al. 2015) proposed that consciousness consists primarily of two aspects: the level of consciousness and the content of consciousness. The level of consciousness (y-axis in Figure 2.1) is controlled by the brainstem and describes low-level sensory stimuli such as wakefulness, arousal, and vigilance. The content of consciousness (x-axis in Figure 2.1) is controlled by cortico-thalamic network and describes high-level abstract representations of awareness, experience, etc.. Awareness can be divided into internal awareness, which is related to inner thoughts, and external awareness, which refers to external environmental stimuli. It may not be possible to detect self-awareness with current technology, but experimental auditory stimuli

can at least be used to determine whether a patient has an awareness of the environment by responding to the patient's reactions. This concept was also used in the design of the Glasgow coma scale (GCS) (Teasdale and Jennett 1974) and the Coma Recovery Scale-Revised (CRS-R) (Giacino et al. 2004), where the diagnosis is established by identifying the level of functional impairment.

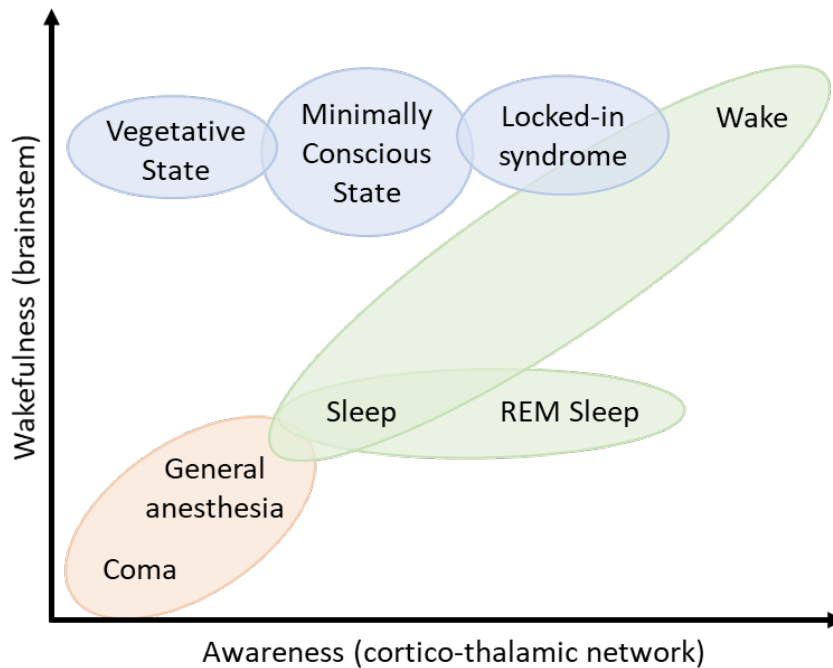


**Figure 2.1:** Clinical scales of consciousness. The x-axis represents awareness, the y-axis represents wakefulness, which are the two major components of consciousness. Healthy consciousness states are indicated in green, patients who are unconscious and unable to wake up are indicated in orange, primary subjects including DOC patients are indicated in blue. Figure is made after the illustrations from (Laureys 2005; Arsiwalla et al. 2017).

The clinical scales of consciousness in Figure 2.1 indicates that in healthy consciousness states, indicated in green, the level of wakefulness and the level of awareness are almost linearly correlated, i.e., when the person is awake (high wakefulness and high awareness), when the person is sleep (low wakefulness and low awareness). An exception are dreams during rapid eye movement (REM) periods, which also present high consciousness (Cologan et al. 2013; Zeman and Coebergh 2013), so the transitions from sleep to REM phases is one dimension. Patients indicated in orange for pharmacological reasons (general anesthesia) or pathological conditions (coma) are unconscious and unable to awaken. The primary subjects of this thesis indicated in blue, which included Disorders of consciousness (DOC) patients. These pathological conditions are the result of brain



---

damage caused by external factors (e.g. traumatic brain injury (TBI)) or internal factors (e.g. anoxia) and these patients maintain high arousal, but awareness is also one dimensional between these pathological states.

DOC is the degree of loss of consciousness, which is usually preceded by a period of unconsciousness in the patient. The DOC dataset used in this thesis contains patients with the following two different pathological states of consciousness:

### **Unresponsive Wakefulness Syndrome/Vegetative State (UWS/VS):**

The vegetative state (VS) is defined as a state of wakefulness without awareness (Laureys et al. 2004), this term was first coined by Jennet and Plum in 1972 (Jennett and Plum 1972), but due to its negative connotation as a long-term and almost irreversible state that can easily be confused with the persistent vegetative state (PVS, UWS/VS due to non-traumatic brain injury for more than three months in the USA and six months in the UK, or due to traumatic brain injury after one year) (Working Party of the Royal College of Physicians. 2003; Giacino et al. 2018). Therefore, Laureys et al. in 2010 suggested to rename it as unresponsive wakefulness syndrome (UWS), implying that this state is not always a long-term chronic state, but may also be a temporary state in the recovery process (Laureys et al. 2010).

Based on the clinical definition, recovery from coma after severe brain injury to unresponsive wakefulness syndrome (UWS) is characterized by opening of the eyes in response to stimulation or spontaneously, which is explained as a symbol of regained arousal. However, eye opening does not mean the restoration of the sleep-wake cycle, and such patients retain autonomic functions such as thermoregulation and cardiovascular regulation, but have no self- or environmental awareness and cannot obey commands, exhibiting only reflexive behavior (The Multi-Society Task Force on PVS 1994). Landsness et al. also reported that that UWS patients had no electroencephalographic (EEG) changes during prolonged eye closure and the absence of common sleep stages such as rapid eye movement (REM) and slow-wave sleep (Landsness et al. 2011).

### **Minimally Conscious State (MCS):**

Reproducible evidence of self- or environmental awareness is a marker of the minimal conscious state (MCS) (Giacino et al. 2002). Patients are able to exhibit non-reflexive and purposeful behaviors that are not associated with language signs of consciousness, such as

visually following and obeying commands, as well as emotional behaviors, such as laughing or crying. Just like UWS, MCS can be a temporary transition to another state of consciousness or it may be permanent.

The targeted pathological states of consciousness for the patients in the dataset used in this thesis are described below:

### **Locked-In Syndrome (LIS):**

Locked-In Syndrome (LIS) patients are characterized by a dissociation of motor and cognitive functions, where cognitive functions such as self-awareness and external awareness are preserved, but motor functions such as aphasia, quadriplegia, or tetraplegia are absent and they can only communicate through eye movements, eye blinking, or lip twitching. This is similar to the behavioral manifestations of unresponsive wakefulness syndrome/ vegetative state (UWS/VS) patients and is often misdiagnosed as persistent vegetative state (PVS) due to the similarity of clinical evaluation results with UWS/VS, but this syndrome is not a disorder of consciousness.

### **Complete Locked-In Syndrome (CLIS):**

Completely locked-in syndrome (CLIS), also known as totally locked-in state (TLS), is a state in which LIS patients slip into, where the patient gradually loses control of these last few remaining muscles, such as the anal sphincter and eye movements or eyebrows (Hayashi and Oppenheimer 2003; Ramos-Murguialday et al. 2011), which is defined as a state in which all motor control is lost but cognition is considered to remain intact, similar to the highly undesirable anesthesia awareness state during anesthesia. The complete inability of CLIS patients to communicate with external environment, as all possible means of communication rely on voluntary motor control of some body muscles, which prevents patients from expressing their thoughts and needs and leaves researchers without a "ground truth" to verify the presence of consciousness in CLIS patients, which is one of the major challenges in this thesis.

## **2.2 Brain-Computer Interface**

Like Jean-Dominique Bauby, the author of "The Diving Bell and the Butterfly" (Bauby 1995), who entered LIS after a massive brainstem stroke, he spells out his feelings after his illness one letter at a time by blinking through the listener-assisted scanning method

(Horki et al. 2015), using the diving bell as a metaphor for his body, which cannot move freely, and the butterfly as a metaphor for his spirit and soul, to tell the world that his imprisoned soul is still alive.

Healthy people communicate their thoughts, feelings and intentions to each other through verbal or non-verbal means. For patients with motor neuron disorders, it is still possible to express their thoughts and feelings through listener-assisted scanning or augmentative and alternative communication (AAC), but when the patient slips from LIS to CLIS, these assistive devices do not work and the patient is thus isolated in his or her body. This is where brain-computer interfaces (BCIs) play an important role for CLIS patients.

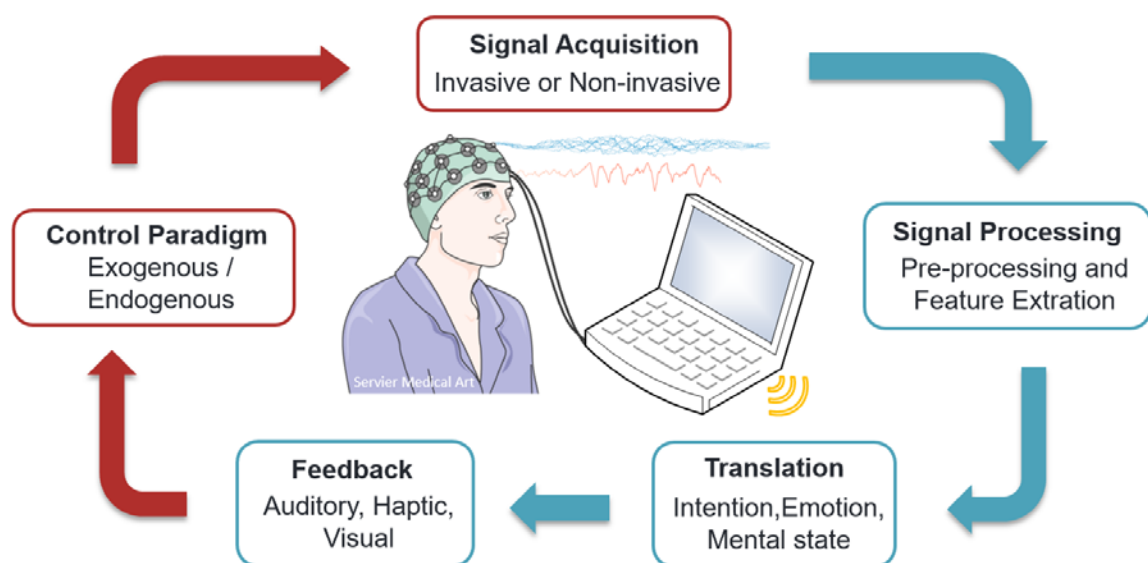


**Figure 2.2:** Schematic of a brain-computer interface (BCI) system, with the red block working on the human brain side and the blue block on the computer side.

Brain-computer interface (BCI) or brain-machine interface (BMI) is a technology that is able to preprocess brain activity and extract relevant features from people's intentions, emotions and mental states, and translate them into control signals or commands to communicate with the external environment, and even control external devices without any kinesthetic movement to replace, supplement, enhance, improve, or restore neuromuscular function from the central nervous system (McFarland and Wolpaw 2017). The final feedback is transmitted to the person through an auditory, tactile, or visual interface. In order to establish communication patterns that elicit specific brain responses, people are often stimulated or tasked, or taught to generate certain features of the signal through exogenous and endogenous paradigms (Kübler and Kotchoubey 2007). A schematic representation of a brain-computer interface (BCI) system is shown in Figure 2.2.

The acquisition devices of BCI systems include invasive or non-invasive techniques to record brain activity. Invasive techniques include electrodes implanted on the surface of the cerebral cortex, electrocorticography (ECoG) (Leuthardt et al. 2004; Schalk and Leuthardt 2011), electrodes implanted in cortical tissue, local field potential (LFP) (Hochberg et al. 2006). Non-invasive techniques include electroencephalography (EEG) (Birbaumer et al. 1999; Kübler and Birbaumer 2008), magnetoencephalography (MEG) (Babiloni et al. 2009), functional near infrared spectroscopy (fNIRS) (Coyle et al. 2004; Coyle et al. 2007), and functional magnetic resonance imaging (fMRI) (Weiskopf et al. 2004). The advantages and disadvantages of signal acquisition for different BCI/BMI modalities in terms of the type of signal, spatial and temporal resolutions, invasiveness, and portability are elucidated in Table 2.1.

**Table 2.1:** Advantages and disadvantages of signal acquisition for different BCI/BMI modalities, the resolution values are references from (Babiloni et al. 2009; Hill et al. 2012; Al-Shargie 2019).

Method	Type of signal	Resolution		Invasive	Portability
		temporal	spatial		
Electroencephalography (EEG)	neuroelectric	High (<1 ms)	Low (1–9 cm <sup>3</sup> )	no	yes
Electrocorticography (ECoG)	neuroelectric	High (<1 ms)	Higher (<1 cm <sup>3</sup> )	yes	yes
Magnetoencephalography (MEG)	electromagnetic	High (<1 ms)	better than EEG (0.5–2 cm <sup>3</sup> )	no	no
functional Near-Infrared Spectroscopy (fNIRS)	hemodynamic/metabolic	Medium (hundreds of ms)	Low (1 cm <sup>3</sup> )	no	yes
functional Magnetic Resonance Imaging (fMRI)	hemodynamic/metabolic	Low (>1 s)	High (1–5 mm <sup>3</sup> )	no	no

For patients who suffer from paralysis, non-invasive methods have been more widely utilized than invasive methods (Birbaumer et al. 2008; van Gerven et al. 2009). Among non-invasive systems, one of the prevalent methods is EEG (Hwang et al. 2013), which is an electrophysiological technique for recording brain electrical activity through electrodes placed on the scalp and was first recorded by German psychiatrist Hans Berger in 1924 (Berger 1929). In this thesis, all EEG datasets were recorded using the International 10-20 system, in which electrodes were placed on the surface of the scalp (Oostenveld and Praamstra 2001; Jurcak et al. 2007).

EEG is mainly used to diagnose and investigate sleep disorders, depth of anesthesia, stroke, epilepsy, coma, and brain death. EEG and recently developed fNIRS have the advantage over other noninvasive methods for monitoring brain activity, such as magnetoencephalography (MEG) or functional magnetic resonance imaging (fMRI), that they are relatively portable, easy to set up and in comparison inexpensive, which are ideal characteristics for such systems. However, the relative distance of the electrodes from the signal source leads to noise and attenuation problems.

The invasive technique of electrocorticography (ECoG) is the technique by which the best signal quality can be obtained and is more precise and sensitive than EEG (Schalk and Leuthardt 2011). However, it requires the surgical implantation of microelectrodes above the cerebral cortex of the brain, which may involve the risk of signal degradation due to the formation of scar tissue around the electrodes as a result of the body's reaction to the foreign object. Its main advantages are high temporal and spatial resolution, high signal fidelity, and less vulnerability to noise and artifacts such as EOG (Ball et al. 2009). As neurosurgical interventions can be risky and expensive, invasive BCI is mainly targeted at paralyzed patients.

Many types of brain imaging can be used in BCI, including measurement of brain electrical activity (EEG and ECoG), measurement of brain magnetic activity (MEG), and measurement of hemodynamic responses (fMRI, and fNIRS). Although fMRI has the highest spatial resolution, it has the worst temporal resolution limited by hemodynamic delay. fNIRS is in between, with better temporal resolution than fMRI and better spatial resolution than EEG, but requires hair to be pushed aside during instrument setup to avoid severely compromising signal quality due to hair obstruction (Coyle et al. 2007); MEG has high temporal and spatial resolution, but requires dedicated electromagnetic interference (EMI) shielding to ensure signal quality; and EEG has high temporal resolution suitable for real-time BCI, but relatively low spatial resolution that can be improved by increasing the number of electrodes. Due to the excessive and bulky equipment of fMRI and MEG, it is limited to clinical applications. Therefore, among the non-invasive techniques, the EEG approach is the most commonly used, except for fNIRS.

The advent of BCI not only gives paralyzed patients hope of being able to control their prosthesis, but also gives patients with late stage ALS the opportunity to communicate with the surrounding people. Similarly, CLIS and LIS patients have inspired researchers to investigate the field of brain-computer interfaces, but due to the lack of ground truth about consciousness, there are few successful cases and many controversies (Chaudhary et al. 2017;

Spüler 2019; The PLOS Biology Editors 2019). In this Thesis due to the limitation of data sources, mainly ECoG and EEG signals are used to compare the different methods of consciousness analysis in CLIS patients.

## 2.3 Sample Entropy

Entropy is a physical concept, which is related to the total amount of disorder within a system. It can be used for nonlinear dynamic analysis in both the time and frequency domain to quantify the regularity (predictability) of a time series. The family of entropy-based methods is frequently used in neuroscience applications (Diambra et al. 1999; Yeragani et al. 2003; Courtiol et al. 2016).

Sample Entropy (SampEn) is a modification of Approximate Entropy (AppEn) proposed by Richman and Moorman (Richman and Moorman 2000) to eliminate some disadvantages of AppEn (Pincus 1991; Yeragani et al. 2003).

Specifically, the advantages of SampEn over AppEn are data length independence and non-inclusion of self-matches in the estimation. Sample entropy is widely applied in neuroscience and has previously been used to determine the level of consciousness, such as during surgical operations (Wu et al. 2014) and in some real-time applications (Wei et al. 2014; Wu et al. 2015). To calculate the sample entropy, a time series  $X = [x(1), x(2), \dots, x(N)]$  is constructed in which  $N$  is the data length, which is divided into several subsequences  $u_m(i)$ , and  $m$  is the dimension:

$$u_m(i) = [x(i), x(i+1), \dots, x(i+m-1)], i = 1 \dots N - m + 1 \quad (1)$$

This must meet the following condition:

$$d[u_m(i), u_m(j)] = \max\{|x(i+k) - x(j+k)|\} < r \times SD \quad (2)$$

where  $SD$  is the standard deviation of the time series  $X$  and  $r$  is the tolerance coefficient. The value of  $r$  was set to 0.2, and the tolerance would be  $0.2 \times SD$  (i.e.,  $x(j)$  was considered to be consistent with  $x(i)$  if  $x(j)$  met  $x(i)$  in this tolerance).  $B^m(r)$  is the summation of the number that  $x(j)$  matches the condition of  $x(i)$ :

$$B^m(r) = (N - m)^{-1} \sum_{i=1}^{N-m} B_i^m(r) \quad (3)$$

Similarly, we set  $m = m + 1$  and repeated Equations (1–3).  $A^m(r)$  is defined as follows:

$$A^m(r) = (N - m - 1)^{-1} \sum_{i=1}^{N-m} A_i^m(r) \quad (4)$$

SampEn is then defined as

$$\text{SampEn}(N, m, r) = \log \frac{A^m(r)}{B^m(r)} \quad (5)$$

Figure 2.3 shows a time series  $X = x[1], \dots, x[i], \dots, x[N]$ . The color band around the data point  $x[1]$ ,  $x[2]$ , and  $x[3]$  represents point  $x[1] \pm r$ ,  $x[2] \pm r$ , and  $x[3] \pm r$ , respectively. All data points in the red band match the data point  $x[1]$ , and similarly, all the data points in the orange and yellow bands match the data points  $x[2]$  and  $x[3]$ .

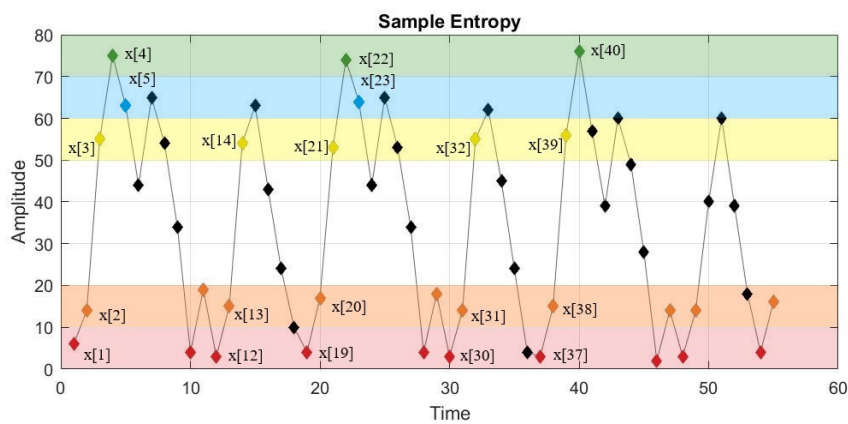


**Figure 2.3:** A diagram where each point represents one data point in time domain to explain the operation of sample entropy depending on the row of occurrence over time

Consider the three components red-orange-yellow as consecutive sequence pattern  $(x[1], x[2], x[3])$  and the four components red-orange-yellow-green as consecutive sequence pattern  $(x[1], x[2], x[3], x[4])$ . In this example, there are four red-orange-yellow sequences,  $(x[1], x[2], x[3], x[4])$ ,  $(x[12], x[13], x[14])$ ,  $(x[19], x[20], x[21])$ ,  $(x[30], x[31], x[32])$ , and  $(x[37], x[38], x[39])$ , they match  $x[1]$ ,  $x[2]$ ,  $x[3]$  on the same color bands, but only two red-orange-yellow-green sequences that match  $x[1]$ ,  $x[2]$ ,  $x[3]$ ,  $x[4]$ . Continuing that way with the next three-component sequence (orange-yellow-green) and the four-component sequence pattern (orange-yellow-green-blue), in this case, the number of matches of three-component pattern matches is two, and only one match for a four-component pattern. These numbers of matches are added to the previous numbers, the total number of three-component matches is six, and the total number of four-component matches is three. Now, repeat all possible sequence patterns,  $(x[3], x[4], x[5], x[6])$ ,  $\dots$ ,  $(x[N-3], x[N-2], x[N-1], x[N])$  to determine the ratio of all three-component pattern matches and four-component pattern matches.

The more complex the series, the higher the value of sample entropy. On the contrary, the more self-similarity in the series, the lower the value of sample entropy. The number of  $N$  was suggested as the average sum of a minimum  $10^m$  and a maximum  $30^m$  by Richman and Moorman (Richman and Moorman 2000) and Pincus and Goldberger (Pincus and Goldberger 1994). Thus, the parameters  $m=3$  is selected according to meet the relationship between  $N$  and  $m$ .

### 2.4 Permutation Entropy

Sample entropy is computationally expensive (Hayashi et al. 2015), and this is important for the future development of a medical device. Therefore, we also investigated the less computationally expensive method of Permutation entropy and compared the results with those from sample entropy.

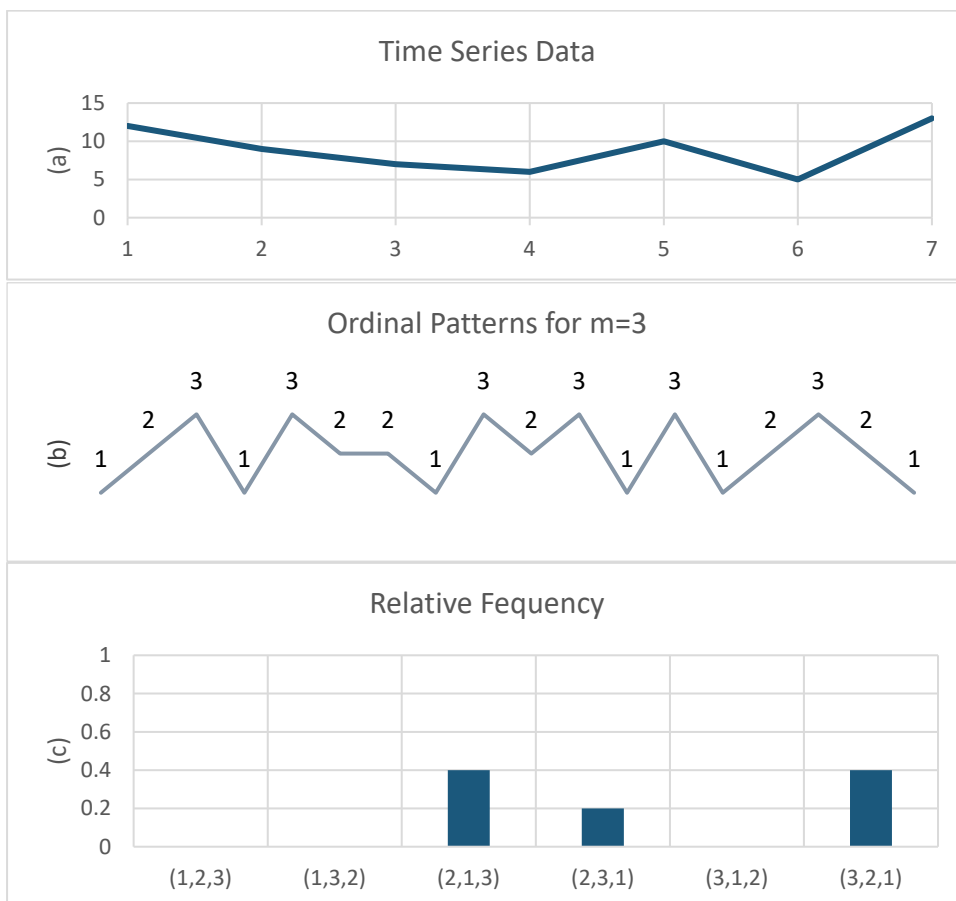


**Figure 2.4:** Example of Permutation Entropy estimation. (a) Time series  $X = (12, 9, 7, 6, 10, 5, 13)$ . (b) The six possible permutation patterns for  $m=3$ . (c) The relative frequency of all possible ordinal patterns for  $n = 3$  for this time series,  $P(2,1,3) = 0.4$ ,  $P(2,3,1) = 0.2$  and  $P(3,2,1) = 0.4$ .



Mathematically, permutation entropy (PE) does not consider the exact values of a time series, but instead considers the ordering of the time series, thus reducing the complexity of its computation (Bandt and Pompe 2002; Kuntzleman et al. 2018). The time series is divided into several non-overlapping subsequences with a length of  $m$  epochs, and each sample is converted into a series of rankings (patterns). An example of PE computation is shown in Figure 2.4. In C(a,b) the time series  $X$  was divided into the values (12,9,7), (9,7,6), ..., (10,5,13), and converted to the patterns (3,2,1), (1,2,3), ..., (2,1,3). Figure 2.4(b) indicates the principle templates of the data sequences and then sums up the number of permutation pattern appearances of each observed sequence. It is different to SampEn since SampEn uses tolerance to ensure whether two time series have similar patterns, whereas PE has a fixed number of  $m!$  ordinal patterns. The complexity of PE is defined by  $m$ , with the possible permutation patterns estimated as  $m!$ . Figure 2.4(c) shows the relative frequency of occurrence of all possible ordinal patterns for this example.

Riedl et al. (Riedl et al. 2013) suggested that a value of  $m$  between 3 and 7 was more appropriate for electroencephalogram (EEG) applications. In order to save computation time, we used a relatively low value of  $m = 3$ , although it may have reduced the sensitivity of the result.

## 2.5 Poincaré plot

The Poincaré plot is a non-linear geometrical representation of successive measurements providing a visual representation of time series variability. A common application of Poincaré plots is the detection of the short-term and long-term variability of a heart rate (Golińska 2013; Henriques et al. 2015), but in recent years, Poincaré plots have also been used in neuroscience applications, such as to detect the depth of anesthesia (Hayashi et al. 2014; Hayashi et al. 2015; Bolaños et al. 2016). For our data set, we used pairs of scatterplots of each ECoG voltage  $x(n)$  versus the next ECoG voltage after a time delay  $\Delta x(n + \Delta)$  for the generation of each Poincaré plot. To quantify the distribution of the ECoG signals in the Poincaré plot, the standard deviation (SD) perpendicular to the diagonal line (SD1) and the SD along the diagonal line (SD2) were measured, as shown in Figure 2.5. Its mathematical expression is as follows: SDX is the standard deviation of time series, and SDSD is the standard deviation of the succeeding difference of time series.

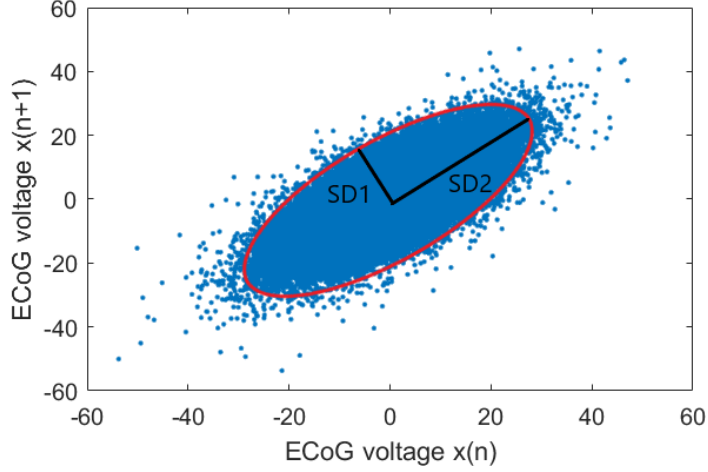


**Figure 2.5:** The Poincaré plot (time delay = 1), standard deviation perpendicular to the diagonal line (SD1) and standard deviation along the diagonal line (SD2) describing the fitted ellipse of the ECoG voltage dispersion along the minor and major axis.

$$SD_1^2 = \frac{1}{2}SDSD^2 = \gamma_X(0) - \gamma_X(1) \quad (6)$$

$$SD_2^2 = 2SDX^2 - \frac{1}{2}SDSD^2 = \gamma_X(0) + \gamma_X(1) - 2\bar{X}^2 \quad (7)$$

where  $\gamma_X(0)$  and  $\gamma_X(1)$  are the autocorrelation function for lag-0 and lag-1 ECoG time series, and  $\bar{X}$  shows the mean of the ECoG time series.

In this study, the Poincaré plots from 30 s epochs of the ECoG signal (the sampling rate was 125 Hz) were plotted. The time delay was thus set to 1/125 s, which must be around one-fifth to one-fourth of the dominant cycle period or a multiple of the signal sampling interval. The choice of the optimum time delay could exactly reconstruct the underlying characteristics of the system (Hayashi et al. 2015).

## 2.6 Multiscacle Approach

Costa et al. (Costa et al. 2002, 2005) reported that multiscale approach was used for analysis based on SampEn estimates of heart rate, and this approach coarse-grained the data by averaging in the range of a given scale. Before using the multiscale approach, white noise was assigned to a higher entropy value than pink noise. However, when the scale size increased, the entropy value of the coarse-grained white noise decreased. Despite this, the change of the scale size had no influence on the entropy value of the coarse-grained pink noise, which was almost constant. If the scale size was more than 4, the entropy value of the white noise was lower than the corresponding value of pink noise. Therefore, in our study, we chose the scale size equal to 4. Figure 2.6 shows the schematic diagram in which the time

series  $b_1, b_2, \dots, b_i$  was created by separating the original time series  $a_1, a_2, \dots, a_{i+3}$  into non-overlapping windows of scale 4 and then averaging the time series in each window.

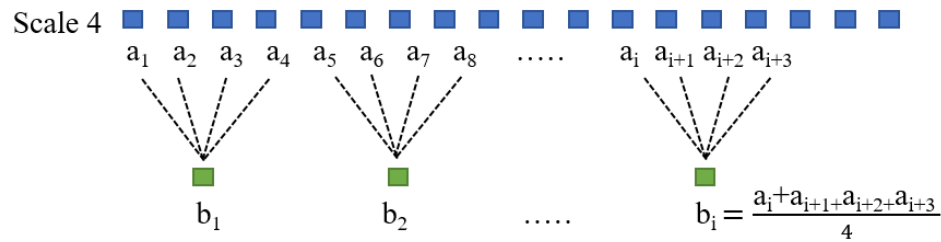


**Figure 2.6:** The coarse-graining procedure for scale 4.

## 2.7 k-Means

Among unsupervised learning algorithms, k-Means is a popular clustering algorithm that divides a given  $n$  points into  $k$  clusters by specifying a fixed number ( $k$ ) of clusters in advance, so that each point belongs to the cluster corresponding to its nearest mean, which is the cluster center (Pham et al. 2005; Kodinariya and Makwana 2013).

The algorithm consists of the following steps:

1. Select  $k$  points (as the black crosses in Figure 2.7) that are initial group centroids in the space represented by the data points to be clustered. Since the different location of the centroids leads to different results, it is better to place them as far away from each other as possible.
2. The next step is to assign each data point to the nearest clusters. The black dashed lines in Figure 2.7 indicate three decision boundaries that divide the data space into three regions which are indicated by blue, green and red circles respectively.
3. When all data point have been assigned, recalculate the locations of the  $k$  new centroids, the black arrows in Figure 2.7 indicate the movements of cluster centroids.
4. Repeat Step 2 and 3 until convergence is achieved and the centroids no longer change.

In this work, multiple runs are executed with random initial group centroids aiming to minimize costs. The cost function is defined in section 2.8.

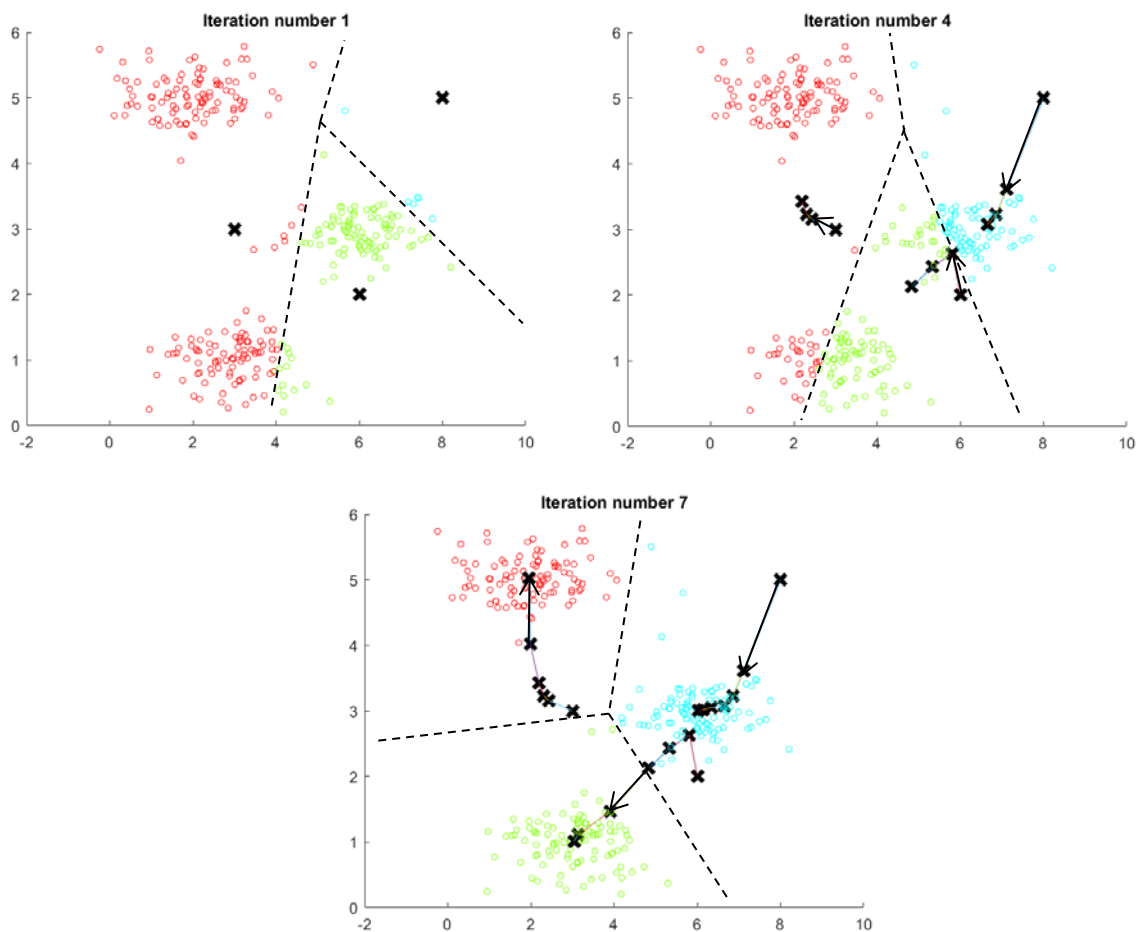


**Figure 2.7:** The schematic illustration of the k-Means algorithm cluster model ( $k = 3$ ). Top left: three clusters are initialized with their initial cluster centroids indicated by black crosses. Top right: the updating of the cluster labels and their cluster centroids after intermediate iterations. Below: the final cluster assignments by K-means algorithm at convergence. The figures were generated with practice materials from the online machine learning course by Andrew Ng on Coursera. <https://www.coursera.org/learn/machine-learning?>

There are two requirements to be considered when using the k-Means method. One is that this algorithm always partitions the dataset at the midpoint between two cluster centers, so the clusters in the dataset must be approximately equal in size. The second is that if the dataset contains a lot of noise or many outliers, then such problematic data objects often cause a significant shift in the calculated cluster centers, and the k-Means algorithm has no precautions against this effect, so the DBSCAN method is added later to analyze the data because it explicitly provides the "noisy" objects.

## 2.8 Elbow method

The oldest method for estimating the number of clusters is intuitively named as elbow method (Kodinariya and Makwana 2013). The elbow method is commonly used to determine the number of clusters in the disease clustering process (Azar et al. 2013).

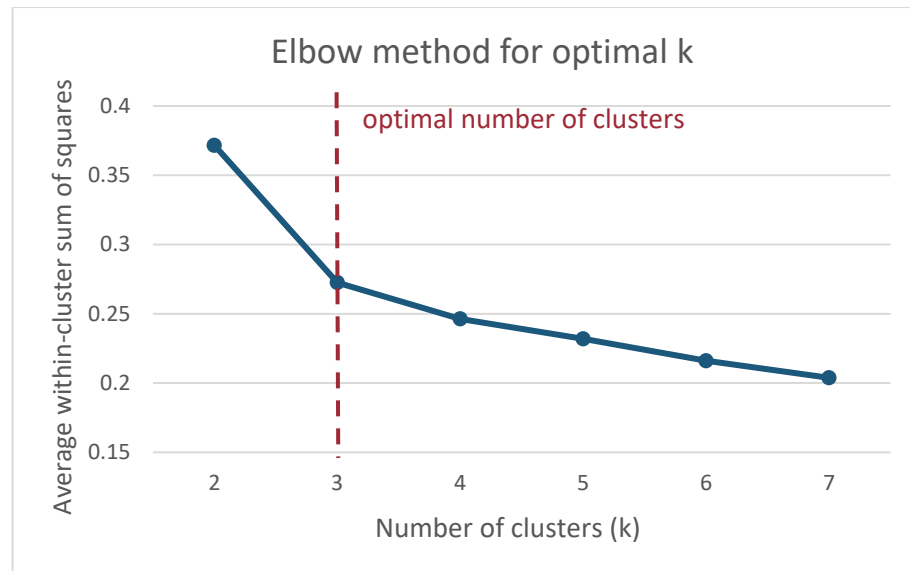


**Figure 2.8:** The elbow method for determining number of clusters, where the x-axis represents the number of clusters and the y-axis represents the cost. The elbow point is indicated by a red vertical dashed line.

In this visual method, as shown in Figure 2.8, which is drawn with the number of clusters on the x-axis and the cost on the y-axis. This method has to calculate the cost for all possible numbers of clusters. In this work, the cost is the average sum of squares within the cluster of distances between each data point and the centroid of each cluster to which it is assigned. The cost function is defined as follows:

$$J = \frac{1}{n} \sum_{i=1}^k \sum_{j=1}^{n_i} \|x_{ij} - \bar{x}_i\|^2 \quad (8)$$

where  $k$  is the number of clusters and  $n$  is the number of data.

The elbow method, as the name implies, is about finding some  $k$ -value below which the costs decrease sharply (upper arm) and reaches a plateau after being greater than this  $k$  value (lower arm), which is the  $k$  value appropriate for this data set.

## 2.9 DBSCAN

DBSCAN (Density-Based Spatial Clustering of Applications with Noise) is a density-based unsupervised learning algorithm original described by Ester et al. (Ester et al. 1996) that classifies objects according to their density so that a number of objects with similar density distributions are assigned to the same cluster. In this analysis, an object is a segment of the sample entropy value (EEG signal). The two input parameters of DBSCAN are as follows:

**MinPts:** Density threshold, which defines the minimum number of points required to form a dense region.

**Eps:** Radius, which defines the maximum distance between a pair of points (Euclidean distance). These two points are considered to be part of the same cluster only if the distance between them is less than or equal to  $\epsilon$ .

Starting from an arbitrary data object (initialized object), DBSCAN estimates the density around each data point by counting the number of objects within the pre-specified radius  $\epsilon$  and applying a specified  $\text{minPts}$  threshold to identify three groups: core, border and noise points, as shown in Figure 2.9 (Ware and Bharathi 2013; Rehman et al. 2014; Pioreckya et al. 2019). For the selection of DBSCAN parameters see the description in section 2.10.

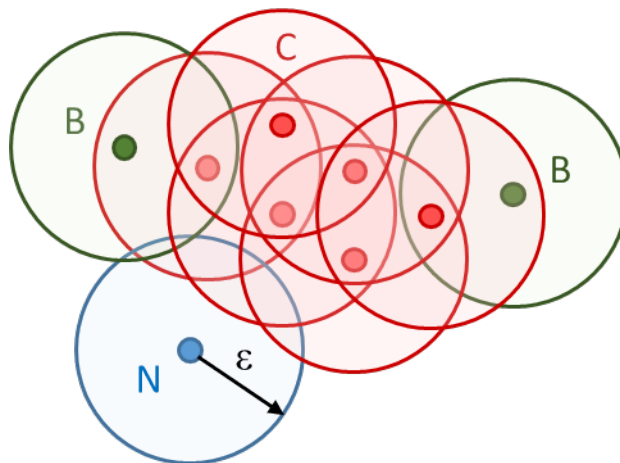


**Figure 2.9:** An illustration of the DBSCAN for  $\text{minPts}$  parameter is 4, and the radius  $\epsilon$  is indicated by the circles. Point C and the other red points are core points which have at least 4 points inside a circle of radius  $\epsilon$  (Eps) including the point itself. Points B are border points that have at least one core point inside a circle of radius  $\epsilon$  (Eps) of this example are indicated in green. Point N is a noise point which is neither a core point nor a border point is indicated in blue. Images are adapted from (Schubert et al. 2017).

---

Based on the above two parameters, the three groups are described in detail as follows:

**Core point:** This is a point that has at least minimum number of points (MinPts) inside a circle of radius epsilon ( $\epsilon$ ) including itself. It means that it is a dense region if there is a core point in this region.

**Border point:** This is a point that has at least one Core point inside a circle of radius epsilon ( $\epsilon$ ), but cannot itself be a core point. It means that the point is near or on the border of dense region.

**Noise point:** This is a point that is neither a core point nor a border point. It means that these points are outliers unrelated to any dense cluster.

The advantage of DBSCAN is that it can find clusters with nonlinear shape or even a cluster that is completely surrounded by other clusters but not connected to them. This algorithm includes only two parameters, and due to the presence of the MinPts parameter reduces the situation of a single-link effect, where different clusters are connected by a thin line. DBSCAN is insensitive to the order of points in the database. If the order of points is changed, points located at the edges of two different clusters may exchange cluster labels, and cluster assignments are unique only if they are isomorphic. Together with the fact that DBSCAN has a cluster of noise, which makes it robust to outliers. DBSCAN does not need to specify the number of clusters in the data in advance, moreover, it uses density as the basis for clustering of categories, which are different from K-means, so DBSCAN is chosen for cross-validation with K-means in this thesis.

## 2.10 K-distance graph

Two parameters, minPts and epsilon ( $\epsilon$ ), need to be adjusted when applying DBSCAN for cluster analysis. The minPts must be chosen to be at least 3. When minPts=1, it is meaningless because each point is already a cluster itself. When minPts $\leq$ 2, the result is the same as the single link hierarchical clustering, in which the dendrogram is cut at height  $\epsilon$ . As a rule of thumb, the smallest minPts value can be obtained from the dimensionality D of the dataset, i.e., minPts  $\geq$  D + 1. Sander et al. suggested minPts=2×D (Sander et al. 1998), but for datasets with noise or with many duplicates or for larger datasets, it is necessary to choose a larger minPts value.

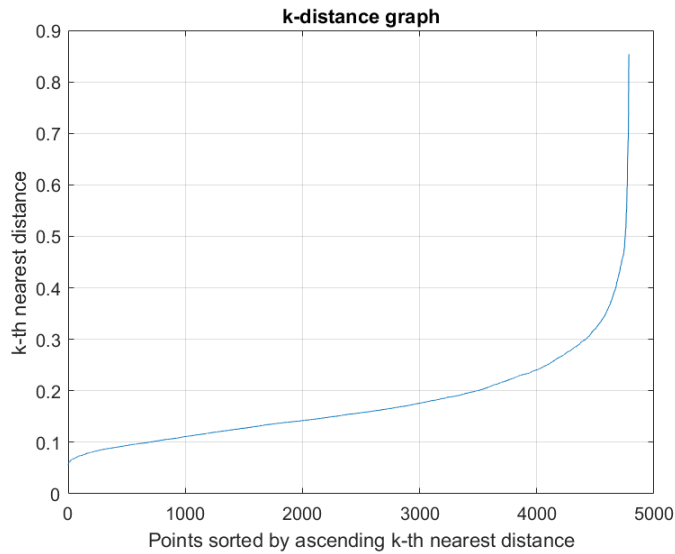


**Figure 2.10:** Plot of the k-distance graph, where the x-axis represents the points sorted by distance and the y-axis represents the epsilon ( $\epsilon$ ) value.

In this study, the k-distance graph is used to find the best epsilon ( $\epsilon$ ) values for different minPts in the data for each patient per day, by plotting the distance to the  $k = \text{minPts} - 1$  nearest neighbors, sorted from the minimum to the maximum value. As shown in Figure 2.10, where the x-axis represents the points sorted by distance and the y-axis represents the epsilon ( $\epsilon$ ) value. The optimal epsilon ( $\epsilon$ ) parameter is located at the elbow of this k-distance graph (Sander et al. 1998; Schubert et al. 2017). If epsilon ( $\epsilon$ ) is chosen too small, a large part of the data will be clustered as noise; conversely, if the epsilon ( $\epsilon$ ) value is chosen too high, the clusters will merge, causing most of the data points to be clustered in the same cluster.



# Chapter 3

## State of the art

*“Can the brain understand the brain? Can it understand the mind? Is it a giant computer, or some other kind of giant machine, or something more?”*

*– David Hubel (1926-2013)*

In this chapter, based on the schematic diagram of the brain-computer interface (BCI) system presented in section 2.2, section 3.1 describes the state of the art techniques applied to the detection of consciousness in CLIS patients with different instruments and different types of signals. It explains as well why most of the channels show similar results that are used as the final result in this thesis. Section 3.2 illustrates the reason for using time-domain algorithms for feature extraction in signal processing instead of frequency-domain algorithms. Finally, in section 3.3, exogenous and endogenous BCI paradigms are presented and the most appropriate one for CLIS patients is proposed based on the literature

### 3.1 CLIS

In the past, CLIS patients were often misdiagnosed as suffering from a disorder of consciousness because it was not possible to verify the presence of cognitive function in CLIS patients without any visible reactions, but by definition they are aware and awake with a level of consciousness comparable to that of healthy individuals (Laureys et al. 2004; Schnakers et al. 2008). Kotchoubey et al. also verified the presence of cognitive function in completely paralyzed patients with ALS through the measurement of event-related potential (ERP) (Kotchoubey et al. 2003). This also inspired the interest of researchers in this area of

consciousness in patients with advanced ALS. Until today, there are only a few papers discussing the issue of consciousness in ALS patients crossing over into CLIS, since there is no ground truth to validate the results. In identifying the consciousness of patients with CLIS, LIS in addition to EEG, ECoG signals, most studies have used the results measured by large medical instruments such as fMRI, PET, and so on.

For example, functional magnetic resonance imaging (fMRI) has been used to overcome the limitations of behavioral assessment (Owen et al. 2009; Monti et al. 2010; Bruno et al. 2011; Cruse et al. 2011). Some findings suggest that some DOC patients retain cognitive function and awareness (Laureys 2005; Schiff et al. 2005; Owen et al. 2006; Owen et al. 2007; Owen and Coleman 2007, 2008). Stender et al. calculated the diagnosis accuracy of both PED and fMRI imaging methods with reference to the Coma Recovery Scale-Revised (CRS-R) to help diagnose the long-term recovery in DOC patients (Stender et al. 2014). Zeman et al. reported the use of positron emission tomography (PET) to measure cerebral metabolism in patients to distinguish between patients with CLIS/LIS and patients in persistent vegetative state (Zeman 2003), and Casali et al. also found different levels of consciousness in LIS, MCS, and VS patients by transcranial magnetic stimulation (TMS) (Casali et al. 2013).

They provide cross-sectional images of the brain, and these brain images are suitable for identifying the location of injuries, tumors, or areas of corresponding motor or language neuronal activity in the brain, but these large instruments are not suitable for daily communication with patients because of their high set-up and maintenance costs. In contrast, the recently developed near-infrared spectroscopy (NIRS) method is a non-invasive optical imaging technique that allows simultaneous measurement of hemodynamic changes in multiple regions. Some researchers attempted to communicate with CLIS patients using NIRS (Gallegos-Ayala et al. 2014; Chaudhary et al. 2017), but controversy persists due to the lack of ground truth about the consciousness of CLIS patients (Spüler 2019; The PLOS Biology Editors 2019).

EEG would be an affordability and ambulatory alternative that could serve as a bridge between patients with advanced ALS and their families and the environment surrounding them in their daily lives. In contrast to other studies that attempt to seek methods of classifying between different clinically defined states of consciousness, such as using event-related synchronization (ERS) and event-related desynchronization (ERD) to distinguish between CLIS/LIS and coma (Markand 1976), the goal of this thesis is to identify patterns that are most likely indicative of a minimum conscious state that will allow successful

communication with ALS patients in CLIS. The research results of EEG and ECoG in this thesis has been peer-reviewed and published in (Wu et al. 2020; Wu and Bogdan 2020; Adama et al. 2022).

In healthy people, the body mapping of the motor cortex follows the cortical homunculus (Penfield and Boldrey 1937; Grodd et al. 2001), but when the brain lesions of CLIS patients are caused by car accidents or strokes, the patients' motor cortex may change. We know from the literature that after amputation of the middle finger in an adult monkey, the neurons innervating the middle finger in the brain were lost by magnetoencephalography (MEG), while the range of neurons innervating the index and ring fingers increased two months later (Lee and van Donkelaar 1995). In the 1960s, the famous American actress Patricia Neal, who was at the peak of her career, suffered a massive stroke that damaged the left side of her brain and paralyzed the entire right side of her body, leaving her unable to speak. But she had a strong will to return to the stage after three years of arduous rehabilitation. Scientists used fMRI to discover that her language area (Broca's area) and motor neurons of the right hand, which were supposed to be dominated by the right hemisphere, were instead dominated by the left hemisphere (Azari and Seitz 2000).

From the above cases, the brain has the capacity for neuroplasticity, which means that the brain has the ability to compensate for damaged areas and reorganize neurons. Just like through magnetoencephalography (MEG) we learned that a professional violinist has a higher number of neuronal cells in the motor neuron cortex area corresponding to the index finger to the little finger of the left hand (Altenmüller 2003). Since fMRI or MEG is required to identify the area of compensatory effect after brain injury, this thesis shows the similar results in most channels as more reliable results.

The choice of methods was guided by the existing literature on the detection of consciousness in other related physiological and clinical states (Laureys 2005; Luauté et al. 2015), such as anesthesia, minimally conscious state and vegetative state (Owen et al. 2006; Casali et al. 2013). Anesthesia in particular provides a useful means of identifying objective patterns that reflect periods of awareness and unconsciousness, as outlined in the literature. One of the methods that has been used in anesthesia for discriminating between awareness and unconsciousness is sample entropy, focusing mainly on calculating the level of brain wave disorder. It is, thus, reasonable to expect that similar patterns reflecting awareness and unconsciousness will also be observed in a CLIS patient. Based on these expected patterns, we were also able to verify our findings using sample entropy (Richman and Moorman 2000; Wei et al. 2014), permutation entropy (Riedl et al. 2013; Kreuzer et al. 2014) and the

Poincaré plot (Hayashi et al. 2014; Hayashi et al. 2015), which were found to have relatively high values during the experiment, indicating a status comparable to the awake period of patients in surgery. Since all of these methods have been applied in the field of anesthesia in real time, and the selection of methods avoids methods with long computation times that are difficult to achieve real-time effects, which greatly increases the possibility of implementing these methods as real-time systems in CLIS and LIS patients, it is expected that the application will gain popularity in the future to help patients' families communicate with patients and further increase the stimulation of patients' brains, with the aim of prolonging patients' lives and improving their quality of life (QOL) (Kögel et al. 2020).

### 3.2 Time Domain vs. Frequency Domain Analyses

In healthy adult individuals, brainwave amplitude typically ranges from 0.5 to 100  $\mu$ V and bandwidth ranges from 0 Hz to half the sampling frequency (Teplan 2002). This bandwidth can be categorized into five basic groups: delta ( $\delta$ ), theta ( $\theta$ ), alpha ( $\alpha$ ), beta ( $\beta$ ), and gamma ( $\gamma$ ) waves corresponding to different frequency spectra. These typical frequency bands of brain waves and their characteristics are listed in Table 3.1.

**Table 3.1:** Typical frequency bands of brain waves in healthy adult individuals.

Band	Frequency range	Corresponding Brain Activity
Delta( $\delta$ )	0.5-4 Hz	Deep sleep
Theta( $\theta$ )	4-8 Hz	Drowsiness, dreaming
Alpha( $\alpha$ )	8-13 Hz	Relaxation, closed-eyes, meditation
Beta( $\beta$ )	13-30 Hz	Psychical activity, thinking, focus, tension
Gamma( $\gamma$ )	>30 Hz	Combination of sensory processing

Whether the frequency range of consciousness of CLIS patients is the same as that of healthy individuals? For brain wave research, there are numbers of studies in frequency domain, such as alpha peak frequency (APF) of 8-13 Hz suggested by Grandy et al. (Grandy et al. 2013) as a stable neurophysiological trait marker of healthy adults, even though it regularly declines with age (Klimesch 1999), Alzheimer's disease (Cantero et al. 2009), schizophrenia (Angelakis et al. 2004), still follow this frequency range, but Hohmann et al. showed that alpha band is not suitable for the CLIS patients with shifts to lower frequency ranges (Hohmann et al. 2018). Babiloni et al. reported that resting-state eyes-closed alpha and delta EEG rhythms were abnormal in LIS patients compared with age-matched healthy

subjects (Babiloni et al. 2010). Birbaumer and colleagues also reported a shift of the EEG spectrum to the low frequency band in LIS and CLIS patients and hypothesized that with underlying neurological function and loss of normal EEG power spectrum may be a long term criterion for determining whether communication ability is still present (Secco et al. 2020; Maruyama et al. 2021). As the available characteristics of the brainwave spectrum in Table 3.1 for healthy individuals is not applicable, frequency domain analysis may be less useful for short time periods of communication in experiments or in the daily lives of CLIS patients.

Similarly, DOC patients have altered Polysomnographic (PSG) signal topography, frequency, and power due to severe brain injury, with the most prominent change in many DOC patients being the general slowing of the EEG. Previous studies have also shown that DOC patients have lower spectral peaks compared to healthy individuals (Fellinger et al. 2011; Lechinger et al. 2013), and UWS patients have lower relative power in alpha band and higher relative power in delta band compared to MCS patients (Sitt et al. 2014; Piarulli et al. 2016).

For both CLIS patients and DOC patients, there are concerns about band shifts to lower frequencies, often without alpha peaks, which may indicate the amount of residual cognitive processing, but are easily recognized as deep sleep states in healthy individuals. Currently, there is no EEG frequency band definition for CLIS/LIS or MCS/UWS patients, and the criteria established based on the EEG frequency band of healthy subjects would misjudge the patient's state of consciousness. Therefore, the sample entropy, permutation entropy, and Poincaré plot are used as the complexity for time-domain signal analysis in this thesis, which avoids the reduction of EEG frequency bands associated with diseases in patients, rendering them more suitable for analysis of CLIS patients and DOC patients compared to features based on the frequency spectrum.

### **3.3 Auditory vs. Motor imagery vs. Visual paradigms**

For paralyzed patients, brain-computer interfaces (BCIs) provide a non-muscular method of communication via brain signals that can be broadly classified into two main BCI paradigms: exogenous and endogenous. The exogenous BCI paradigm uses external stimuli, such as flashing LEDs or auditory cues, to evoke specific brain patterns to respond accordingly; P300 (Cipresso et al. 2012; Guy et al. 2018) and steady-state visually evoked potential (SSVEP) (Lim et al. 2017) both fall into this category. Endogenous BCI requires patients to perform designated mental tasks, and motor imagery (MI) (Müller-Putz et al.

2010) falls into this category. Most EEG-based endogenous BCI systems have been tested on healthy individuals over the past two decades (Blankertz et al. 2006). More recently, Han et al. reported successful online communication with a CLIS patient using an EEG-based endogenous BCI system (Han et al. 2019). One of these verbal feedbacks to a specific brain response (e.g., "yes" or "no") is also known as the reflexive semantic classical conditioning (based on Pavlovian theory) paradigm. The main goal of this paradigm is to deal with communication problems in patients with severe motor disorders, such as CLIS (Birbaumer et al. 2012; Furdea et al. 2012; Ruf et al. 2013; Gallegos-Ayala et al. 2014; Chaudhary et al. 2016).

Feedback at the auditory (Nijboer et al. 2008), tactile, or visual (Caria et al. 2007) interface in BCI, thus enabling the user to modulate their brain activity, is a very important part of BCI to be able to successfully control external devices. The Glasgow coma scale (GCS) (Teasdale and Jennett 1974) and the Coma Recovery Scale-Revised (CRS-R) (Giacino et al. 2004) were also developed to diagnose the degree of dysfunction through auditory and motor as well as visual stimuli, and are commonly used in experiments to test the presence or absence of external consciousness.

CLIS and LIS patients with ALS have reduced or absent voluntary motor capacity and are more likely to exhibit sleep-wake disturbances than healthy individuals in the later stages of ALS (Lo Coco et al. 2011). They may experience periods of fluctuating consciousness that are not easily identified, which, combined with the impaired vision of such patients due to dry eyeballs and subsequent corneal necrosis, may limit the use of eye-tracking devices or other AAC devices that require a healthy visual system (Okahara et al. 2018; Beukelman and Light 2020; Chaudhary et al. 2020). Therefore, CLIS and LIS patients should avoid using visual BCI feedback systems. However, motor imagery this type of BCI paradigm typically requires lengthy training sessions for training classifiers prior to each use of the system, which leads to patient fatigue before they even begin using the system (Nicolas-Alonso and Gomez-Gil 2012). In addition, many individuals have difficulty performing motor imagery tasks and are unable to have a specific sense of motor imagery, preferring instead to imagine images of moving hands or legs (Hwang et al. 2009). Vidaurre and Blankertz et al. also reported that 15-30% of BCI users have "motor imagery illiteracy" (Vidaurre and Blankertz 2010). For CLIS and LIS patients with ALS, auditory BCIs are most important and seem to be the only way to prevent extinction of thought. Loss of communication can negatively impact their quality of life (Felgoise et al. 2016), and such

---

patients would benefit from a BCI system that would allow them to live more independently with a view to a relatively high recovery of their social life.

### 3.4 Summary

To determine whether CLIS and LIS patients retain cognitive function and consciousness, most studies use results from large medical instruments such as fMRI and PET in addition to EEG and ECoG signals. These large instruments are mainly used to identify the location of damage or the corresponding areas of motor or speech neuron activity in the patient's brain. Most of the state of the art techniques have been used to help physicians diagnose and understand the long-term course of patients' disease or to differentiate between different disease types on the clinical scales of consciousness. However, there is a lack of a brain-computer interface-based communication method that is easy and inexpensive to set up and maintain, and suitable for reliable daily communication with CLIS patients. Despite the breakthrough in near-infrared spectroscopy (NIRS), it is still quite controversial.

The approaches in this thesis mainly utilize EEG, a relatively affordable and mobile option, and the database of both CLIS and LIS patients in this thesis uses an auditory paradigm that bypasses the effects of visual impairment and "motor imagery illiteracy". Due to the shift of the EEG spectrum to lower frequency bands in LIS and CLIS patients, frequency domain analysis may be a long-term criterion to assess whether the communication ability is still present, but may be less useful for experimental or short-term communication in the daily life of CLIS patients. According to section 2.1, the span of consciousness during anesthesia includes the CLIS/LIS and DOC patient consciousness, which provides an objective model to distinguish between presence and absence of consciousness in conjunction with the large number of cases in the field of anesthesia and real-time demand. This thesis mainly refers to the algorithms of sample entropy, permutation entropy and Poincaré plot time-domain analysis in this related field of anesthesia as indicators to possibility of implementation in CLIS and LIS patients as a bridge between patients and their families and the environment surrounding them in daily life, in order to increase patients' willingness to live with a view to a relatively high recovery of their social life.

## Chapter 4

# Modus Operandi

*“The brain is a complex biological organ of great computational capability that constructs our sensory experiences, regulates our thoughts and emotions, and control our actions.”*

*– Eric Kandel*

In this thesis, the state of consciousness in CLIS patients should be detected by continuously recorded electroencephalography (EEG) or electrocorticography (ECoG) with a priori knowledge of the “ground truth”. The five key advantages of this work are as follows:

- i. The all-important “ground truth” is accessible and can provide objective means of detecting the presence of consciousness in such patients. It was able to obtain such a “ground truth” from one CLIS patient, who successfully communicated and answered patient-specific questions asked by an investigator using a brain-computer interface system. To the best of my knowledge, there is no other such dataset in existence.
- ii. The analysis of time domain signals using sample entropy, permutation entropy, and Poincaré plot can avoid the disease-related reduction of EEG frequency bands in CLIS/LIS or MCS/UWS patients, which would misjudge the patient's consciousness state if judged based on the EEG frequency bands of healthy persons, and there is currently no definition of EEG frequency bands for patients with these diseases.



- iii. In this thesis sample entropy, permutation entropy, and Poincaré plot are implemented not only in ECoG signals, but also sample entropy and Poincaré plot in EEG signals to successfully identify the difference in consciousness status of CLIS/LIS and DOC patients. Compared with large instruments such as fMRI, the portability of EEG signals and the feasibility of implementing sample entropy, permutation entropy, and Poincaré plot into a real-time system can be expected to become a communication bridge between patients and their family members in the future.
- iv. Sample entropy can be used as a reference indicator for communication with patients to avoid making experimental results dependent on patient willingness, who may have a psychological-emotional problem (e.g., depression) or a physiological problem (e.g., pain) during the experimental period. It also can help researchers understand the patient's physical and psychological state.
- v. All the methods mentioned currently in the feature extraction section have different parameter choices and individual patient differences, it is difficult to establish a threshold as a universal criterion for the presence or absence of consciousness in patients. In this thesis unsupervised learning methods (k-Means and DBSCAN) are used to provide a threshold of consciousness for individual participation in the experiment from the feature extraction results for each patient, so that in the future families and researchers will have a more objective reference indicator for communicating with patients.

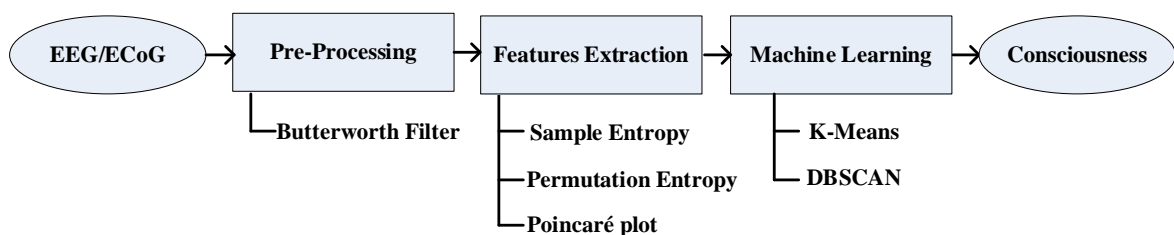


**Figure 4.1:** The data processing flow chart of Modus Operandi.

The data processing flow chart of modus operandi of the presented approach in the thesis is shown in Figure 4.1. First, a the Butterworth bandpass filter is used in the pre-processing to reduce the 50Hz power-line noise, and then different feature extraction methodologies (sample entropy, permutation entropy, and Poincaré plot) are used to obtain a value representing the conscious state. Third, unsupervised learning (k-Means and

DBSCAN) was used to find the individual threshold values of the patient's state of consciousness during the experimental and during the resting period. The ultimate goal is to develop a method in order to detect consciousness in CLIS patients to re-establish communication during the time they are conscious.

## 4.1 Pre-Processing

Medical equipment as well as daily care activities are known to introduce a lot of noise, especially when recording brainwave signals for long periods of time. Among others, PSG recordings in DOC patients can be affected by dysregulation of the vegetative nervous system, resulting in abnormal sweating, spasms that can cause huge muscle artifacts, etc. (Wisłowska et al. 2017).

In this section, considering the reduction of the computational load, first, down-sampling was carried out to 100/125 Hz, while the original sampling rate was 200/500 Hz depending on the data set at our disposal. Second, to avoid interference at 50 Hz power-line frequency and to focus on the beta band (13-30 Hz), which frequency band are closely related to consciousness for thoughtfulness and awareness (Schwender et al. 1996), a sixth-order Butterworth filter (1–45 Hz) was used to bandpass filter the down-sampled signals.

## 4.2 Feature Extraction

For the feature extraction part, there are some slight differences in the algorithms used in the thesis for ECoG and EEG signals, so the detailed flowcharts are shown in Figure 4.2- Figure 4.3 respectively.

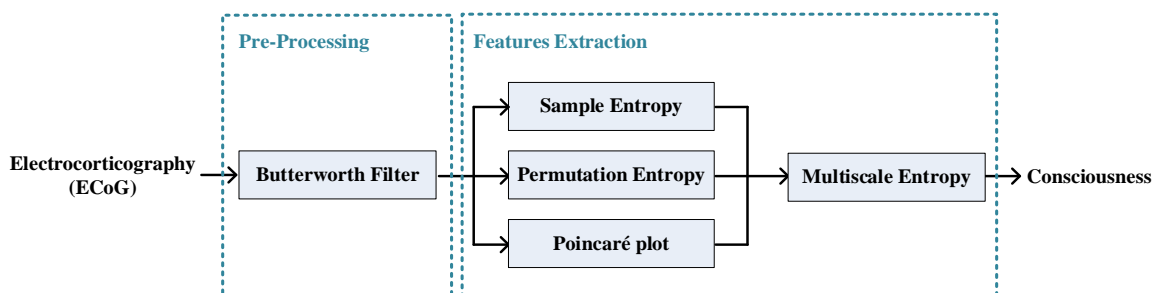


**Figure 4.2:** The data processing flow chart of ECoG signals.

Figure 4.2 shows the ECoG signal processing flowchart for the multiscale-based method analysis for the CLIS patient GR dataset, which will be presented in details in section

5.1. The original ECoG signals were down-sampled to 125 Hz to reduce the processing time, and a sixth-order Butterworth bandpass filter from 1 to 45 Hz was used to remove the power line noise of 50Hz and retain the beta band (13-30 Hz), which is considered to be closely associated with consciousness for thoughtfulness and awareness (Schwender et al. 1996), to obtain the filtered signal. Then, sample entropy, permutation entropy and Poincaré plot were applied on the filtered data. Finally, multiscale entropy (Costa et al. 2002, 2005) was utilized to reduce the white noise and estimate the consciousness levels.

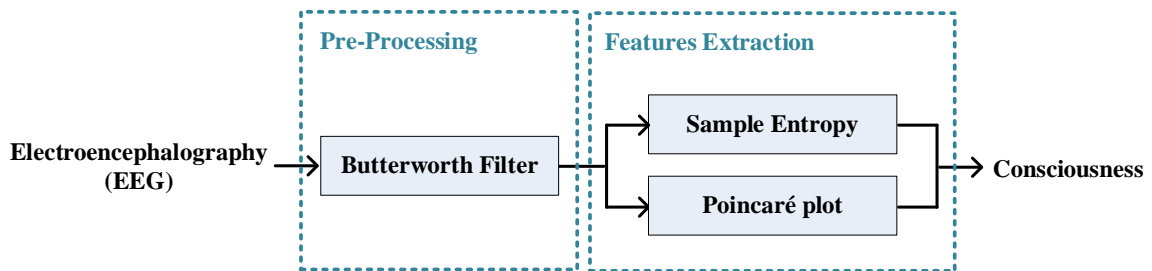


**Figure 4.3:** The data processing flow chart of EEG signals.

Figure 4.3 shows the EEG signal processing flowchart for the analysis of sample entropy and Poincaré plot methods of the CLIS/LIS and DOC patient datasets from section 5.2-5.4. Again, in order to reduce the computational load, down-sampling was carried out to 100/125 Hz, while the original sampling rate was 200/500 Hz. Second, the down-sampled signals were band pass filtered by a sixth-order 1–45 Hz Butterworth filter, since thoughtfulness and awareness, which is closely related with consciousness, are considered to be in the beta band (13–30 Hz) (Schwender et al. 1996) and interference of the 50 Hz power-line frequency is avoided, as already mentioned above. Finally, the sample entropy and Poincaré plot algorithm was applied to obtain an individual level of consciousness. All analyses were conducted using MATLAB R2018b (The Mathworks, Inc.).

### 4.3 Machine Learning

Currently, many brain disorders are identified by machine learning, such as epilepsy (Pioreckya et al. 2019), Alzheimer/Parkinson, and schizophrenia (Dvey-Aharon et al. 2015), etc. It is also used to distinguish sleep stages (Güneş et al. 2010). It follows that both unsupervised learning methods (k-Means and DBSCAN) and supervised learning methods (random forest and support vector machine (SVM)) can be used to estimate whether a patient

is stimulated during certain time periods or whether a participant suffers from a certain disease, etc.

As mentioned earlier, CLIS patients are supposed to be fully conscious but cannot perform any muscle movements or produce any speech to make a clear statement. There is no "ground truth" that can be used as teaching input to correct outcomes in supervised learning methods. Although researchers were able to obtain such from a CLIS patient when the patient successfully communicated and answered patient-specific questions asked by the researchers using the brain-computer interface system, this was sometimes influenced by whether the patient fully participated in the experiment. Since unsupervised learning methods that do not require any user input are appropriate for this condition and they are more time efficient and objective compared to supervised learning methods.

In addition, all the methods mentioned in the feature extraction section so far have different parameter choices and individual patient differences, so it is difficult to establish a threshold as a criterion for the presence or absence of consciousness in all patients. However, it is possible to obtain a threshold of consciousness for individual participation in the experiment from the feature extraction results for each patient using unsupervised learning methods (k-Means and DBSCAN), so that in the future families and researchers will have a more objective reference indicator for communicating with patients.

# Chapter 5

## Datasets

*“If the human brain were so simple that we could understand it, we would be so simple that we couldn’t.”*

*– Emerson M. Pugh*

### 5.1 ECoG recordings of a CLIS patient

The dataset was recorded by electrocorticography (ECoG) from a 40-year-old male in a completely locked-in state (CLIS) over 24 h at a sampling rate of 500 Hz with a 64-channel brain amplifier (Brainproducts GmbH, Munich, Germany). He was diagnosed with ALS in 1997 and entered CLIS in 2008. Based on studies by Bierbaumer and colleagues (Ramos-Murguialday et al. 2011; Soekadar et al. 2013; Bensch et al. 2014; Adama et al. 2019; Wu et al. 2020), we know that this CLIS patient learned to use this brain–computer interface in an attempt to communicate with the external environment through muscle twitching. The patient had a strong will to live before entering CLIS, but after falling into CLIS, there was only one successful communication out of several attempts. As Soekadar et al. (Soekadar et al. 2013) reported that the circadian rhythm in CLIS patients is unpredictable, it can lead to a higher frequency of dozing during the day than in healthy individuals. One hypothesis was that this lack of communication was due to a result of the experimenter arriving at the wrong time (i.e., when the patient was not in a consciousness state) and, thus, the patient was unable or unwilling to communicate. As described in the introductions, the goal was to identify, if

possible, when the patient was in a conscious state and hence most likely to be able to communicate successfully.

Figure 5.1 (right) shows the position of the ECoG grid electrodes on the left side of the patient's frontal and parietal lobes (Graumann et al. 2010). The functional channel locations of the ECoG electrode array are shown in yellow (Figure 5.1, left panel). The ground channel was S032, and the reference channel was G102 (orange channels, Figure 5.1, left panel). The implantable electrode was made of material that was difficult to bend; thus, the curvature of the brain could not be fully matched. This probably led to a recording hole in the middle of the electrode array (white channels in Figure 5.1, left panel) due to channel losses or high impedances. The reference and ground channels were not part of the recording hole.

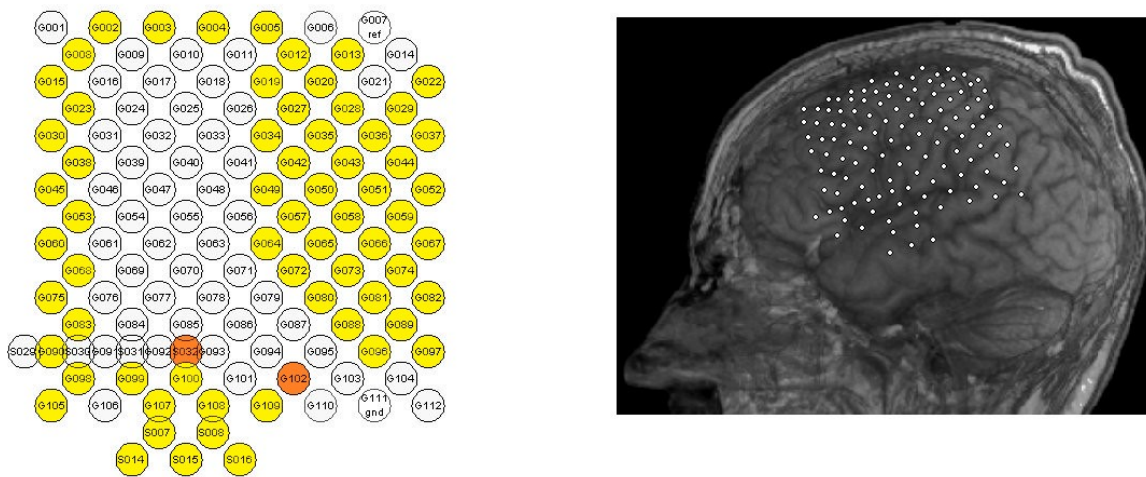


**Figure 5.1:** Channel locations of the electrocorticography (ECoG) electrode array in a CLIS patient. Left: channel names, the functional channels shown in yellow, and ground channel (S032) and reference channel (G102) in orange. Right: the position of implanted ECoG grid electrodes. Photo courtesy of the Institute for Medical Psychology and Behavioural Neurobiology, University of Tübingen.

During the day of recording, an auditory experiment as described in (Adama et al. 2019) was performed from 14:50 to 17:00. This was the period in which the experimenter was present, and includes both experimental setup and communication with the patient. During the experiment, the patient was expected to answer some paired yes or no open personal questions, such as “You feel good today?” or “You feel bad today?” Personal questions with known answers such as “Are you German?” or “Are you Dutch?” were also asked in order to control the correctness of detection. The patient in question was previously trained to use the brain–computer interface (BCI) while he was in LIS status and was thus

aware of how to use the BCI correctly. The patient not only answered the paired questions correctly, but also through questions like “Are you positive regarding the future?” and “Are you negative for the future?” These kinds of questions showed a positive attitude to life during the time of the experiment. The experimental protocol as supplemental material in section Appendix A that shows the list of questions and answers during the experiment, in which a + sign means yes and a – sign means no. In order to present the original situation of the experiment, we did not correct the accuracy of the English grammar and the representation of the answers, but excluded the patient’s personal data. We summarized the proportion of correct answers through semantic and contextual judgments, and even if the experimenter asked a paired yes or no question that was not the direction he wanted to go, he expressed his will strongly, and he let the experimenter know the third idea he was trying to express after answering the two opposite meanings. The patient answered 18 yes or no questions during the experiment. One answer was incorrect, and one was unclear, so the CLIS patient had an 88% accuracy rate in the experiment. In the experimental protocol, we indicated the questions with correct answers in green, those with incorrect answers in red and those with unclear answers in black.

## 5.2 EEG recordings of CLIS patients

The dataset in question comprises the signals of electroencephalography (EEG) and electrooculography (EOG). The dataset provider published the analysis results from four CLIS patients (Chaudhary et al. 2017). The same codename is used to facilitate comparison for readers. All these patients completed more than 250 sessions over several weeks: patient B completed 56 sessions, patient F completed 80 sessions, patient G completed 51 sessions, and patient W completed 74 sessions.

The EEG data was recorded with an EEG amplifier (Brain Amp DC, Brain Products, Germany). Figure 5.2 shows the channel positions which were used to acquire EEG signals and four electrodes which were used to acquire the vertical and horizontal EOGs. Since this data set does not standardize the channels and sampling rates used for all patients and for each visit, the same channels and sampling rates are usually used only at the same visit (usually a visit contains several experiments within a week), Table 5.1 shows the electrodes and sampling rates used to record the EEG signals for different CLIS patients on different days.

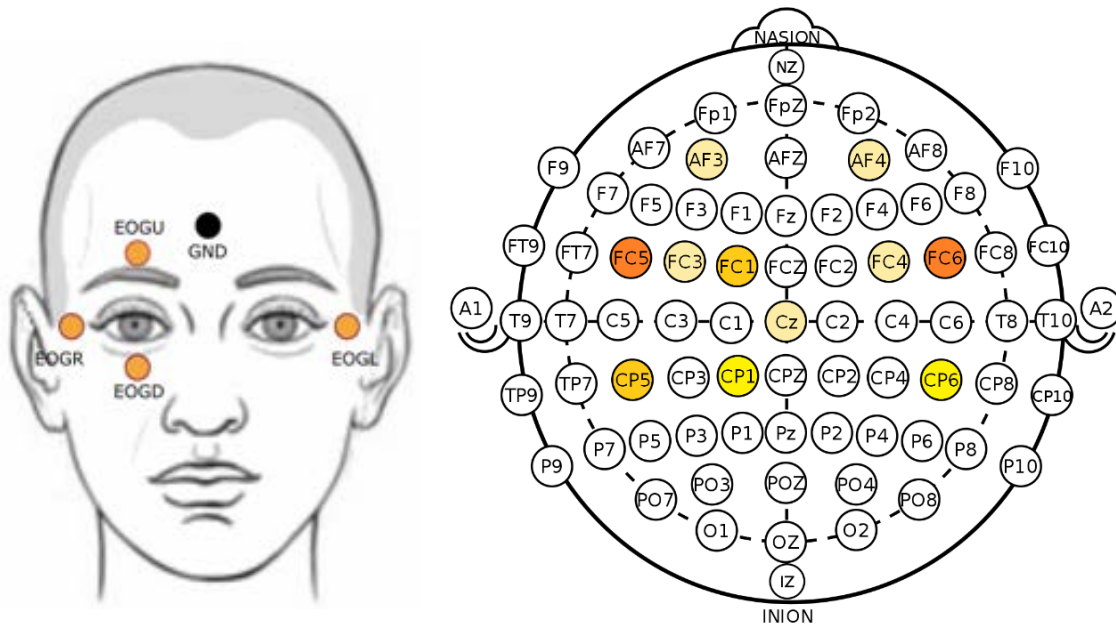


**Figure 5.2:** Channel positions of CLIS patients. Left: the channel positions of electrooculographic (EOG), courtesy of the Institute for Medical Psychology and Behavioural Neurobiology, University of Tübingen. Right: the channel positions of electroencephalography (EEG).

**Table 5.1:** Electrodes and sampling rates recording the EEG signals of the four CLIS patients on different days.

Codename	Day	EEG channels	Sampling rates
Patient B	Day1	FC5, FC1, FC6, CP5, CP1, CP6, AF3, AF4	200
	Day2	FC5, FC1, FC6, CP5, CP1, CP6, AF3, AF4	200
Patient F	Day1	FC5, FC1, FC6, CP5, CP1, CP6	200
	Day2	FC5, FC1, FC6, CP5	200
Patient G	Day1	FC4,FC5,FC3,FC6,Cz	500
	Day2	FC4,FC5,FC3,FC6,Cz	500
Patient W	Day1	FC5, FC1, FC6, CP5, CP1, CP6	500
	Day2	FC5, FC1, FC6, CP5, CP1, CP6	500

Beside the effect that in LIS the EOG signals that are measured to reject its influence in the recorded EEG data, during the course of disease in ALS toward CLIS, the patients gradually lose the ability to control muscles and even eye movements, and thus, the EOG disappears. Therefore, in this dataset, we focus only on the analysis of the source of brain waves, EEG signals.



Patient B is a 61 year old CLIS patient. He was diagnosed with ALS in May 2011. From April 2012 to December 2013, he was able to communicate with the MyTobii eye-tracking device. His family members attempted to train him to move his eyes to different sides to express “yes” and “no,” but the response was unstable. Since August 2014, a communication was no longer possible.

Patient F is a 68-year-old completely locked-in state patient. She was diagnosed with ALS in May 2007, locked-in syndrome (LIS) in 2009, and CLIS in May 2010. No communication channel was realized since 2010. Gallegos-Ayala et al. (Gallegos-Ayala et al. 2014) described the details of this patient.

Patient G is a 76-year-old completely locked-in state patient. She was diagnosed with ALS in 2010 and in the same year lost the capability to walk and talk. In February 2013, she started using one finger to communicate through an augmentative communication device. Unfortunately, seven months later, communication via the finger communication device failed as she was diagnosed with a corneal defect that caused her vision to deteriorate. She switched to using eye tracking for communication in early 2014, but since August 2014, before BCI was implemented, her husband and caregivers lost communication with her.

Patient W a 24 year old LIS patient, who is on the verge of CLIS. She was diagnosed with ALS in December 2012, and six months later she was completely paralyzed. From early 2013 to August 2014, she was able to communicate with eye tracking. After that, she attempted to turn her eyes to different directions to answer yes and no questions by training until December 2014. She completely lost control of her eyes in January 2015 and attempted to twitch the right corner of her mouth to answer yes, but the response was variable, so her parents lost reliable communication contact with her.

In total, over 45 h (250 sessions) of auditory experiments like (Ramos-Murguialday et al. 2011) were recorded including trigger marks, the states of baseline, presentation, last word, and response. Beforehand of the study, the investigators discussed with family members in order to compile 200 personal questions known by the patients for sure and 40 open questions.

First, the investigators trained the patients ahead the experiments by asking the known questions, for example: “Berlin is the capital of Germany?”/“Berlin is the capital of France?,” in which the patient was expected to answer these paired “yes” or “no” questions.

During the experiments, the investigators asked the patients personal questions as well, such as “Is your husband’s name Joachim?” and also open questions the like “You feel good

today?”/“You feel bad today?” related to the topic around the quality of life and compare the answers with the actual physiological status reported by the caretakers.

All the known questions and personal questions included 10 questions with answers of "yes" and 10 questions with answers of "no". The order in which these 20 questions are presented is random. The entire process of EEG data recording was continuously monitored by the investigators to avoid long periods of slow wave sleep (SWS) during the experimental period.

Two days were selected for each of CLIS patients B, F, G, and W, in addition to the fact that the experimenter reserved rest periods between experiments on these two days and that the patients were more conscious on these two days than on the other days, as the analysis results responded accordingly to whether the experiment was performed or not.

### **5.3 EEG recordings of LIS patients**

In this dataset there are EEG recordings from four LIS patients P11, P13, P15 and P16 at a sampling rate of 500 Hz with a 16 channel EEG amplifier (V-Amp DC, Brain Products, Germany). We kept the denomination as in (Tonin et al. 2020; Jaramillo-Gonzalez et al. 2021). Most file formats of P11 and P13 are .vhdr/.vmrk files, but almost all file formats of P15 and P16 are .ahdr/.amrk encrypted files locked by encryption keys.

The experimenter later converted all files in .ahdr/.amrk format to .vhdr/.vmrk format and provided them in the supplementary material of the published article (Jaramillo-Gonzalez et al. 2021). Unfortunately, rest periods were not reserved in most experimental sessions for P15 and P16, and on the few days when rest periods were reserved, patients did not complete the correct copy spelling as requested by the experimenter, so it was not possible to compare the differences between experimental and rest periods.

Considering we are interesting on the days with spelling session records, so in this dataset the focus is on description of P11 and P13. Figure 5.3 shows the channel positions where EEG signals were acquired according to the international 10-20 standard electrode system (Oostenveld and Praamstra 2001; Jurcak et al. 2007) and the four electrodes which were used to acquire vertical and horizontal EOGs. Table 5.2 shows the electrodes used to record the EEG signals for different LIS patients on different days. The C1, Cz and C2 channels of patient 13 did not work properly on day one, so these data will not be included in the analysis.

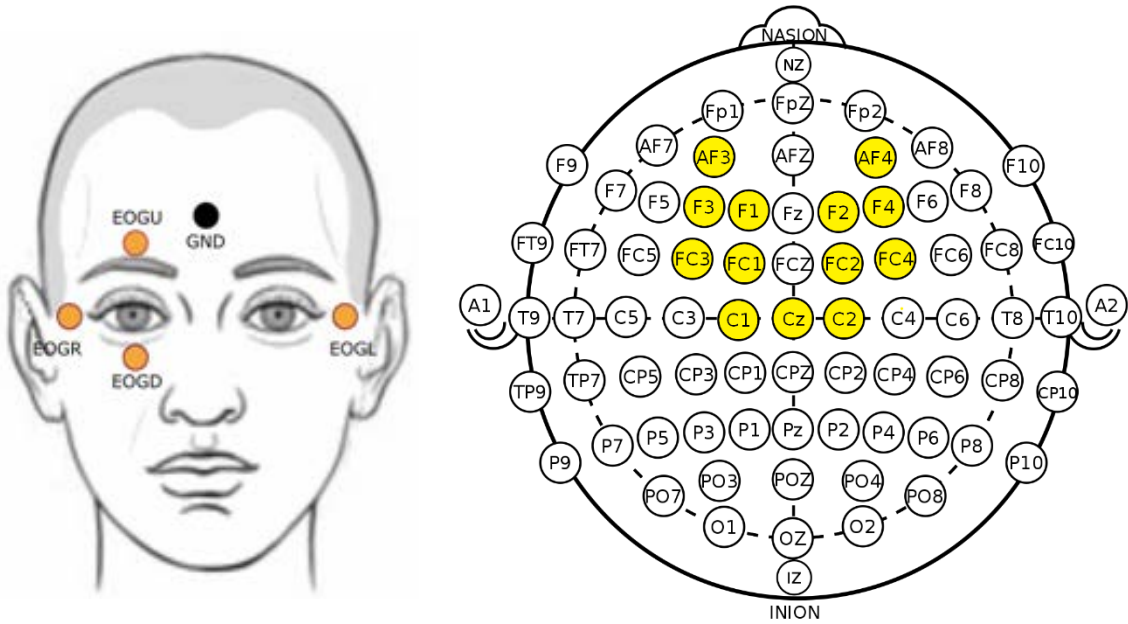


**Figure 5.3:** Channel positions of LIS patients. Left: the channel positions of electrooculographic (EOG), courtesy of the Institute for Medical Psychology and Behavioural Neurobiology, University of Tübingen. Right: the channel positions of electroencephalography (EEG).

**Table 5.2:** Electrodes recording the EEG signals of the two LIS patients on different days.

Codename	Day	EEG channels
Patient 11	Day1	F2, F4, FC2, FC4, C2, Cz, C1, FC1, FC3, F1, F3
	Day2	F4, FC2, FC4, C2, Cz, C1, FC1, FC3, F3
Patient 13	Day1	AF3, F3, AF4, F4
	Day2	AF3, F3, C1, Cz, C2, AF4, F4

In the paper (Tonin et al. 2020), the authors have used the EOG signal amplitude to determine whether the patient answered "yes" or "no". Based on this, in this dataset, we focused on the analysis of the EEG signal, the source of the brain waves, as a cross-validation of the EOG results.

P11 and P13 are native German speakers. Patient 11 is a 33-year-old locked-in state patient who was diagnosed with ALS in August 2015. He was able to communicate with Augmentative and Alternative Communication (AAC) until August 2017. Patient 13 is a 58 year old LIS patient. He was diagnosed with ALS in January 2011, AAC was possible until January 2018. Both were at the verge of CLIS with ALS Functional Rating Scale-Revised (ALSFSR-R) (Cedarbaum et al. 1999) score of 0. They were no longer able to use a

commercial eye-tracking device, but they could still communicate by selecting groups of letters to organize sentences through eye movements.

The auditory experiment procedure in one day included four different sessions of training, feedback, copy spelling and free spelling, which check step by step whether the patients were willing to communicate, and the free spelling session was implemented only when the cross-validation accuracy of each session of training, feedback and copy spelling exceeds 75%.

In preparation for the study, the patient's family or caregiver formulated and recorded more than 100 questions with known "yes" and "no" answers in their own voice, and this salient stimulus in the familiar voice of a relative could enhance patient responses and increased the probability that investigators would observe meaningful behaviors in these patients (Del Giudice et al. 2016).

Patients were asked to answer 10 questions with known answers of "yes" and 10 questions with known answers of "no" at each training and feedback session. The order of presentation of these 20 questions was randomized. Instead of containing pre-recorded personal questions, in the copy and free spelling sessions, patients are asked to select a group of letters or a specific letter to further spell a complete word or an entire sentence based on the answers to a series of yes/no questions. Whereas the difference between the two sessions is that the patient is asked to spell a predetermined phrase in the copy session, in the free spelling session, the patient can spell any sentence he/she wants. The details of the auditory experimental procedure are described in (Tonin et al. 2020; Jaramillo-Gonzalez et al. 2021). Three supplementary videos also provided in (Tonin et al. 2020) show the process of spelling a sentence for three patients.

Despite the fact that spelling communication is very slow for healthy people, the average spelling speed mentioned in the article was  $0.57 \pm 0.29$  (char/min) for P11 and  $0.48 \pm 0.24$  (char/min) for P13, indicating that it is a long spelling process for LIS patients to express a sentence, but when patients were asked "Would you like to continue?" the patients spelled out sentences such as "I am happy to see my grandchildren grow up," "I am looking forward to the holidays," and "I am happy" to show their willingness to communicate. From these formed sentences we can see that the patient did not show frustration because of this slow speed, from which we speculate that perhaps being able to communicate with someone is more exciting than the isolated experience of lying alone in an immobile body?

### 5.4 EEG recordings of DOC patients

To ensure a broader application of the methods, this thesis includes a dataset from Salzburg, Austria and Liege, Belgium (Wielek et al. 2018), which contains EEG signals from patients with disorders of consciousness (DOC) and diagnosed patients by behavioral assessments of auditory, visual, motor, verbal, communication and arousal functions according to the Coma Recovery Scale Revised (CRS-R) (Giacino et al. 2002; Giacino et al. 2004). The main application of this dataset is sleep analysis, but there are also some event notes that can be used as evidence of the patient's response to environmental stimuli. This dataset included seven MCS patients and eleven UWS patients. We selected cases with long-period events, such as nursing actions (e.g., repositioning, cleaning, feeding) and Coma Recovery Scale-Revised (CRS-R) score tests, to ensure that the events in the environment had some degree of influence on the patient's consciousness, and excluded cases with only multiple single-point-in-time events, such as check electrodes. Therefore, this thesis mainly presented the results of two MCS and four UWS patients.

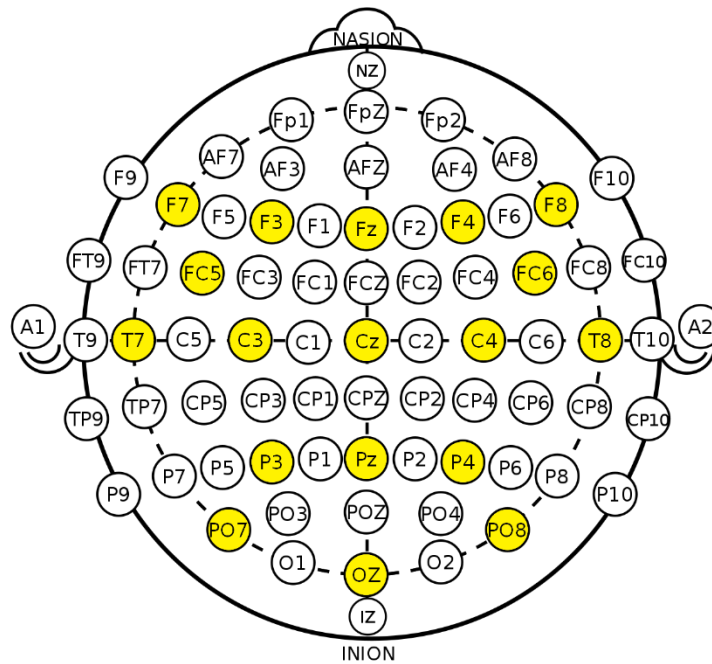


**Figure 5.4:** The channel positions of electroencephalography (EEG) for DOC patients.

In this dataset there are Polysomnographic (PSG) recordings from DOC patients at a sampling rate of 500 Hz with Brain Products amplifiers (Brain Products, Gilching, Germany). EEG signals were recorded from 18 electrodes at locations F3, F4, FC5, FC6, C3, C4, P3, P4, T3, T4, F7, F8, PO7, PO8, Fz, Cz, Pz, Oz, based on the international 10-20 electrode

system. Note that the new electrode naming system Modified Combinatorial Nomenclature (MCN) system renames the four electrodes of the 10-20 system. T3 is now T7 and T4 is now T8 (Sharbrough et al. 1991; Acharya et al. 2016). Besides EEG, electrooculography (EOG), electromyogram (EMG), electrocardiogram (ECG), and respiratory signals were also recorded for all DOC patients. Figure 5.4 shows the channel positions where EEG signals are located based on international 10-20 electrode system. Table 5.3 shows the Demographic information of all DOC patients.

**Table 5.3:** Demographic information of all DOC patients. The analyzed patient sample consisted of two MCS and four UWS patients. Abbreviations: Etiology: CVA-Cerebrovascular Accident; Diagnosis: UWS = Unresponsive Wakefulness Syndrome, MCS = Minimally Conscious State; CRC-R = Coma Recovery Scale-Revised.

Patient ID	Gender	Age	Diagnosis	CRS-R Total score	Period since injury (months)	Etiology
MCS1	male	57	MCS	12	135	Anoxia
MCS2	male	73	MCS	17	8	CVA
UWS1	female	65	UWS	4	4	Anoxia
UWS2	female	58	UWS	4	28	CVA
UWS3	male	61	UWS	4	32	Anoxia
UWS4	female	50	UWS	4	45	CVA

## 5.5 Discussion of datasets

In order to expand the field of application of the methods and also to verify the effectiveness of each method, these methods were applied in four different datasets. These four datasets include not only different types of brain waves, intracranial ECoG signals and non-invasive EEG signals, but also patients with different diseases of CLIS, LIS, MCS and UWS.

Although the invasive ECoG signal has several advantages over noninvasive EEG signal, such as greater Signal-to-noise ratio (SNR), higher signal amplitude, higher spatial resolution, broader frequency bandwidth, and less vulnerability to artifacts such as EMG (Leuthardt et al. 2009; Bensch et al. 2014; Martens et al. 2014), there are surgical risks, i.e. relative fewer cases than EEG signals. Because of the convenience of EEG signals, EEG signals are widely used in brainwave research.

Both patients in the CLIS and LIS datasets suffered from ALS and it was more feasible to investigate the function of the various topographies (Brodmann area), whereas patients in the MCS and UWS datasets had etiologies due to anoxia, traumatic brain injury (TBI),

cerebrovascular accident (CVA), and not ALS. Without the aid of fMRI, there is concern that the neural distribution of the brain in patients with causes such as stroke and cerebral ischemia does not follow the traditional Brodmann area (Azari and Seitz 2000). Therefore, we will focus on consistent results across multiple channels in the DOC patient dataset to avoid compensatory effects of brain injury.

All of the databases, based on the provider's investigations, show evidence of the existence of certain consciousness activities in patients, based on this as a cross-validation of the results of the method applied in this thesis.

# Chapter 6

## Results

*“Anyone who has never made a mistake has never tried anything new.”*

*– Albert Einstein (1879-1955)*

In this chapter, the results of feature extraction and machine learning are presented separately, based on the data processing flowchart of Modus Operandi introduced in Chapter 4. In the feature extraction part, multiscale-based methods (multiscale sample entropy, multiscale permutation entropy and multiscale Poincaré plots) were first applied to analyze ECoG signals from a completely locked-in state (CLIS) patient, then the application of sample entropy and Poincaré plot were extended to the EEG signal.

The permutation entropy was not used here because the method transfers the time series to the  $m!$  patterns, and even with higher  $m$  parameters, the method still ignores too much detail of the time series, but relatively, permutation entropy is an appropriate method to reflect circadian rhythms in healthy subjects and minimally conscious state (MCS) patients as reported by Wislowska et al. (Wislowska et al. 2017).

All four datasets only the ECoG recordings of the CLIS patient and the disorders of consciousness (DOC) dataset contain night periods. Section 6.1.3 presents the permutation entropy results of the ECoG recordings, while the DOC dataset, as already analyzed by Wislowska et al. using this method (Wislowska et al. 2017), the analysis is not repeated here.

To confirm the usability of the sample entropy, the method was applied to CLIS, LIS and DOC datasets to detect potential stages of consciousness. Since the results of sample entropy and Poincaré plot in sections 6.1.6-6.1.7 are similar, but Poincaré plot directly uses the voltage amplitude of the time series and is more sensitive due to the need to remove some



peaks to see the consciousness results, future extensions to LIS, MCS and unresponsive wakefulness syndrome (UWS) patients will be based on the results of sample entropy in this work.

Finally, the clinical scales of consciousness introduced in section 2.1 shows that LIS patients have the closest level of consciousness to healthy individuals, and with residual eye movements as the "ground truth" of consciousness, LIS patients thus have the highest probability of being conscious among all patients. Therefore, in the machine learning part, the k-means and density-based spatial clustering of applications with noise (DBSCAN) methods were applied to cluster the sample entropy results of LIS patients in order to cluster the difference between the patient's consciousness during the rest and experimental periods as a manifestation of the patient's response to external stimuli.

## **6.1 Feature Extraction part**

In sections 6.1.1-6.1.4, the ECoG signal of the CLIS patient GR was analyzed using multiscale-based methods for the dataset in section 5.1. In section 6.1.6-6.1.7, the EEG signals of four CLIS patients B, F, G, and W were analyzed using the sample entropy and Poincaré plot methods for the data set in section 5.2. In section 6.1.8, the data set from section 5.3 was added to perform sample entropy analysis of the EEG signals from LIS patients 11 and 13. Finally, the DOC dataset from section 5.4 was extended in section 6.1.9 to perform sample entropy analysis of the EEG signals from 2 MCS patients and 4 UWS patients.

### **6.1.1 Multiscale Approach result**

For the ECoG signal of a CLIS patient GR dataset from section 5.1, Figure 6.1 is the result of sample entropy without the multiscale approach, which is very noisy. As proposed in section 6.1.2, Figure 6.2 shows the results with the multiscale approach for 24 h. In order to obtain the main trend and reduce the effect of white noise, we utilized the multiscale approach after sample entropy, permutation entropy and Poincaré plot to extract a cleaner result from all approaches.

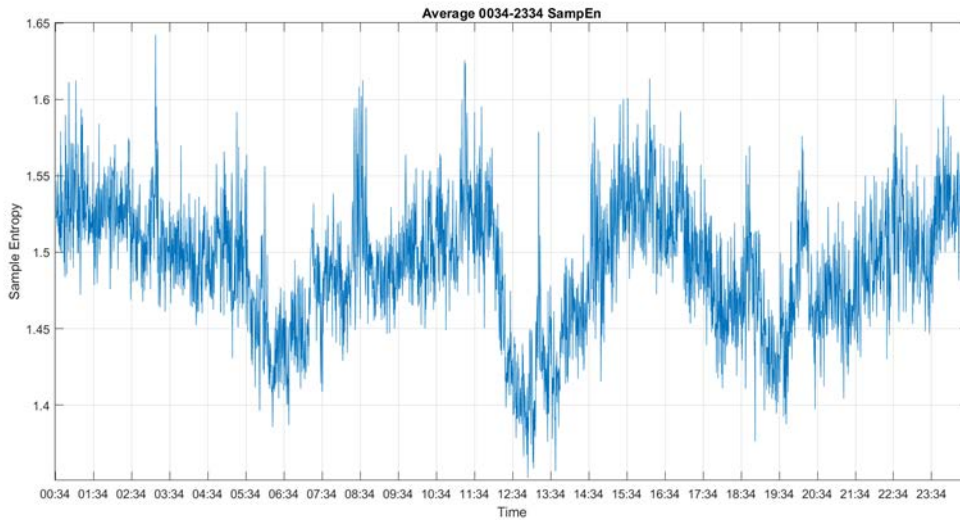


**Figure 6.1:** The result of Sample Entropy for 24 h.

### 6.1.2 Multiscale Sample Entropy result

As proposed in section 2.3 and 2.6 (Barnett et al. 2009; Adama et al. 2019; Wu and Bogdan 2020), the results of the sample entropy were utilized to analyze consciousness. A higher value of multiscale sample entropy (MSE) indicated increased complexity within the ECoG signals, which was more indicative of periods of consciousness. The average MSE from all 59 usable channels over the 24 h recording period is shown in Figure 6.2. There are 5 channels that are considered to be operating incorrectly due to too high voltage amplitude. As we know from the experiment performed the day of recording, the patient answered the questions correctly during the auditory experiment, which took place from 14:50 to 17:00. The average value of MSE during the experiment was 1.5242. Using this information as the ground truth, and thus setting the consciousness threshold value at 1.52, above which a period of consciousness was presumed, shown in red blocks. The periods between 15:18–15:56, 16:04–16:22 and 16:52–17:02 could be labelled as periods of consciousness. Under this premise, we could label the periods between 08:28–08:36, 11:12–11:42, 11:50–12:02, 23:40–01:34, 01:46–02:32 and 03:06–03:16 as periods of consciousness as well, shown in red blocks.

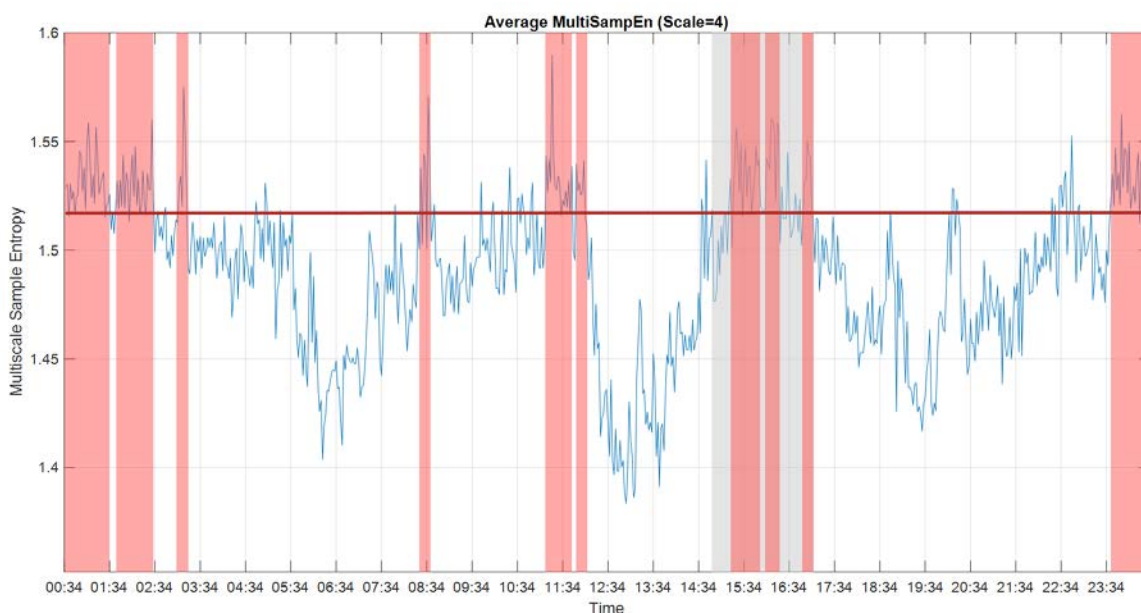


**Figure 6.2:** The results of multiscale sample entropy (MSE) (scale = 4) for 24 h. The period of the experiment is indicated by the grey block. The threshold value is indicated by a red horizontal line. The periods of presumed consciousness are indicated by the high values of MSE, shown in red blocks. To avoid the plot being too crowded, we marked the predicted conscious periods, which are predicted conscious periods of more than 6 min for every 10 min overlapping time window.

### 6.1.3 Multiscale Permutation Entropy result

In order to reduce the computation time, we also applied multiscale permutation entropy (MPE) in this approach to investigate this option and analyze the consciousness state in the time domain. Smaller MPE values imply increased pattern similarity in the time series and, hence, less complex brain activity. Figure 6.3 shows the average MPE from all 59 usable channels over 24 h. The average value of MSE during the experiment was 2.388. Using this MPE value as a consciousness threshold, we could identify the periods between 15:46–16:10 and 16:26–16:50, but also between 09:06–09:42, 09:58–10:10, 10:46–11:02 and 12:26–12:58, as periods of consciousness.

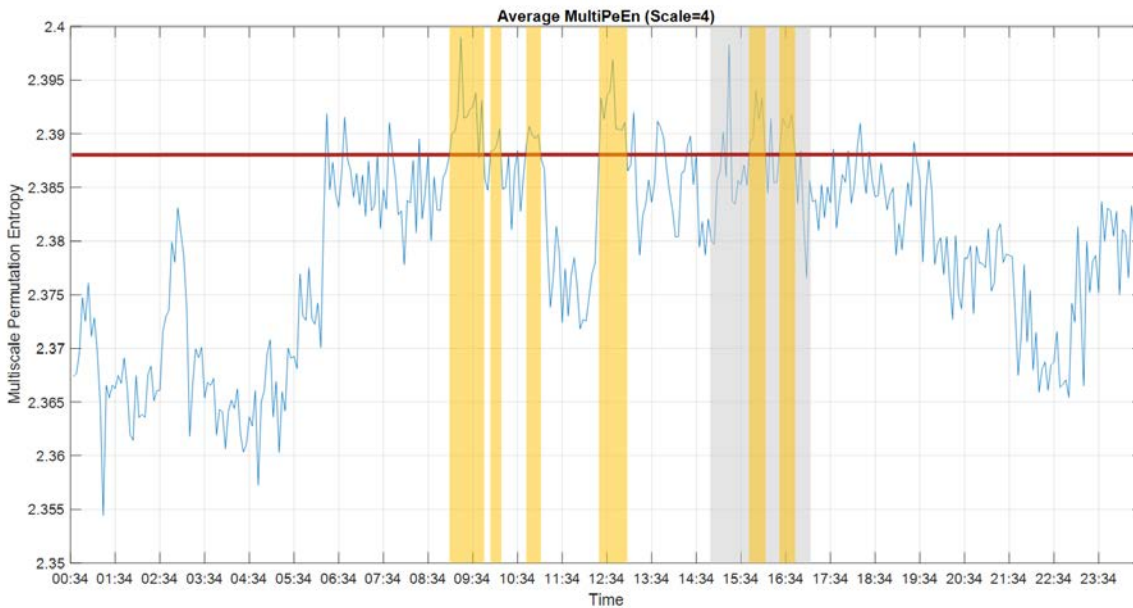


**Figure 6.3:** The results of multiscale permutation entropy (MPE) (scale = 4) for 24 h. The period of the experiment is indicated by the grey block. The threshold value is shown by a red horizontal line. The periods of consciousness as presumed by the high values of MPE are indicated in the yellow blocks. To avoid the plot being too crowded, we marked the predicted conscious periods, which are predicted conscious periods of more than 8 min in every 12 min overlapping time window.

#### 6.1.4 Multiscale Poincaré plot result

Golińska (Golińska 2013) reported that the Poincaré plot showed a fluffy (Hayashi et al. 2014) pattern during light anesthesia and an elongated pattern during deep anesthesia. We used this interpretation in our application, i.e. if the CLIS patient was conscious and participated in the experiment, a fluffy pattern was displayed in the results of the Poincaré plot, as shown in Figure 6.4 (left). In contrast, if the CLIS patient was unconscious and only the ECoG signals were recorded through the BCI interface without the researcher stimulating the patient, the results of the Poincaré plot displayed an ellipse pattern, as shown in Figure 6.4 (right). To distinguish the difference, SD1 represents the instantaneous variability, and SD2 shows the ECoG voltage variability of the 30 s recording time window. We show the 24 h results of SD1 and SD2 in Figure 6.5 and Figure 6.6.

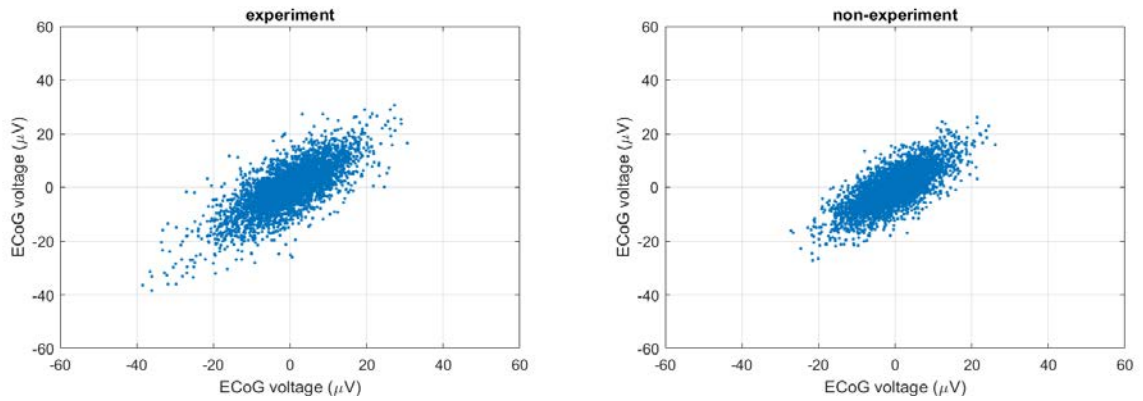


**Figure 6.4:** The Poincaré plot. Left: 30 seconds during experiment. Right: other 30 seconds during non-experiment.

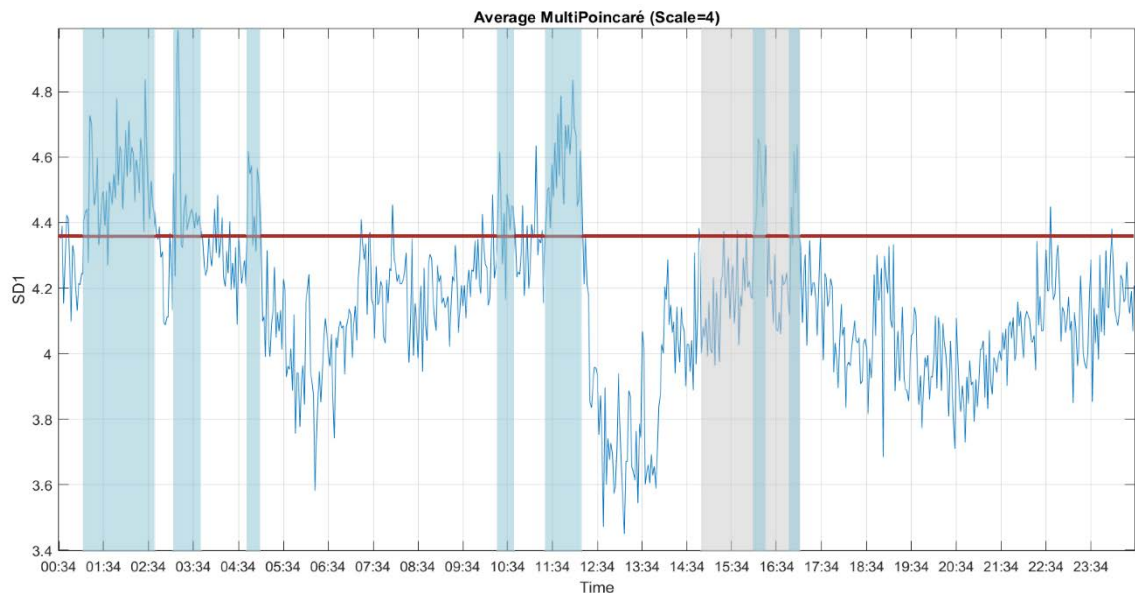


**Figure 6.5:** The SD1 of the multiscale Poincaré (MSP) plots (scale = 4) for 24 h. The period of the experiment is indicated by the grey block. The threshold value is indicated by a red horizontal line. The presumed periods of consciousness, as indicated by high values of SD1, are shown in blue blocks. To avoid the plot being too crowded, we marked the predicted conscious periods which were more than 6 min for every 10 min overlapping time window.

To reduce white noise in the result of the Poincaré plot, we utilized the multiscale approach, which is an approach also described by Henriques for heart rate variability (Henriques et al. 2015). The SD1 and SD2 of the MSP plots for 24 h are shown in Figure 6.5 and Figure 6.6. The result of SD1 was the average of all 59 usable channels. For SD2, there were seven channels where the whole trend was not visible due to the presence of some peaks, so only the average of 52 usable channels was used for SD2. The trend of SD1 and SD2 was similar to MSE. The distributions of MSP plots during the experiment had the high-peaked and heavy-tailed characteristics, which are different from the flat-topped characteristic of MSE and MPE. The kurtosis of MSE distribution was leptokurtic, and the

MSE and MPE distributions were platykurtic. Considering the preparation during the experiment, we raised the threshold to the average of the upper half of the sorted data during the experiment. With a threshold value of SD1 at 4.36, the ground truth periods at 16:04–16:22 and 16:56–17:04 exceeded the threshold. Using this consciousness level threshold, the periods between 10:22–10:44, 11:24–12:14, 01:08–02:46, 03:10–03:44 and 04:46–05:04 could be labelled as periods of consciousness. Both SD1 and SD2 showed similar trends, but the results of SD2 have more peaks and it is not easy to observe the whole trend, so we will use the results of SD1 to compare with other methods.

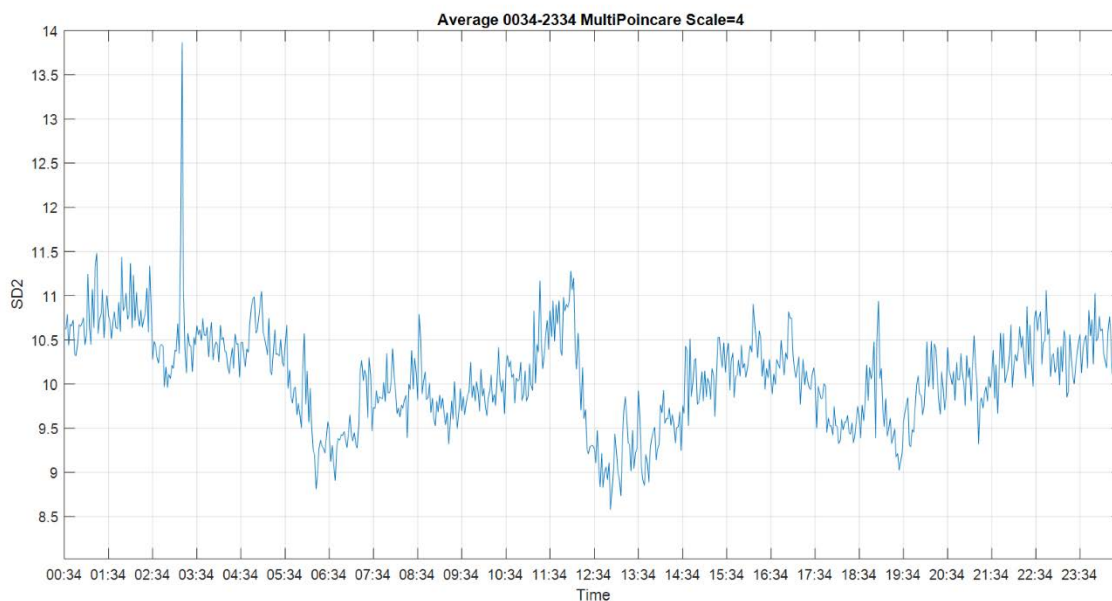


**Figure 6.6:** The SD2 of multiscale Poincaré (MSP) plots (Scale=4) for 24 h.

### 6.1.5 Discussion of ECoG signal results

The results of the three different approaches of MSE, MPE, and MSP plot applied to the ECoG signals suggest that this CLIS patient was conscious between approximately 16:04–16:10. This time window corresponds to the period during the experiment in which the CLIS patient correctly answers the pairwise yes or no questions via a BCI (Ramos-Murguialday et al. 2011; Adama et al. 2019).

The results of the MSE and MSP plots indicate that this patient was probably awake during the night, supporting the result of (Soekadar et al. 2013), which reported that sleep fragmentation of slow wave sleep (SWS) increases during the process of ALS patients slipping into CLIS.

The trend of the results was similar for the MSE and MSP plots, but different from MPE. Permutation entropy represents the time series in  $m!$  possible ordinal patterns, attenuating the information from voltage variation and thus reducing the sensitivity of the result. In (Wisłowska et al. 2017), it was reported that the permutation entropy results showed that the complexity of EEG signals decreased in both healthy subjects and MCS patients from day to night, reflecting the circadian rhythm of arousal. Therefore, it is possible that the CLIS patient dreams during the night. The voltage amplitude variations are large, but the ordinal patterns are similar because there are fewer environmental stimuli to induce brain activity when the patient sleeps at night. It should also be noted that during dreaming, one can state there is consciousness (Cologan et al. 2013; Zeman and Coebergh 2013).

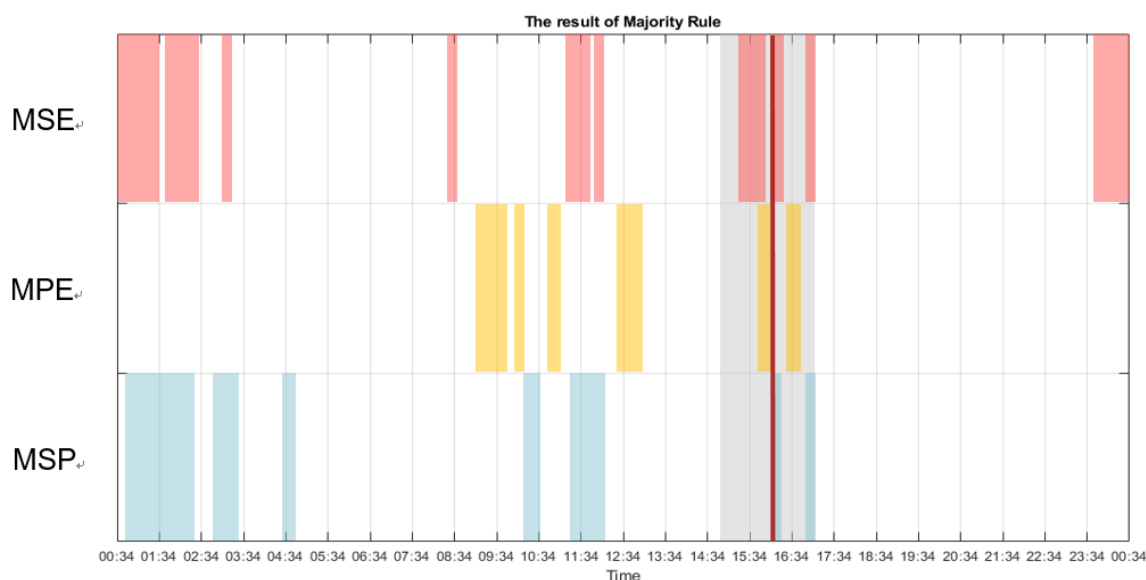


**Figure 6.7:** The result of the majority decision of three methods is indicated by the dark red block. The period of the experiment is shown in the grey block. The state of consciousness over 24 h identified by the different methods is enclosed by magenta (MSE), yellow (multiscale permutation entropy (MPE)), and blue (multiscale Poincaré (MSP)) blocks.

Figure 6.7 shows the result of the majority decision of the three methods over a period of 24 h. From 16:04 to 16:10, the MSE, MPE, and MSP plots show that this CLIS patient was in a conscious state. Even though all methods indicated more or less precisely the reported time of consciousness of the patient by the experimenter that day, the exact times differed from one method to another. In addition, other time periods of detected consciousness were not consistent over all methods. Thus, the level of sensitivity of the applied methods can be interpreted as being different and thus more or less responsive to the

change of consciousness. This indicates that a single method may not be an appropriate approach to identify exactly the levels of consciousness in CLIS patients. Currently the definition of the threshold is based only on the value of each method in the time window of the experiment that the patient communicated with the investigators. In the future, when there are more cases of this type of disease with a proofed moment of consciousness, we hopefully can define the threshold for consciousness and unconsciousness in CLIS patients in a more general way.

Because the experimental period was 14:50–17:00 and there was an 88% accuracy response rate, we used the 15:00–17:00 experimental period to compare the distribution of values with all other 2 h non-experimental slots, these research results are published in (Wu et al. 2020). We used the Z-test, and since the value ranges of the individual methods were different, we normalized the value of the individual methods to (0,1). The result for MSE is shown in Figure 6.8(a). The Z-test revealed that the multiscale sample entropy (MSE) value was significantly different in all non-experimental periods compared with the experimental period, except for the nighttime period, and the higher MSE values could probably be attributed to the rapid eye movement (REM) during dream sleep, which indicates consciousness (Cologan et al. 2013; Zeman and Coebergh 2013).

Figure 6.8(b) shows the statistical results for multiscale permutation entropy (MPE), illustrating that there is no significant difference in the 09:00–11:00 time period. Since the multiscale Poincaré (MSP) plots also showed the same results, and the majority decision of all three methods (Figure 6.7) had higher values, the patient may have been conscious in the morning.

Although the statistical results of the multiscale Poincaré (MSP) plots in Figure 6.8(c) showed higher values at night, the Z-test showed significant differences at these time periods compared with the experimental period. As proposed in section 2.3-2.5, the Poincaré plot equations were calculated by the voltage amplitude, but the sample entropy equations have a tolerant coefficient, and the permutation entropy method transfers the time series to the  $m!$  patterns. Therefore, the Poincaré plot equations were not tolerant compared with the sample entropy and permutation entropy methods, so the rapid eye movement (REM) during the sleep phase may have led to higher values of the multiscale Poincaré (MSP) plots, as shown by the values. Please note that during the probable REM phase, the values were significantly higher than during the experimental phase, which is in accordance to the relation between consciousness and dreaming. Therefore, combining the results from a number of methods, as we have done in this work, leads to a higher likelihood of correctness.



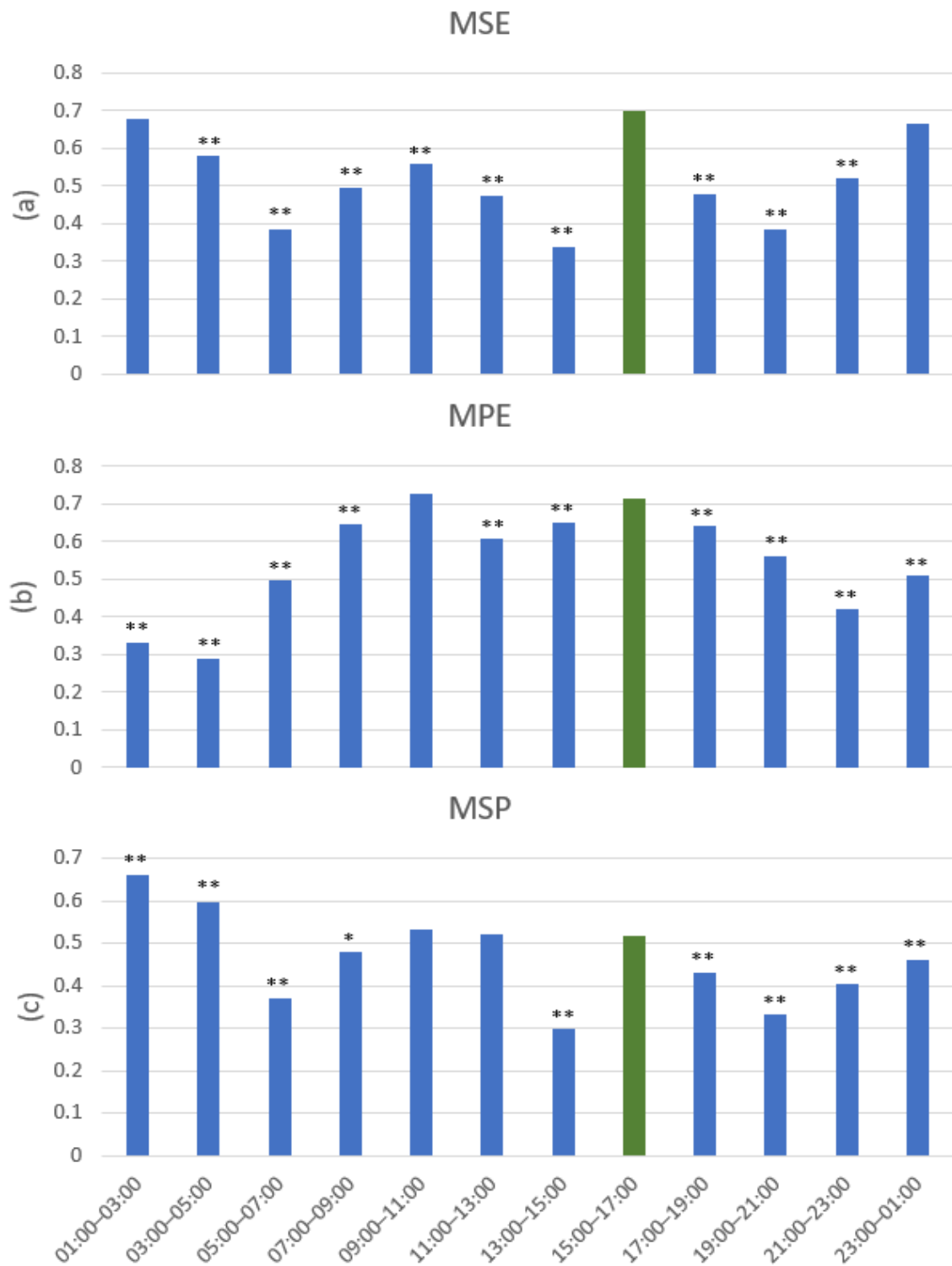


**Figure 6.8:** The statistical results (Z-test) for (a) MSE, (b) MPE, and (c) MSP over 24 h. The period of the experiment is shown in green. Significant differences are identified by \*  $p < 0.05$  and \*\*  $p < 0.01$  in respect to the values from the proven communication time.

### 6.1.6 Poincaré plot results from CLIS patients

For the CLIS dataset from section 5.2, the top diagram of Figure 6.9-Figure 6.12 shows the result of the Poincaré plot: We assume that the higher the value, the higher the relative consciousness of the patient. The figure below shows the trigger marks, those with numbers represent experimental state and those without numbers represent resting state. Between two red vertical lines indicate sessions, each session lasts around 10 minutes. To more clearly distinguish the difference between experimental and rest time, in these datasets all sessions in a day are combined in chronological order in the same figure.

As proposed in section 2.5, we have applied Poincaré plot to the dataset as shown in Figure 2.5. We interpret therefore a higher value of Poincaré plot as higher brain activity and thus hypothetically more consciousness. This interpretation is based on the results shown in (Chaudhary et al. 2017) where during the corresponding time slots (see Figure 6.9-Figure 6.16 trigger marks), the experimenter received a good number of correct answers, thus indicating the consciousness of the patient.

Figure 6.9-Figure 6.12 are showing the results for CLIS patients B & F over two days for each patient. These data were selected, in addition to the fact that the experimenter reserved rest periods between experiments on these two days and that the patients were more conscious on these two days than on the other days, as the analysis results responded accordingly to whether the experiment was performed or not.

#### CLIS patient B on day 1

In Figure 6.9, we combined seven consecutive sessions over 69 min for patient B during day one. The Figure 6.9 below shows the time window between 10 and 60 min in which the investigators asked the questions. The time windows from 0 to 10 min and 60–69 min are the rest states. The top diagram shows the result of the Poincaré plot: We assume that the higher the value, the higher the relative consciousness of the patient. After 9th min, the value rises obviously, clearly showing the difference between resting and experimental state as at that point the questions were started. The Poincaré plot value was higher at the beginning, probably due to lunch, and the first session was recorded from 12:22 to 12:32. This Poincaré plot result shows a high similarity to the sample entropy result in Figure B.1.

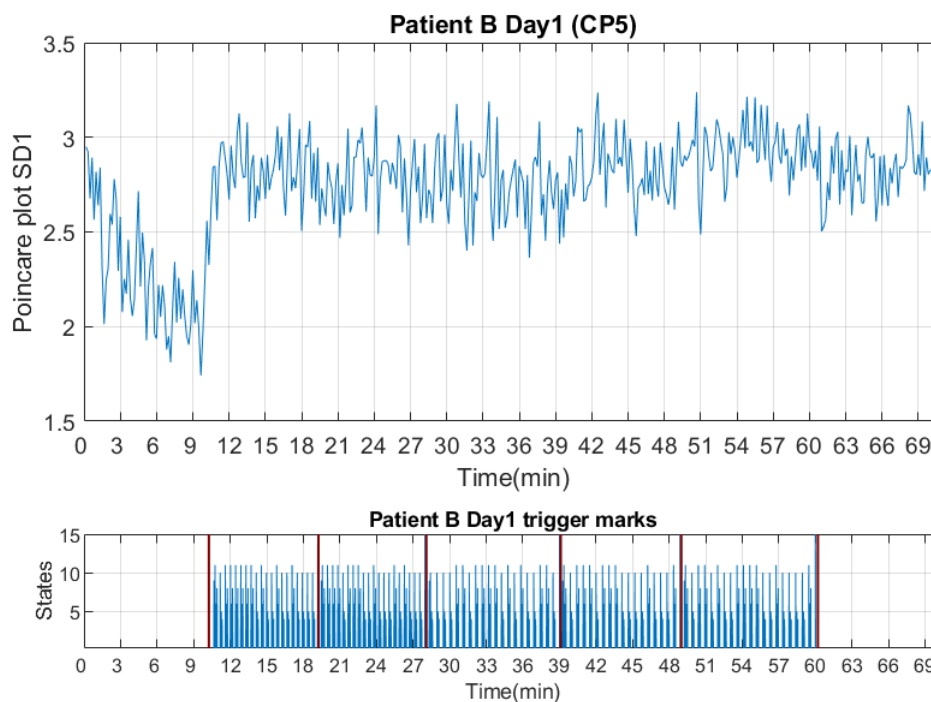


**Figure 6.9:** The SD1 result of Poincaré plot for CLIS patient B on day 1. Top: the channel CP5 result of the Poincaré plot. Bottom: The trigger marks for patient B on day 1. The sessions are indicated between two red vertical lines. The periods with numbers are experimental state, and those without numbers are rest state.

## CLIS patient B on day 2

In Figure 6.10, we combined seven consecutive sessions for patient B during day two all in all over 64 min. The Figure 6.10 below shows the time window between 10 and 59 min in which the investigator asked the questions. The periods from 0 to 10 min and 59–64 min are the rest states. After 10<sup>th</sup> min, the value of Poincaré plot rises obviously as well, what we would interpret again as a higher level of consciousness. There is a slow decline after the 59<sup>th</sup> min. The results of patient B in these two days are consistent with the time window of trigger marks. The results for patient B in all other channels (FC5, FC1, FC6, CP5, CP1, CP6, AF3, AF4) have a similar trend. This Poincaré plot result shows a high similarity to the sample entropy result in Figure B.2.

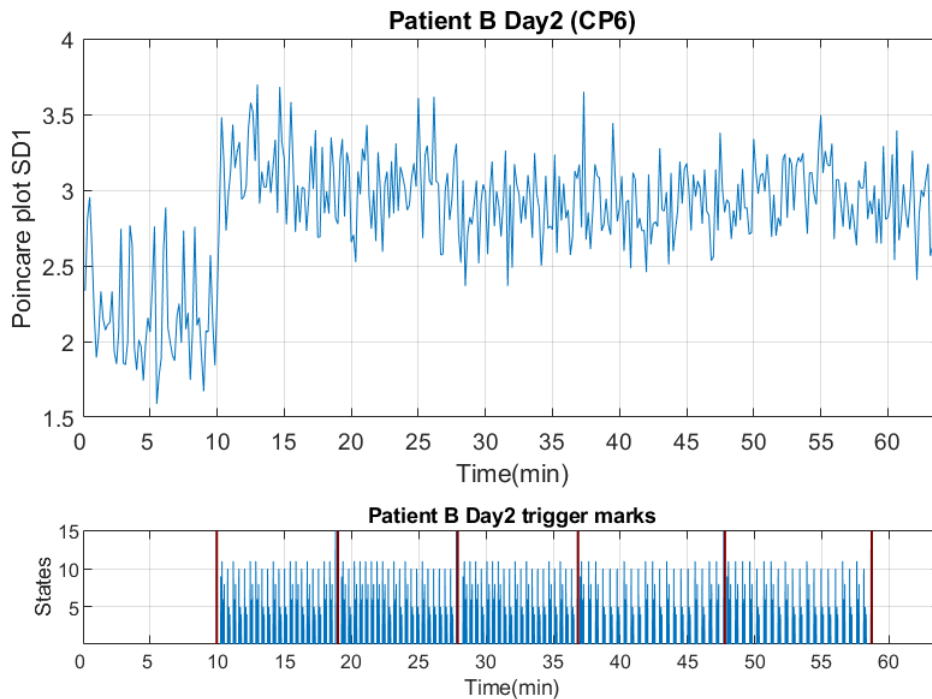


**Figure 6.10:** The SD1 result of Poincaré plot for CLIS patient B on day 2. Top: the channel CP6 result of the Poincaré plot. Bottom: The trigger marks for patient B on day 2. The sessions are indicated between two red vertical lines. The periods with numbers are experimental state, and those without numbers are rest state.

### CLIS patient F on day 1

In Figure 6.11, a combination of six consecutive sessions during day one over 90 min is shown for patient F, who performed less good as patient B in general. The Figure 6.11 below shows the time windows between 0 and 39 min and 68–90 min in which the investigator asked the questions. The period of 39–68 min is a rest state. After the 38<sup>th</sup> min, the value of Poincaré plot rises slowly. After the 74<sup>th</sup> min, the value declines slowly. It presents the opposite result to patient B, but compared to the sample entropy results in Figure B.3, although there are some peaks in the Poincaré plot results. These two different methods still present consistent results. The trend of symmetrically positioned electrodes (CP5 vs. CP6, FC5 vs. FC6) is similar, whereas not symmetrical positioned electrodes differ. So, depending on the area over which the electrode is placed (e.g., over the Broca area or the Wernicke area), the task-related signal must be different and thus will indicate different corresponding aspects and show different trends on the related electrodes. We speculate that the level of consciousness depends on how difficult the questions were. Perhaps the questions asked by the investigators can promote the patients' thinking?

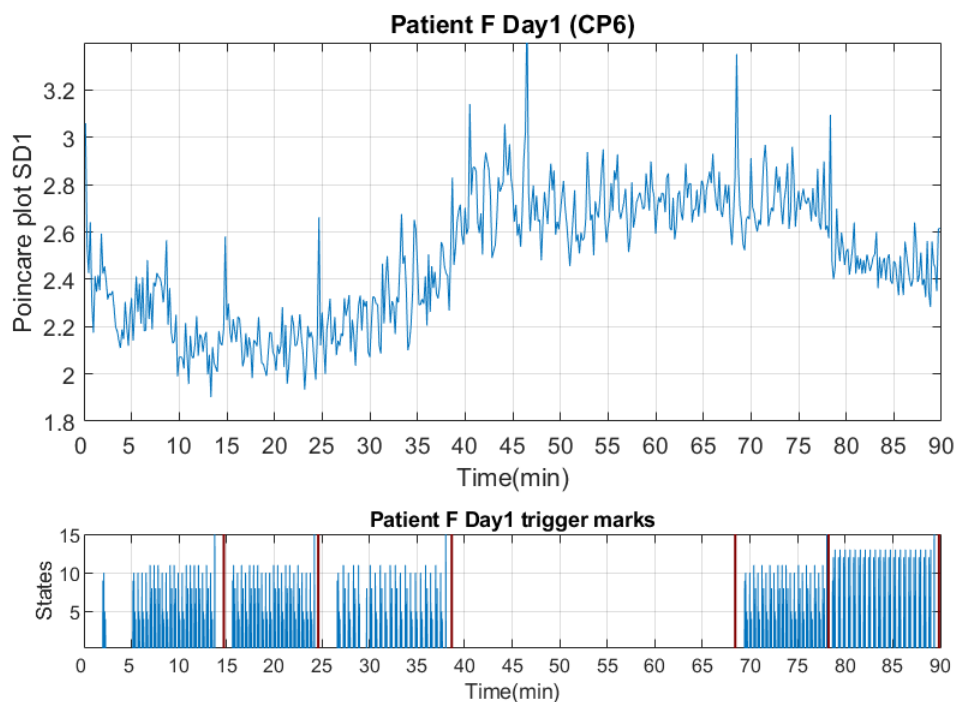


**Figure 6.11:** The SD1 result of Poincaré plot for CLIS patient F on day 1. Top: the channel CP6 result of the Poincaré plot. Bottom: The trigger marks for patient F on day 1. The sessions are indicated between two red vertical lines. The periods with numbers are experimental state, and those without numbers are rest state.

### CLIS patient F on day 2

In Figure 6.12, we show the consecutive combination of seven sessions during another day over all in all 70 min during day two. The Figure 6.12 below shows the time windows between 10 and 35 min and 37–60 min in which the investigator asked the questions. The time windows of 0–10 min and 60–70 min are the rest states. After the 36<sup>th</sup> min, the value of Poincaré plot rises slowly. The value declines slowly after the 48<sup>th</sup> minute. The correct response rate is around 70% by functional near-infrared spectroscopy (fNIRS) and support vector machine (SVM) to ensure that patients are awake (Chaudhary et al. 2017). There is a similar result between channel CP5 and the other channels (FC5, FC1, FC6) for patient F on day two, and compared to the sample entropy results in Figure B.4, these two different methods show consistent results. In the future, we will correlate the different types of questions and related feedback in order to refer to the value of Poincaré plot and to obtain further results.

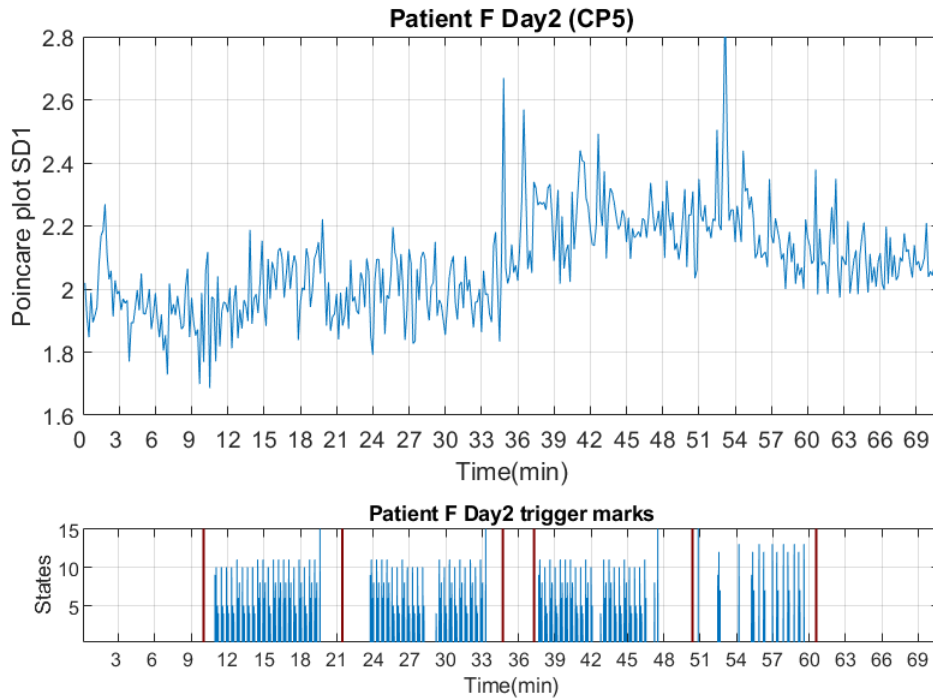


**Figure 6.12:** The SD1 result of Poincaré plot for CLIS patient F on day 2. Top: the channel CP5 result of the Poincaré plot. Bottom: The trigger marks for patient F on day 2. The sessions are indicated between two red vertical lines. The periods with numbers are experimental state, and those without numbers are rest state.

It is speculated that patient F allowed her mind to wander when she was not in the experimental time period, resulting in more brain activity during the rest time period than during the experimental time period. This patient showed the same phenomenon as the LIS patient during the spelling experiment, and the sample entropy results of the LIS patient during the spelling experiment are presented later in section 6.1.8.

### 6.1.7 Sample Entropy results from CLIS patients

Since the results of the Poincaré plot are similar to those of the sample entropy, the Poincaré plot results for the other CLIS patients G and W over two days are presented in section Appendix C. Correspondingly, the sample entropy results for the other CLIS patients B and F over two days are presented in section Appendix B.

For the CLIS dataset from section 5.2, the top diagram of Figure 6.13-Figure 6.16 shows the result of the sample entropy. The figure below shows the trigger marks, those with numbers represent experimental state and those without numbers represent rest state. Between two red vertical lines indicate sessions, each session lasts around 10 minutes. In order to distinguish more clearly the difference between experimental and rest time, in these datasets all sessions in a day are combined in chronological order in the same figure.

As proposed in section 2.3, we have applied sample entropy to the dataset as shown in Figure 2.3. We interpret therefore a higher value of sample entropy as higher brain activity and thus hypothetically more consciousness. This interpretation is based on the results shown in (Chaudhary et al. 2017) where during the corresponding time slots (see Figure 6.13 - Figure 6.16 trigger marks), the experimenter received a good number of correct answers, thus indicating the consciousness of the patient.

Figure 6.13-Figure 6.16 are showing the results for CLIS patients G & W over two days for each patient. These data were selected, in addition to the fact that the experimenter reserved rest periods between experiments on these two days and that the patients were more conscious on these two days than on the other days, as the analysis results responded accordingly to whether the experiment was performed or not.

### CLIS patient G on day1

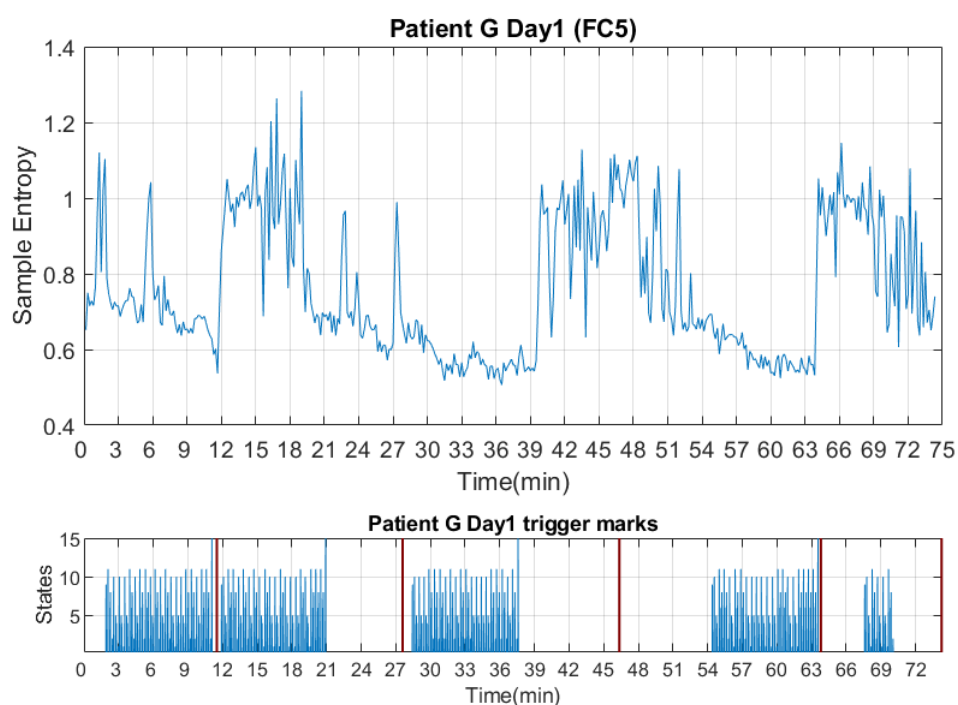


**Figure 6.13:** The sample entropy result for CLIS patient G on day 1. Top: the channel FC5 result of the sample entropy. Bottom: The trigger marks for patient G on day 1. The sessions are indicated between two red vertical lines. The periods with numbers are experimental state, and those without numbers are rest state.

For patient G, five consecutive sessions over 74 min were combined on the day one, as shown in Figure 6.13. In the second session, the value of sample entropy increased accordingly as the experimenter continued with the auditory experiment. However, in the

third, fourth, and fifth sessions, the value of sample entropy increased when the experimenter stopped the auditory experiment. Patient G was presumed to be more focused at the beginning of the experiment on this day, and gradually decreased as he became more skilled. Biederman et al. (Biederman and Vessel 2006) describe why people like new stimuli and that repeated stimuli weaken the brain's response. It may help us to explain this phenomenon. This sample entropy result shows a high similarity to the Poincaré plot result in Figure C.1.

Consequently, patient G was able to let her mind wander when she was not in the experimental time period, resulting in higher brain activity during the rest period after the second session. This patient showed the same phenomena as the LIS patients during the spelling experiment, the sample entropy results of LIS patients during the spelling experiment are presented later in section 6.1.8.

In this thesis, we focus on all cases in which significant index changes occurred at the beginning and at the end of the experiment, and overall, the patients responded accordingly to the external stimuli.

## CLIS patient G on day 2

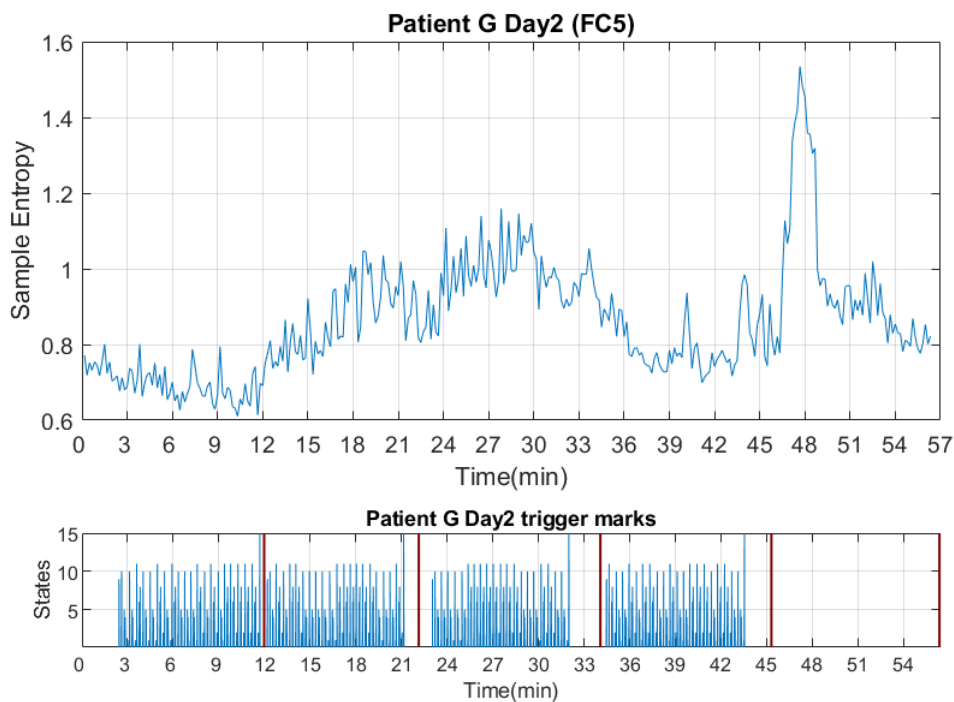


**Figure 6.14:** The sample entropy result for CLIS patient G on day 2. Top: the channel FC5 result of the sample entropy. Bottom: The trigger marks for patient G on day 2. The sessions are indicated between two red vertical lines. The periods with numbers are experimental state, and those without numbers are rest state.



For patient G, five consecutive sessions over 56 min were combined on the day two, as shown in Figure 6.14. Session 1-4 are the experimental periods where the sample entropy values undergo a slow increase and then decrease. In the rest period (fifth session), there was a peak at about 48<sup>th</sup> minute, and usually the investigators would keep quiet during the rest period. We asked the experimenters and they replied that there was no record of possible effects causing this peak. Of course, it is not excluded that this patient does some thinking in her own mind. The results for patient G in all other channels (FC4, FC5, FC3, FC6, Cz) have a similar trend. This sample entropy result shows a high similarity to the Poincaré plot result in Figure C.2.

### CLIS patient W on day 1

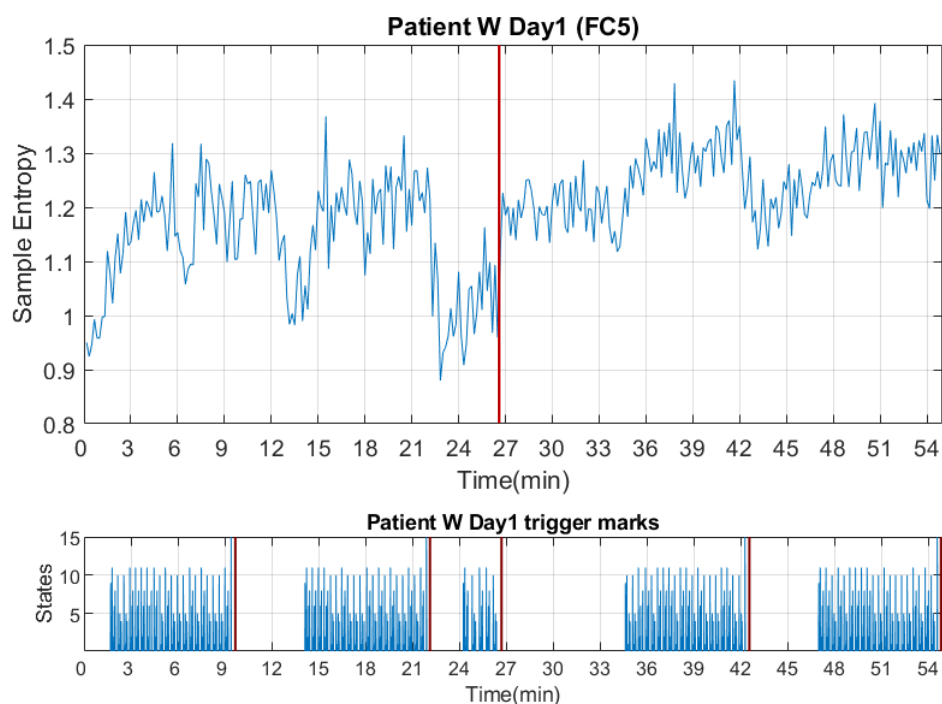


**Figure 6.15:** The sample entropy result for CLIS patient W on day 1. Top: the channel FC5 result of the sample entropy. Bottom: The trigger marks for patient W on day 1. The sessions are indicated between two red vertical lines. The periods with numbers are experimental state, and those without numbers are rest state.

Remark: the data before 27<sup>th</sup> minute was recorded in the morning and the other part in the afternoon.

Five consecutive sessions over 55 min were combined on the day one for patient W, as shown in Figure 6.15, who performed better as patient G in general. The Figure 6.15 below shows the time windows between 2-10, 14-22, 35-42, and 47-54 min in which the investigators asked the questions. The time windows from 0 to 2 min, 10-14 min, 27-35 min,

and 42-47 min are the rest states. Remark that in most cases the time difference between each session is short, but in this case the data before 27<sup>th</sup> minute was recorded in the morning and the other part in the afternoon. So the baseline is different, but we can still see the difference between experimental and resting period clearly.

The values increase significantly at the 2<sup>nd</sup>, 14<sup>th</sup>, 35<sup>th</sup>, and 47<sup>th</sup> minutes. Conversely, the values decreased significantly at the 12<sup>th</sup>, 22<sup>nd</sup>, and 42<sup>nd</sup> minutes, showing more clearly the difference between the resting state and the experimental state at the beginning and the end of the questions compared to the Poincaré plot results in Figure C.3. In the third session, although slight differences between the experimental and the resting period could still be seen, the number of questions in this session was not 20 as usual. Perhaps the experiment was stopped because of some necessary nursing actions. As described by (Jaramillo-Gonzalez et al. 2021), they put the patients' care and health in the first priority.

### CLIS patient W on day 2

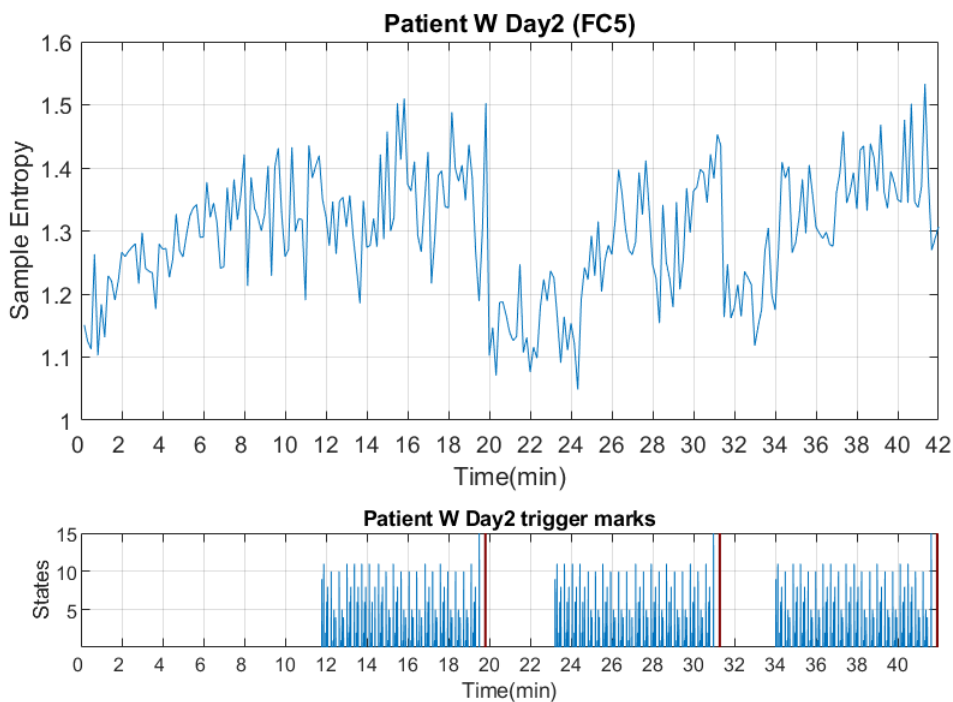


**Figure 6.16:** The sample entropy result for CLIS patient W on day 2. Top: the channel FC5 result of the sample entropy. Bottom: The trigger marks for patient W on day 2. The sessions are indicated between two red vertical lines. The periods with numbers are experimental state, and those without numbers are rest state.

Three consecutive sessions over 42 min were combined on the day two for patient W, as shown in Figure 6.16. The Figure 6.16 below shows the time windows between 12-20, 23-31, and 34-42 min in which the investigators asked the questions. The time windows

from 0 to 12 min, 20-23 min, and 31-34 min are the rest states. The values increase significantly at the 14<sup>th</sup>, 24<sup>th</sup>, and 34<sup>th</sup> minutes. Conversely, the values decreased significantly at the 20<sup>th</sup> and 31<sup>st</sup> minutes, which clearly shows the difference between the resting state and the experimental state at the beginning and the end of the questions. The results of patient W in these two days are consistent with the time window of trigger marks.

There is a similar result between channel FC5 and the other channels (FC1, CP1, CP5) for patient W, all these channels are located in the left hemisphere. Through the medical records we learned that in January 2015, when she completely lost control of her eyes, she tries to twitch the right corner of her mouth to answer yes. As we know, the muscles on the right side of the body are controlled by the left hemisphere, while the muscles on the left side are controlled by the right hemisphere. From the fact that her remaining controllable body muscles are on the right side, we can infer that her left hemisphere is more active.

Although the results of sample entropy and Poincaré plot are similar, Poincaré plot is more sensitive one needs to remove some peaks in order to see the consciousness results, so the results of later extensions to LIS, MCS, and UWS patients will be dominated by the results of sample entropy in this work.

### **6.1.8 Sample Entropy results from LIS patients**

For the LIS dataset from section 5.3, the top diagram of Figure 6.17-Figure 6.20 shows the result of the sample entropy. The figure below shows the trigger marks, those with numbers represent experimental state and those without numbers represent rest state. Between two red vertical lines indicate sessions. In order to distinguish more clearly the difference between experimental and rest time, in these datasets all sessions in a day are combined in chronological order in the same figure. The free spelling experiment lasted longer, but the experimenter tried to keep the experiment to about 2 hours a day to avoid patients' fatigue affecting the experiment results.

As the results shown in (Tonin et al. 2020), the LIS patients spelled logical sentences during free spelling experiments. The experimenter also received a good number of correct answers during training and feedback sessions, thus indicating the consciousness of the P11 and P13. Figure 6.17-Figure 6.20 are showing the results for two LIS patients over two days for each patient. These dates were chosen because there are free spelling sessions on the two days and also because consciousness was reported to be better than on the other experimental days, and therefore suitable to reliable check for the plausibility of the results.

Since the period of spelling sessions indicates more consciousness compared to the yes and no questions, since free spelling is a more active action than passively answering yes and no questions (Lesenfants et al. 2018), the results of LIS patients focus on the spelling sessions and the rest period around them.

### LIS patient 11 on day 1

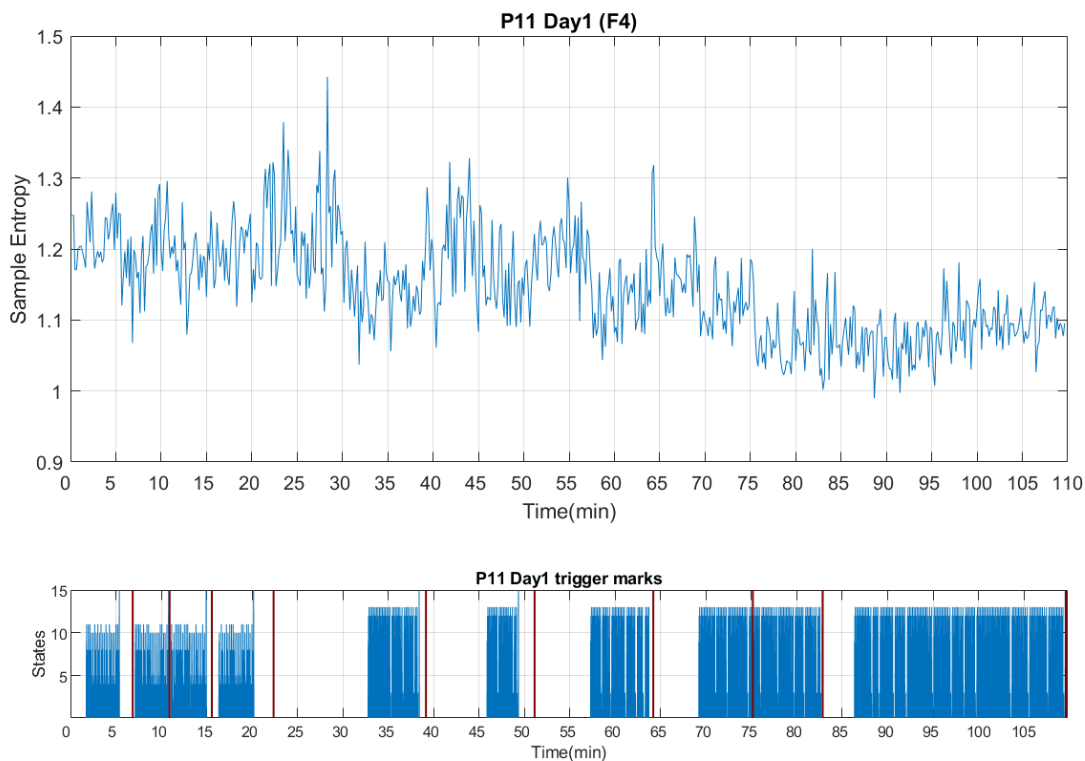


**Figure 6.17:** The sample entropy result for LIS patient 11 (ALSFRS-R=0) on day 1. Top: the channel F4 result of the sample entropy. Bottom: The trigger marks for patient 11 on day 1. The sessions are indicated between two red vertical lines. The periods with numbers are experimental state, and those without numbers are rest state.

Ten consecutive sessions over 110 min were combined on the day one for patient 11, as shown in Figure 6.17. The first two sessions are training sessions, the third and fourth sessions are feedback sessions, and the other six sessions are spelling sessions. The Figure 6.17 below shows the time windows between 33-38, 46-49, 57-64, 69-83, and 87-110 min in which the patient spelling sentences. The time windows from 22 to 33 min, 38-46, 49-57, 64-69, and 83-87 min are the rest states. Most of the rest periods before spelling showed higher sample entropy values, presumably caused by patients using rest periods to organize sentences. When the three experiments of train, feedback and spelling were conducted on

the same day, the sample entropy values for most of the rest periods before spelling were also higher than those for the train and feedback sessions, which is consistent with active action being more conscious than passive action.

## LIS patient 11 on day 2

Twelve consecutive sessions over 130 min were combined on the day two for patient 11, as shown in Figure 6.18. The first six sessions and the second last session are training sessions, the seventh, eighth, and the last sessions are feedback sessions, and the ninth and tenth sessions are spelling sessions.

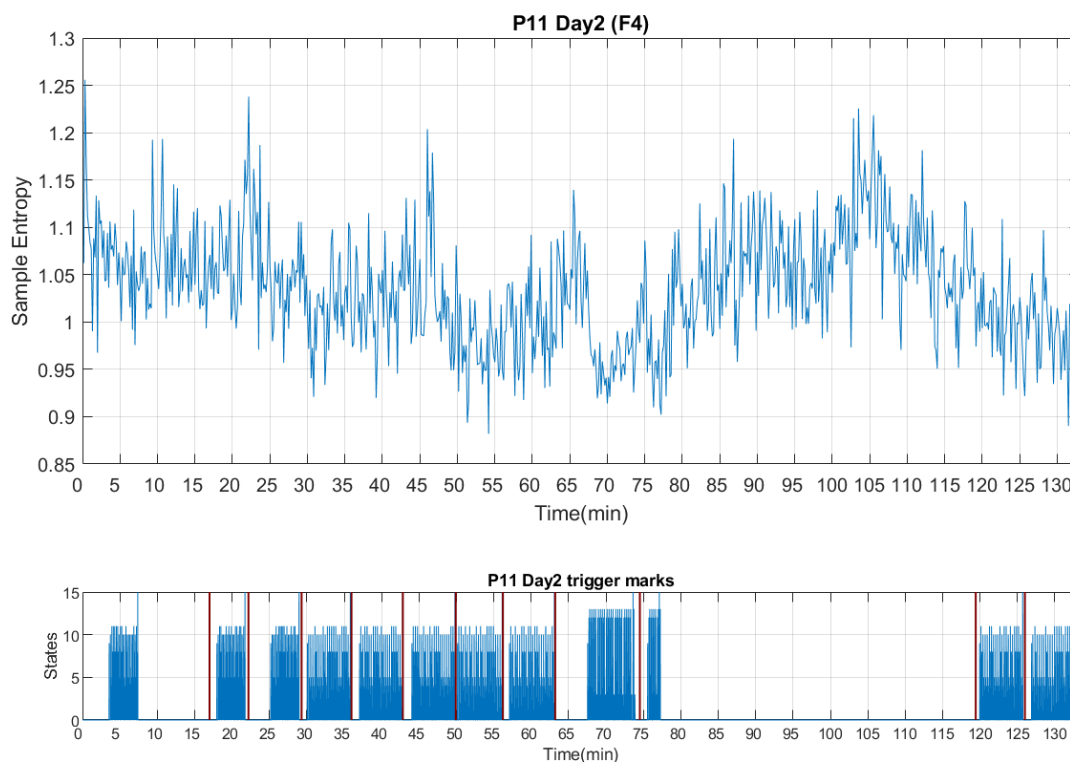


**Figure 6.18:** The sample entropy result for LIS patient 11 (ALSFRS-R=0) on day 2. Top: the channel F4 result of the sample entropy. Bottom: The trigger marks for patient 11 on day 2. The sessions are indicated between two red vertical lines. The periods with numbers are experimental state, and those without numbers are rest state.

The Figure 6.18 below shows the time windows between 68-74 and 76-78 min in which the patient spelling sentences. The time windows from 63 to 68 min and 74-76 min are rest periods before spelling sessions, and 78-120 min is the rest period after spelling session. All rest periods showed high sample entropy values, and patient 11 had similar trends in results for all other channels (FC2, FC4, C2, Cz, C1, FC1, FC3, F3) over these two

days. This case is the visit 10 in (Tonin et al. 2020), where they reported that during this visit the eye-movement amplitude of patient 11 was lower than the other nine visits previously, although the accuracy rate for training sessions was 80%, but they defined that no success was achieved in feedback and spelling sessions.

All LIS patients in this dataset are affected by motor neuron disease of ALS, which is a neurodegenerative neuromuscular disease that patients in the progressive loss of muscle control. When we followed the investigator (Tonin et al. 2020) to visit this patient in early 2020, patient 11 can still spell logical sentences at this visit, indicating that although the result showed that this patient was more conscious during the rest periods, he was not willing to communicate at this time. Secco et al. also report that P11 maintains a consistent EEG spectral distribution between May 2018 and September 2019 (Secco et al. 2020), a period that spans data from both experiments for P11.

Due to the absence of a voluntary response at this time in this patient, we presume that this patient didn't want to participate in the experiment at this time due to some psychological-emotional problem, such as depression, or some physiological problem, such as pain.

Depending on these kind of observation and in accordance with the presented results, it can be argued that sample entropy can be used as a reference indicator for communication with patients to let the investigators know the real situation of patients. In order to avoid making the experimental results depend on patients' willingness, and also to help the investigators to understand and respect the patients' willingness.

### **LIS patient 13 on day 1**

For patient 13, eight consecutive sessions over 125 min were combined on the day one, as shown in Figure 6.19. The first three sessions are training sessions, the fourth session is feedback session, and the other four sessions are spelling sessions. The Figure 6.19 below shows the time windows between 25-37, 41-71, 85-98, and 103-126 min in which the patient spells sentences. The time windows from 19 to 25 min, 37-41, 71-85, 98-103, and 126-129 min are the rest states. Most of the rest periods before spelling showed higher sample entropy values, presumably caused by patients using rest periods to organize sentences. When the three experiments of train, feedback and spelling were conducted on the same day, the sample entropy values for most of the rest periods before spelling were also higher than those for the train and feedback sessions, which is consistent with active action being more conscious than passive action.

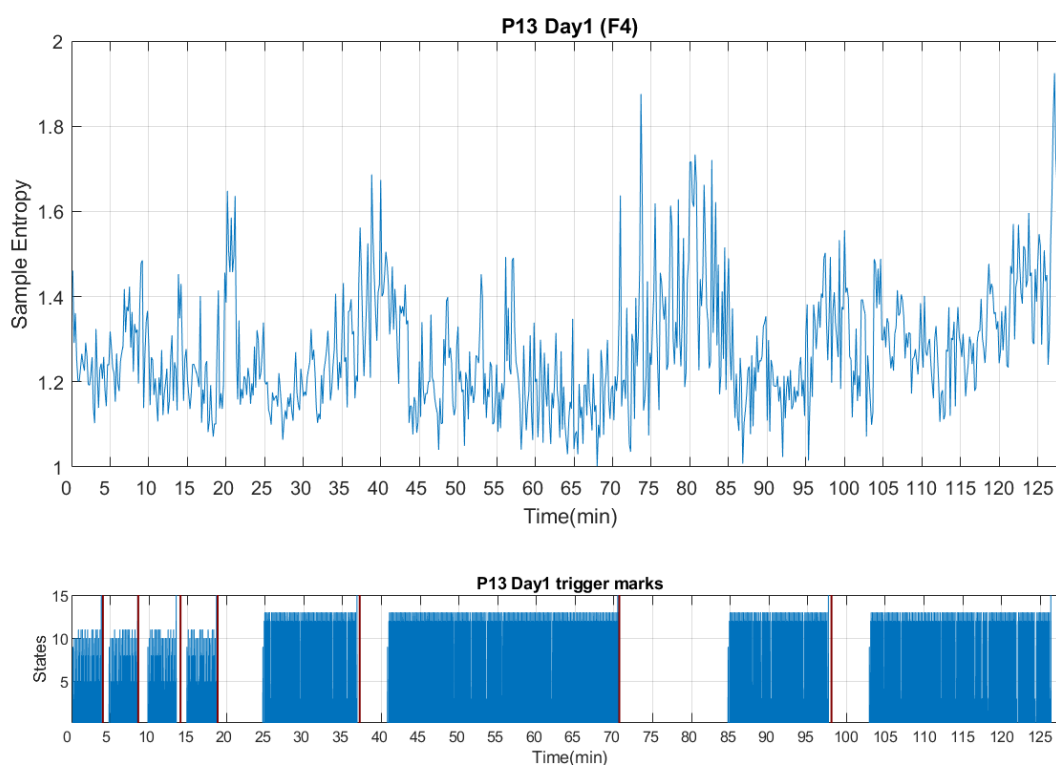


**Figure 6.19:** The sample entropy result for LIS patient 13 (ALSFRS-R=0) on day 1. Top: the channel F4 result of the sample entropy. Bottom: The trigger marks for patient 13 on day 1. The sessions are indicated between two red vertical lines. The periods with numbers are experimental state, and those without numbers are rest state.

## LIS patient 13 on day 2

For patient 13, six consecutive sessions over 100 min were combined on the day two, as shown in Figure 6.20. The first two sessions are training sessions, the third session is a feedback session, and the other three sessions are spelling sessions. The Figure 6.20 below shows the time windows between 17-38, 45-61, and 62-102 min in which the patient spelling sentences. The time windows from 12 to 17 min, 38-45, 61-62, and 102-103 min are the rest states. We observed that if the rest time between two spelling sessions is too short, for example the rest time in 61-62 min, then the value of sample entropy will not increase too high, just like the result 74-76 min on the day two for patient 11. The other rest periods before and after spelling showed higher values for sample entropy, which were also higher than the training and feedback sessions, consistent with active actions being more conscious than passive actions. In the last session, the patient freely spelled out "I look forward to a vacation", demonstrating a strong will to live. The results for patient 13 in all other channels (AF3, F3, C1, Cz, C2, AF4) have a similar trend.

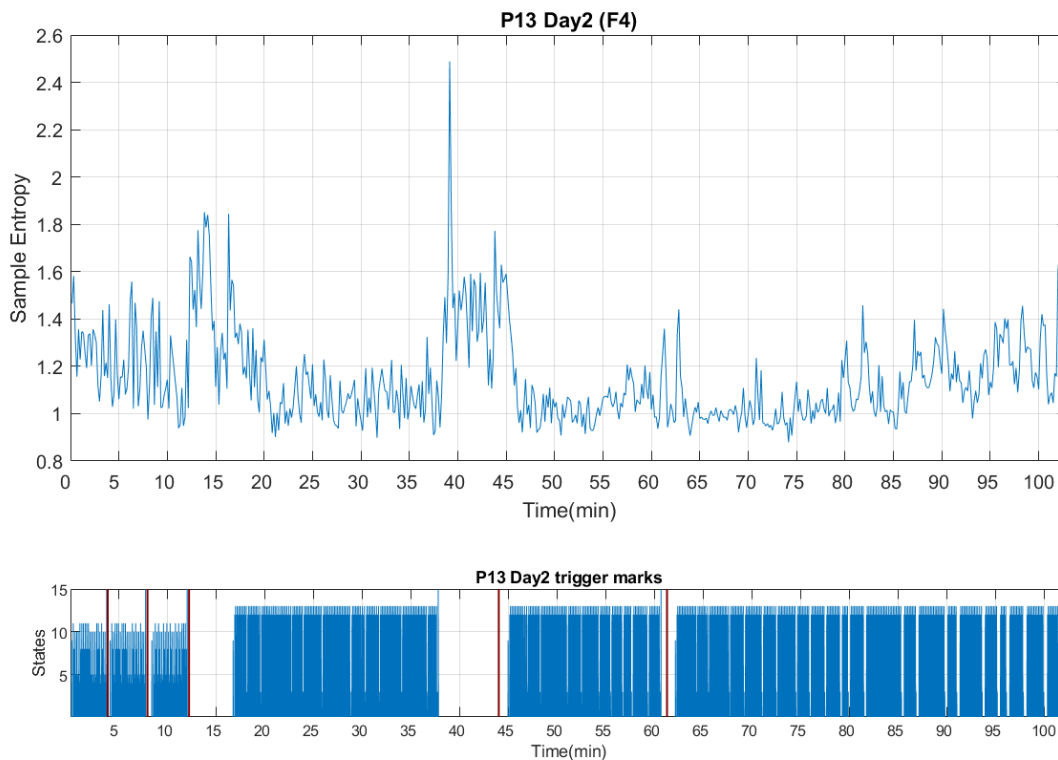


**Figure 6.20:** The sample entropy result for LIS patient 13 (ALSFRS-R=0) on day 2. Top: the channel F4 result of the sample entropy. Bottom: The trigger marks for patient 13 on day 2. The sessions are indicated between two red vertical lines. The periods with numbers are experimental state, and those without numbers are rest state.

### 6.1.9 Sample Entropy results from DOC patients

In this disorders of consciousness (DOC) dataset, MCS and UWS patients had etiologies due to anoxia, traumatic brain injury (TBI) and cerebrovascular accident (CVA). To avoid compensatory effects of brain damage such as stroke and cerebral ischemia, the resulting distribution of brain functions does not follow the standard Brodmann area (Azari and Seitz 2000). Therefore, the consistent results for multiple channels are shown in the following sections with the aim of finding an appropriate approach for all patients.

This DOC dataset from section 5.4, the results of the sample entropy are shown in Figure 6.23-Figure 6.29 for a total of 9 segments of polysomnogram (PSG) recordings from two minimally conscious state (MCS) patients and four unresponsive wakefulness syndrome (UWS) patients. It is assumed that the higher the value, the higher the relative consciousness of the patient. The red line indicates that an event occurred near that time point. The magenta block indicates events that persist over a period of time to be defined by the relationship of



two successive events or the description of the event itself, referred to here as a continuous event.

Cologan et al. suggested that if UWS patients have REM sleep stages or facial expressions consistent with stimuli, it is recommended to perform MCS testing first, which has a better chance of recovery than patients without REM sleep stages. Based on this dataset providers Wielek et al. used unsupervised learning in their paper (Wielek et al. 2018) to reveal the presence of different sleep stages in MCS patients, so we will build on this and compare whether the sample entropy results are event-related. These data were selected because, in addition to the more significant effect of continuous event recording on results, consciousness was reported to be better than in the other patients. Therefore, results should be more reliable in the context otherwise here presented work.

### MCS patient 1

Figure 6.21 shows 213 minutes PSG recording of patient MCS1. At around the 156<sup>th</sup> minute, the sample entropy value began to increase, and the 186<sup>th</sup> minute event showed that the patient started lunch half an hour ago, so the sample entropy values are consistent with this event. Another event (the 204<sup>th</sup> minute) was that the investigator re-glued the EMG channel, but this was a single point event to which the patient did not respond, so it did not affect the sample entropy results. The results for patient MCS1 in all other channels (F4, FC5, FC6, C3, C4, P3, P4, T3, T4, F7, F8, PO7, PO8, Fz, Cz, Pz, Oz) have a similar trend.

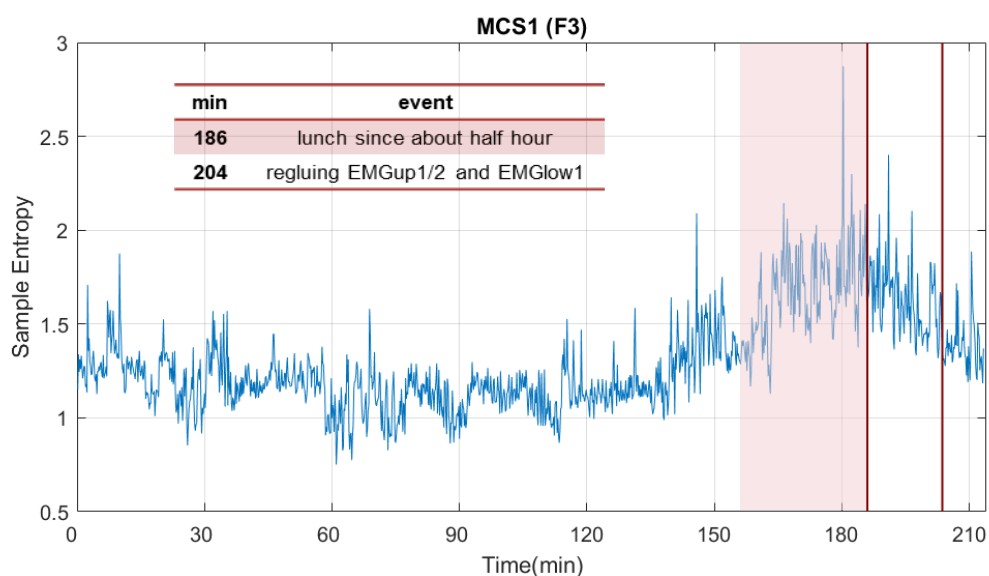


**Figure 6.21:** The channel F3 result of sample entropy for Patient MCS1. The time points with events are indicated in red vertical lines. Continuous event is indicated in magenta block.

## MCS patient 2

Figure 6.22 shows 260 minutes PSG recording of patient MCS2. This recording was made from 11:23 to 15:43, so we presume that the higher value of the sample entropy at the beginning was caused by lunch. After lunch the patient slept for a while and at around the 156<sup>th</sup> minute the patient was woken up for the CRS-R (Giacino et al. 2004) test, which took 20-30 minutes according to the event notes of other patients, which is consistent with the relatively high value of sample entropy before the 180<sup>th</sup> minute. The results for patient MCS2 in all other 17 channels have a similar trend.

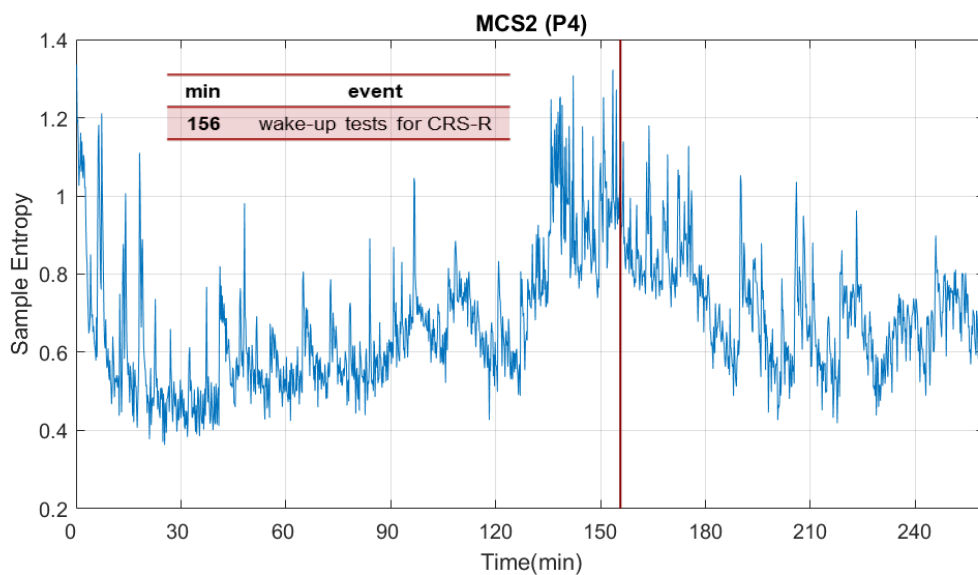


**Figure 6.22:** The channel P4 result of sample entropy for Patient MCS2. The time point with events are indicated in red vertical lines.

## UWS patient 1

Figure 6.23 shows over 12 hours PSG recording of patient UWS1. The gray block shows the night time period according to the internet to check the sunrise 06:28 and sunset 19:51 on the day of the location where the experiment was implemented. The nursing staff turned off the lights at 185 min and turned them on at 707 min, but it seems that the sunlight outside had a greater effect on patient UWS1. No event occurred at sunrise, but the sample entropy increased significantly. This is consistent with (Wisłowska et al. 2017) indicating that light gives “Zeitgebers” to humans, which in turn changes the dynamics of the brain between day and night.

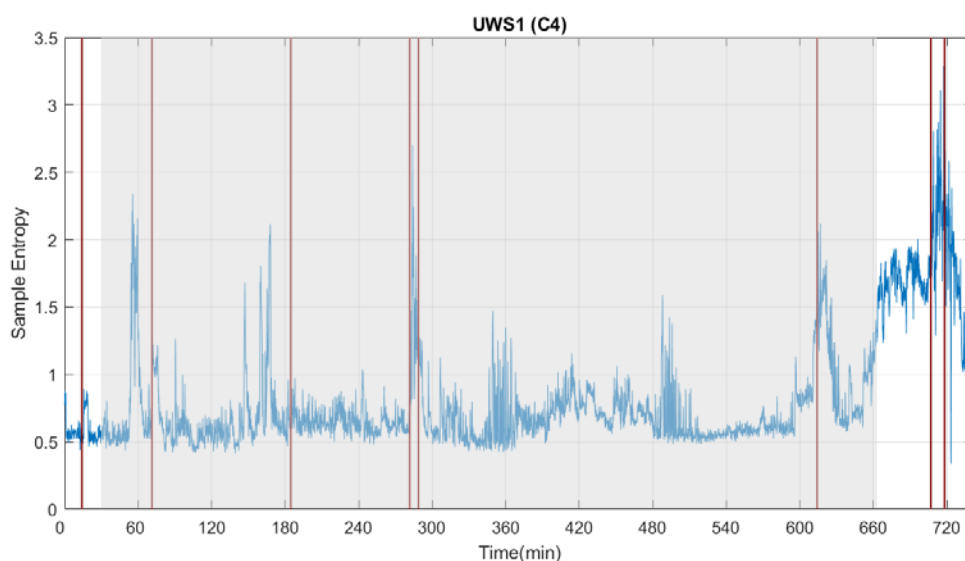


**Figure 6.23:** The channel C4 result of sample entropy for Patient UWS1. The night period is shown in gray block. The time points with events are indicated in red vertical lines.

Several care actions were performed by nursing staff at 282, 614 and 718 minutes, and at 718 min the care action started 5 min ago. All of these actions had an effect on the patient also reflected in the rapid rise in sample entropy values. At minute 14, the investigators left the room and at 71 minutes and 289 minutes they checked the electrodes. These effects were also reflected in a slight increase in the sample entropy values. Channels F3 and F4 lost signals after 70 minutes and thus not included, perhaps because the two electrodes were disconnected when the EMG electrodes were reconnected at the 71<sup>st</sup> minute. Similar trends to Figure 6.23 were observed in the results of UWS1 for the other 15 channels.

**Table 6.1:** The event notes for Patient UWS1.

min	event	min	event
14	AG leaving room after talking	289	eleks adjust
71	fixed upper EMG	614	Patient is repositioned
185	lights off	707	light on
282	care	718	care start 5min ago

## UWS patient 2

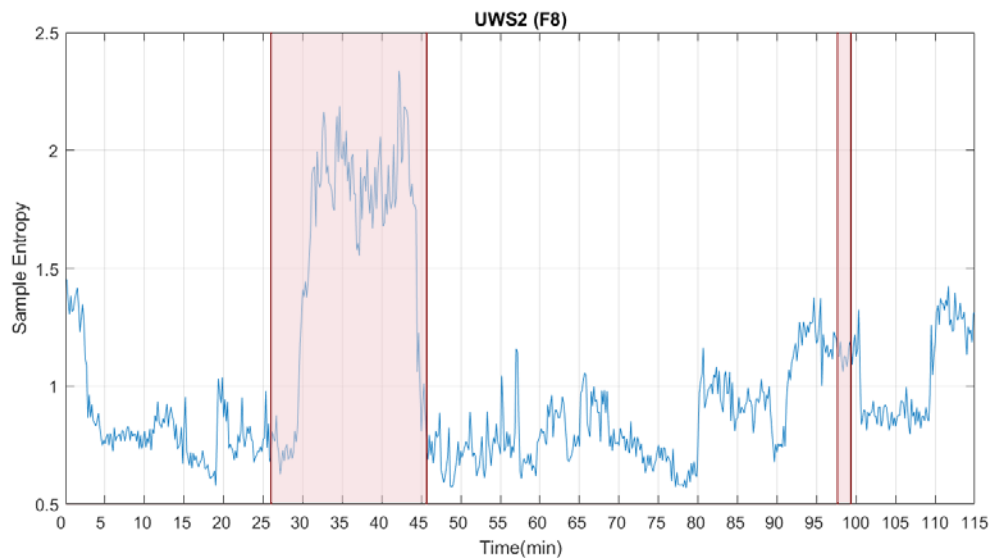


**Figure 6.24:** The channel F8 result of sample entropy for Patient UWS2. Continuous events are indicated in magenta blocks.

Figure 6.24 shows 115 minutes PSG recording of patient UWS2. From 26<sup>th</sup> to 46<sup>th</sup> min and from 98 min to 99 min the nursing staff did some care actions. 20 min of care actions had a greater effect on this patient effect than 1 min of care actions. The sample entropy showed higher values during the care actions despite a 2-3 minute delay during the 20 minute care actions. The results for patient UWS2 in all other channels (F3, F4, FC5, FC6, C3, C4, P3, P4, T3, T4, F7, PO7, PO8, Fz, Cz, Pz, Oz) have a similar trend.

**Table 6.2:** The event notes for Patient UWS2.

min	event	min	event
26	care start	98	care start
46	care end	99	care end

## UWS patient 3 (PSG1)

The results of patient UWS3 for a total of 21 hours in a single day are shown in Figure 6.25-Figure 6.27. Figure 6.25 shows the PSG recordings of the patient's UWS3 overnight for over 12 hours. From 297<sup>th</sup> min to 311<sup>th</sup> min and from 564<sup>th</sup> min to 590<sup>th</sup> min the nursing staff did some care actions. The sample entropy showed higher values in the care actions, and there is a time point of care action at 90 min, we also see a peak of sample entropy before 90 min. The nursing staff did insulin administration at 666 min, started the medication at 702 min, and changed the patient's position at 732 min, so we saw three continuous peaks in

the morning. The remaining event was at 153min when the investigator re-glued the electrode, but it didn't have a significant effect on the sample entropy results.

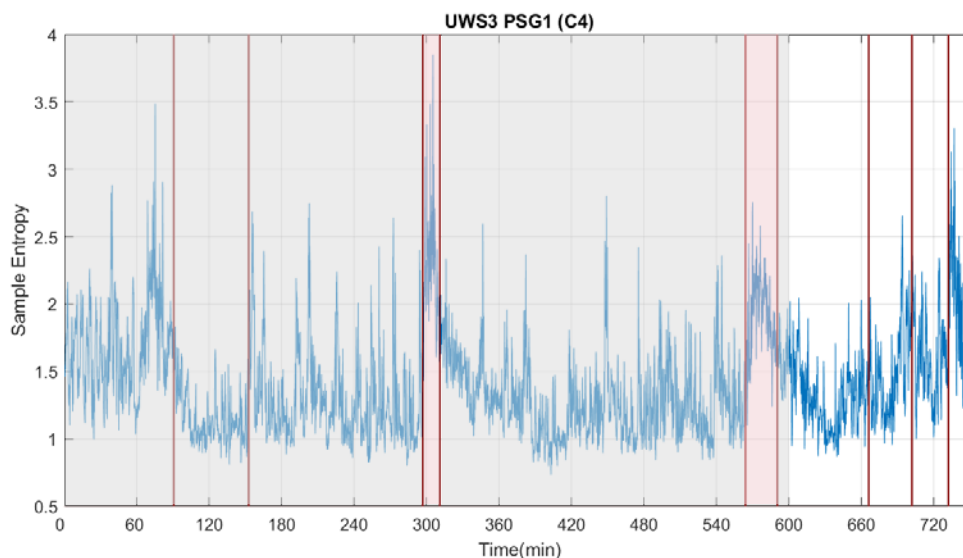


**Figure 6.25:** The channel C4 result of sample entropy for Patient UWS3 (PSG1). The night period is shown in gray block. The time points with events are indicated in red vertical lines. Continuous events are indicated in magenta blocks.

**Table 6.3:** The event notes for Patient UWS3 (PSG1).

min	event	min	event
90	care	564	care start
153	reglue chin electrode	590	care end
297	care start	666	07:30 Insulin administration
311	care end	702	medication start
		732	positioning

### UWS patient 3 (PSG2)

The second PSG recording of the patient UWS3 over seven and a half hours is shown in Figure 6.26. At 60 and 360 minutes, several care actions were performed by nursing staff. Both impacted the patient and are also reflected in the rapid increase in sample entropy values. At 267<sup>th</sup> and 329<sup>th</sup> minutes, the investigators checked the electrodes. These impacts caused the sample entropy values to increase relatively slightly.

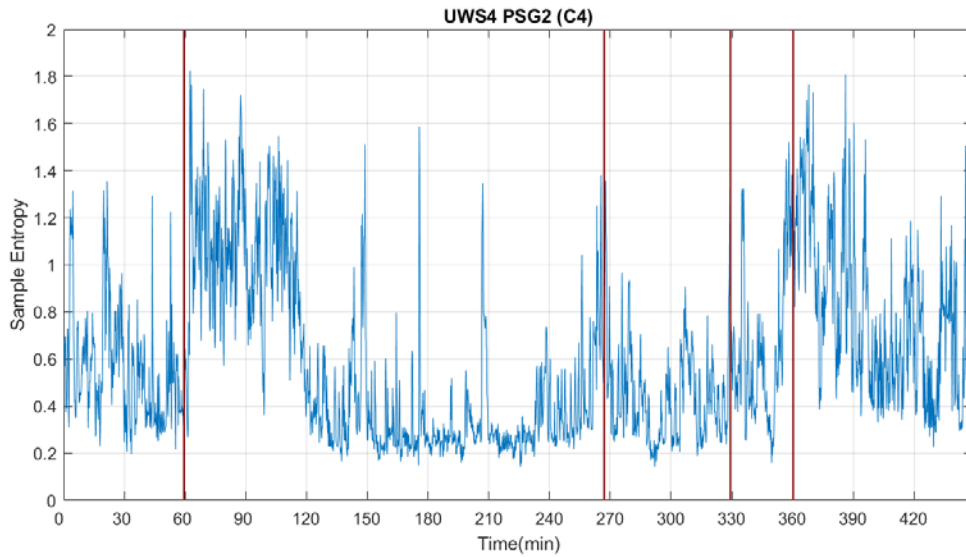


**Figure 6.26:** The channel C4 result of sample entropy for Patient UWS3 (PSG2). The time points with events are indicated in red vertical lines.

**Table 6.4:** The event notes for Patient UWS3 (PSG2).

min	event	min	event
60	care action	329	check electrodes
267	check electrodes	360	start of care action

### UWS patient 3 (PSG3)

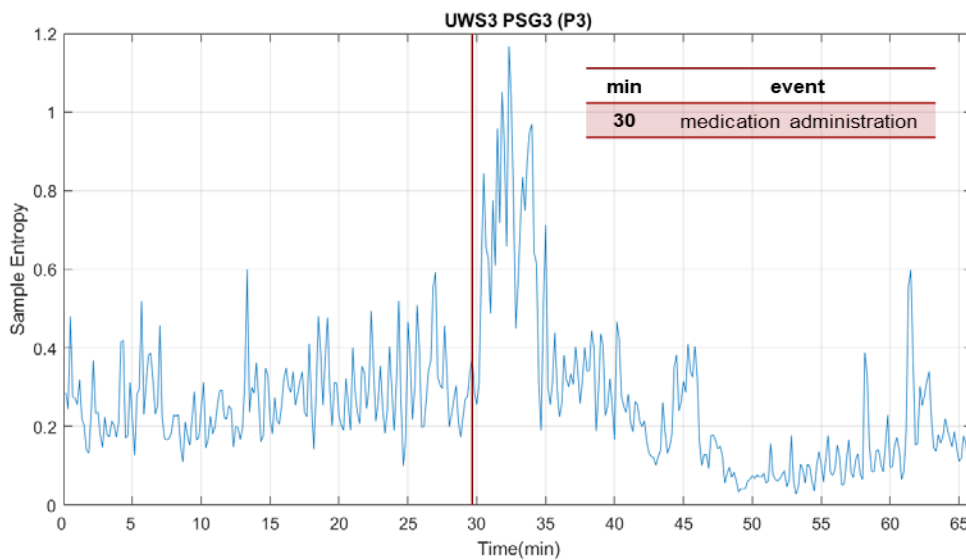


**Figure 6.27:** The channel C4 result of sample entropy for Patient UWS3 (PSG3). The time point with events are indicated in red vertical lines.

The third PSG recording of the patient UWS3 over 65 minutes is shown in Figure 6.27. The only event is that the nurse performed a medication administration at the 30<sup>th</sup> minute,

which obviously caused 5 minutes of relatively higher sample entropy values. The three PSG recordings for patient UWS3 in other 17 channels have a similar trend.

### UWS patient 4

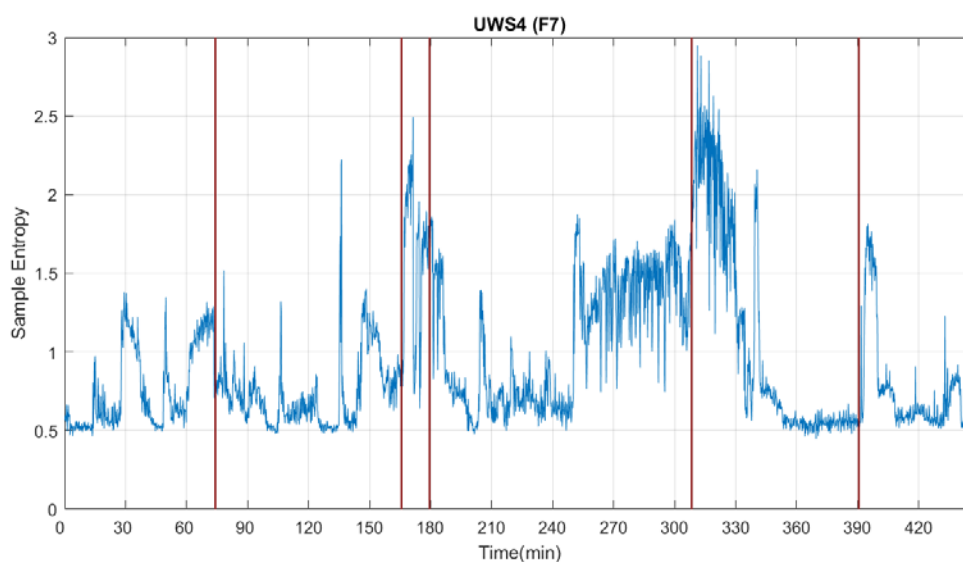


**Figure 6.28:** The channel C4 result of sample entropy for Patient UWS4. The time points with events are indicated in red vertical lines.

Figure 6.28 shows over seven and a half hours PSG recording of patient UWS4. This recording was made from 6:43 to 14:10, so the meal events around 74<sup>th</sup> and 308<sup>th</sup> minutes were breakfast and lunch times, respectively, and the effect of lunch reflected in sample entropy values was more significant than breakfast. Nursing staff performed some care actions at 166 and 390 minutes. The impact of these two events on the patients is also reflected in the rapid increase in the sample entropy values. The effect of these two events on the patient is also reflected in the rapid increase in the sample entropy value. The event at 180<sup>th</sup> min was nutritional intake, which showed a relatively higher sample entropy value. Although for this patient there was no record of how long the events lasted, we still found relatively high values around the events. The results for patient UWS4 in all other 17 channels have a similar trend.

**Table 6.5:** The event notes for Patient UWS4.

min	event	min	event
74	eat	308	eat
166	care action	390	care action
180	nutrition		

### 6.1.10 Discussion of EEG signal results

In section 6.1.6-6.1.9, the sample entropy and Poincaré plot methods were applied to EEG signals of different patients with different diseases. In the CLIS dataset, most results from four patients for a total of eight days showed relatively higher sample entropy values, during the time windows where consistent with the communication period. However, the results for patient F on day one and part of results for patient G on day one are not in line with this trend. Perhaps the patients were able to let their minds wander during the time they were not in the experimental period, resulting in higher brain activity during the resting period than experimental period. The same phenomena as in the LIS patients occurred during the rest periods, when they presumably organized the sentences. Nevertheless, globally, the obtained results are correlating with the observations in (Chaudhary et al. 2017). Even though this does not prove the correctness of the approach in terms of levels as used in medicine, but it indicates that the approach might be correct. Therefore, in this thesis, we focus on all cases in which significant changes occurred at the beginning and at the end of the experiment, and overall, the patients responded accordingly to the external stimuli.

We obtained similar results for the sample entropy and Poincaré plot methods, but the application of Poincaré plots to the EEG signal requires modification. Since the Poincaré plot equation has no tolerance, it directly uses the voltage amplitude of the EEG signal, unlike the sample entropy equations have a tolerant coefficient. If some peaks of the Poincaré plot exceed one standard deviation of the entire time series of the day, one standard deviation needs to be subtracted to obtain a result similar to the sample entropy method. Therefore, we focus on the sample entropy method, which can be applied not only to CLIS/LIS patients but also to patients with disorders of consciousness (DOC).

A total of four patients with CLIS and two patients with LIS were analyzed for non-invasive brain waves, EEG signals, and the following three patterns were observed:

1. The sample entropy value changed due to the stimulation of the auditory experiment.
2. Patients were presumed to be more focused at the beginning of the experiment, and gradually decreased as they became more skilled. As Biederman et al. (Biederman and Vessel 2006) describe why people prefer new stimuli and that repeated stimuli weaken the brain's response.
3. Patients were still organizing sentences or thinking before spelling session, resulting in higher sample entropy values before the experiment than during the experiment.



For the Patient 11 on day two, Tonin et al, reported that the patient did not perform well in this experiment, the sample entropy results showed that the patient performed more brain activity during the resting period than the spelling experiment, as shown in Figure 6.18. These two contrasting results indicated that this patient was not ready for communication at this time. Moreover, the patient was still able to spell logical sentences when we visited him in 2020. Thus, sample entropy can be used as a reference indicator for communication with patients to avoid making experimental results dependent on patient willingness and also to help investigators understand and respect patient willingness.

After the experiment of visiting P11, as mentioned in the paper (Tonin et al. 2020) in a supplementary video, P11 spelled "Ich brauchen andere Stimme" ("I need another voice") in the first free spelling. It took him about 38 minutes and answered 206 questions to spell this sentence, which, combined with the fact that the average spelling speed of the patients in the experiment mentioned in the article was about 0.5 (chat/minute), indicated that the expression of a sentence is a long spelling process for them. I hypothesized that BCI users in general need to organize the sentences in their minds during the rest time and try to streamline the words as much as possible to achieve the best spelling efficiency.

We also tried to use permutation entropy in EEG signals, since the method transfers the time series to  $m!$  patterns, even with higher  $m$  parameters, this method still ignores too much detail of the time series, so permutation entropy does not perform well compared to poincaré plots and sample entropy, but as the result of Figure 6.3 and the report of (Wisłowska et al. 2017) show, permutation entropy could be a suitable method to reflect the circadian regulation of arousal in healthy subjects, CLIS and MCS patients.

In the disorders of consciousness dataset in section 6.1.9, in total 7 MCS patients and 11 UWS patients, for the MCS patients who reported to have the REM sleep stage, we choose two cases, whereas for the UWS patients, four patients also show the results in the same section. Of the experimenters each investigator has a different habit of recording events. Nevertheless, if there is only one time point of event notes, we still have some relatively high sample entropy values around the event notes. We may not be able to explain every peak, but at least for each recorded event in Figure 6.21-Figure 6.28, the sample entropy showed an increase in the patient's brain activity for reported events during the experiment.

As Cologan et al. suggested, if UWS patients have REM sleep stages, it is recommended to do MCS testing first. Sample entropy could be a reference index indicating that patients' brain activity matches the stimuli, giving them a better chance of recovery than patients without this phenomenon. As Wielek et al. have indicated the existence of different

sleep stages in MCS patients, not only MCS patients show the expected event response, but also unexpected results were seen in UWS patients. Therefore, we hypothesized that in addition to measuring sleep stage integrity in UWS patients, perhaps sample entropy could be the basis for measuring whether UWS patients are responsive to environmental stimuli. In (Wisłowska et al. 2017) also revealed that in single-subject analyses, some UWS patients may also exhibit circadian differences of brain activity in entropy.

The main problem with CLIS patients in general is the lack of ground truth. Although at night they had healthy sleep and normal circadian rhythms, they often dozed off during the day (Lo Coco et al. 2011), so we cannot be certain that the patients answered all questions correctly. This is because in order to obtain the baseline from patients, they have to answer many questions with known answers and copy spelling of words, caused sometimes they were distracted, fatigued, bored, or habituated, which may have resulted in patients answering in a way that did not meet the investigator's expectations. In the CLIS and LIS datasets, the experimenter controlled the duration of the experiment to about 2 hours per day to try to ensure that patient fatigue would not affect the results of the experiment.

The LIS patients are closest to the state of healthy subjects in the clinical scales of consciousness, and with the residual eye movements as the “ground truth” of consciousness, in addition to the fact that LIS patients can freely spell out meaningful sentences. These data might have more brain activity than the other datasets, so we select them as the dataset for machine learning.

## **6.2 Machine learning part**

Machine learning is commonly used in the field of brain waves to identify whether a patient has a disease such as epilepsy (Pioreckýa et al. 2019), schizophrenia (Dvey-Aharon et al. 2015), or to distinguish sleep stages (Güneş et al. 2010), etc. Since all the methods mentioned in the feature extraction section currently have different parameter choices and individual patient differences, it is difficult to establish a threshold as a general criterion for the presence or absence of consciousness in patients. Therefore, in this section, the LIS data with the most active brain activity in all datasets are selected and unsupervised learning methods are applied to find an individual threshold for each patient

Many clustering algorithms use distance measures to calculate the similarity between observations, such as K-Means or DBSCAN. For this reason, these methods perform better in the case of continuous attributes, so here the sample entropy results are subdivided into several consecutive 1-minute time series instead of being based on data features. As

described in section 6.1.10, the LIS patients are closest to the state of healthy subjects in the clinical scales of consciousness, and they can freely spell out meaningful sentences using residual eye movements as the "ground truth" of consciousness. These data might have more brain activity than the other datasets, which is why we select the LIS patient dataset in section 5.3 as the dataset for machine learning. In this section, the k-means and density-based spatial clustering of applications with noise (DBSCAN) methods were applied to the sample entropy results of the EEG signal datasets from LIS patients 11 and 13. To cluster the differences in consciousness between the rest and spelling experimental periods of the 2 LIS patients, the performance of the patients in response to external stimuli was analyzed. This section also presents the cost calculation results of the Elbow method (Kodinariya and Makwana 2013) for different k values of k-means and the k-distance graph results for the parameter selection of DBSCAN.

### 6.2.1 k-Means results

As proposed in section 2.7, this section presents the application of k-Means method to the sample entropy results in section 6.1.8, focusing on the clustering analysis during the spelling experimental period and the resting period before and after the experiment. The k-Means results are shown in the odd numbered figures in Figure 6.29-Figure 6.37, where the x-axis and y-axis show the values of sample entropy after mean normalization and feature scaling. The black cross is the center of the cluster at each iteration.

To increase the amount of data, the 1-minute time series were overlapped with a 10-second moving window, and the overlap also made the data features (maximum, minimum, median, mean, standard deviation, median, and variance) more similar to improve the homogeneity of the input data and reduce outliers. Since the data characteristics are similar for each series (t=1,2,3,4,5,6), only the t=1 vs. t=2 figures are shown here.

Since an algorithm like k-Means always partitions the dataset at the midpoint between the centers of two clusters, and the original two periods vary in size, the period with less data is used as the basis in this approach to make the two periods approximately equal in size. In addition, if the sample entropy values after mean normalization and feature scaling of the two periods overlap, these overlapping values may come from either the experimental period or the resting period, which will cause instability in the clustering results (Pham et al. 2005).

The elbow method is used to show the cost of k-Means with different numbers of clusters, as shown in the even numbered figures in Figure 6.30-Figure 6.38, where the x-axis

represents the number of clusters and the y-axis represents the cost. The costs are calculated with reference to section 2.8. For all k-Means results, we already know that there are at least two clusters for the spelling experimental and resting periods. As the results of elbow method shows that  $k=3$  is the appropriate cluster size, the results for  $k=2$  and  $k=3$  will be presented in the odd numbered figures in Figure 6.29-Figure 6.37.

### LIS patient 11 on day 1

Figure 6.29 shows the k-Means results for patient 11 on day one, including 914 1-minute time series, half of which are from the spelling experimental period and the other half from the rest period. If the sample entropy values after mean normalization and feature scaling of the two periods still overlap, leading to unstable clustering results, the data analysis here is based on the data volume on another day of the same patient in the less spelling experimental period.

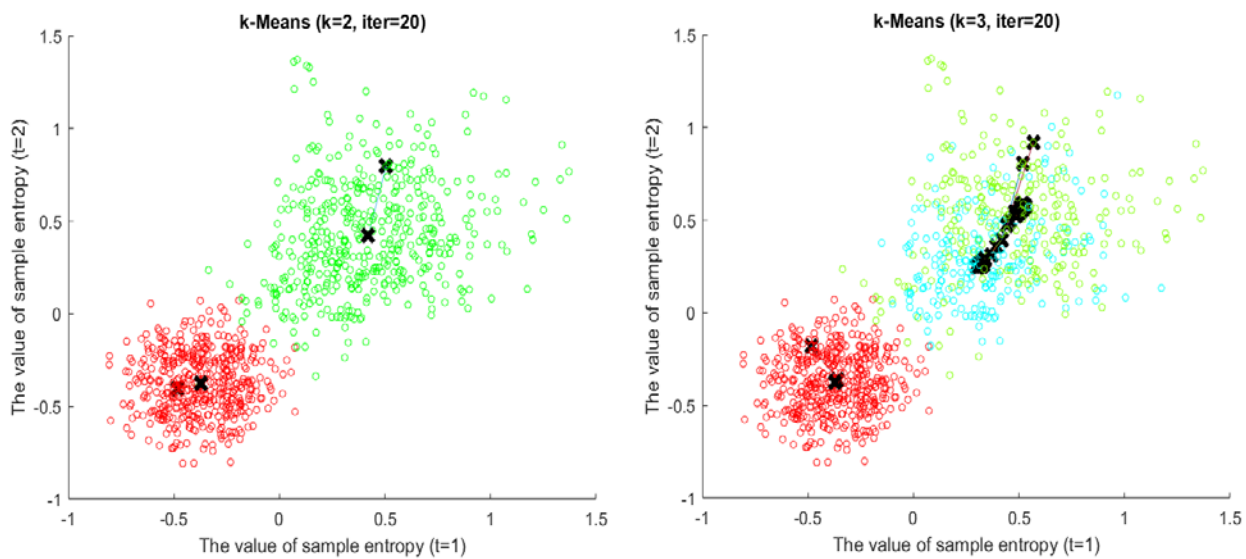


**Figure 6.29:** The k-Means results for LIS patient 11 (ALSFRS-R=0) on day 1, where the x-axis and y-axis show the sample entropy values after mean normalization and feature scaling at different time points ( $t=1$  vs.  $t=2$ ). The black crosses are the centers of the clusters at each iteration, both figures show the results after 20 iterations. Left:  $k=2$ . Right:  $k=3$ .

For all k-Means results, we already know that there are at least two clusters for the spelling experimental and resting periods. The elbow method in Figure 6.30 shows the cost of k-Means for patient 11 on the day one in different clusters. Although it is less obvious compared to Figure 6.32, it can still be seen that the cost decreases rapidly as  $k$  increases from 1 to 3, and then reaches an elbow where the cost equals 0.3051, after which the

deviation decreases slowly. Since the cost at this point is at the elbow of this curve,  $k$  equals 3 is the appropriate number of clusters.

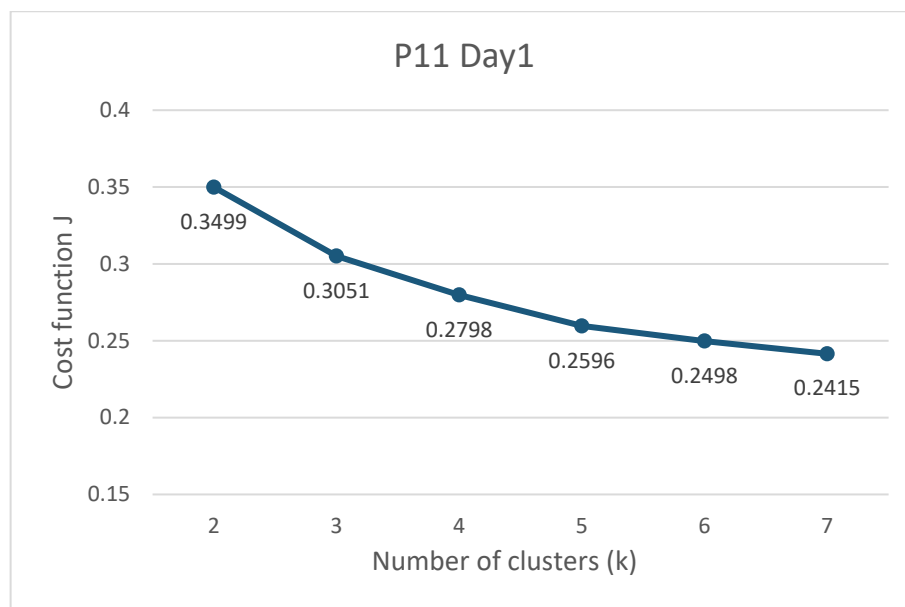


**Figure 6.30:** Cost of k-Means for LIS patient 11 on day 1, where the x-axis represents the number of clusters and the y-axis represents the cost.

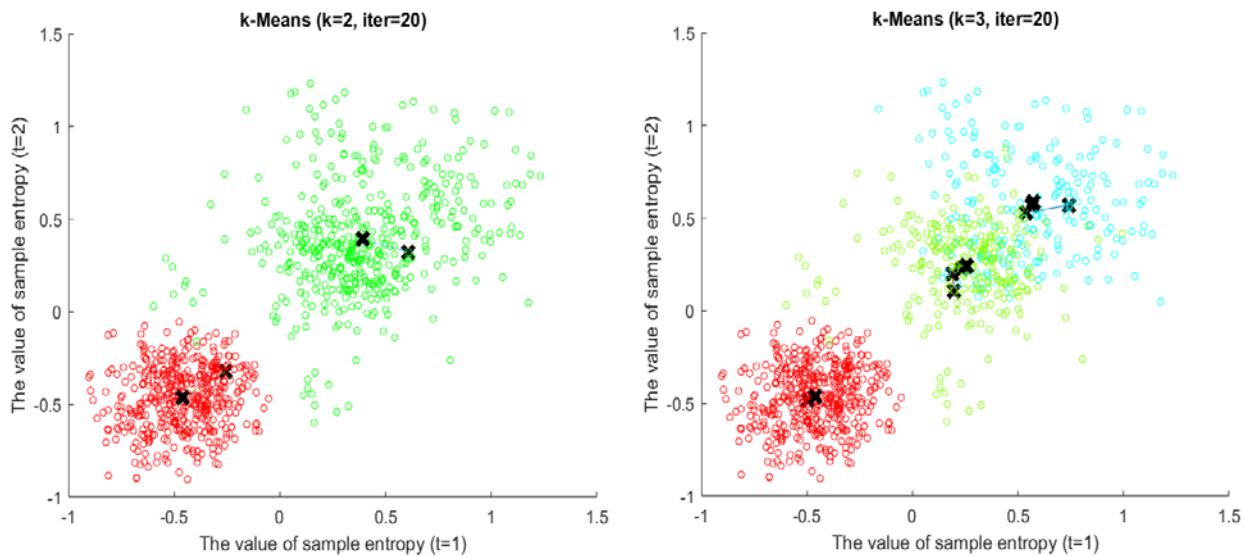
The third cluster, based on the original sample entropy results in Figure 6.17, is presumed to be caused by the different rest periods, where patients may have less need to think about new sentences in the later period because they have already organized the sentences in the previous period. Even in the result with the lower cost of  $k=4$ , the clusters of the spelling experimental period (red) were not separated into two clusters, but the resting period was divided into three clusters, which shows that the brain activity of the patients was quite consistent when the spelling experiment was performed.

For the spelling experimental periods of patient 11 on day one, the sample entropy value after mean normalization and feature scaling was approximately below 0. This is the same as the clustering result for this patient on another day, but different from patient 13, probably due to individual differences between patients. The clustering number of 3 is generally consistent with the DBSCAN results in Figure 6.40.

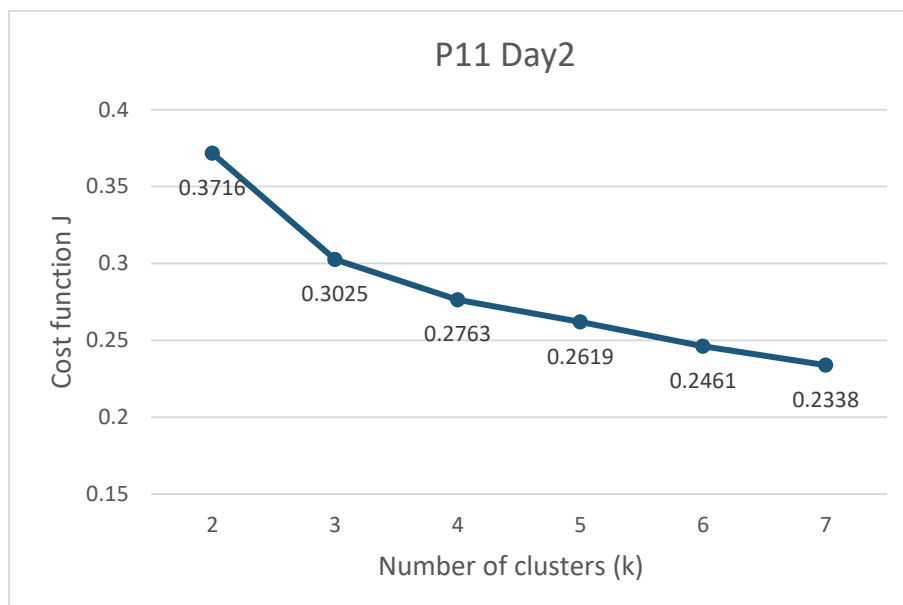
### LIS patient 11 on day 2

Figure 6.31 shows the k-Means results for patient 11 on day two. On this day, the data amount of the spelling experimental period with less data was used as the basis, and the same data amount was taken during the rest period, so that the data amounts of the two periods

were equal, including a total of 908 1-minute time series, half of which are from the spelling experimental period and the other half from the rest period.



**Figure 6.31:** The k-Means results for LIS patient 11 (ALSFRS-R=0) on day 2, where the x-axis and y-axis show the sample entropy values after mean normalization and feature scaling at different time points ( $t=1$  vs.  $t=2$ ). The black crosses are the centers of the clusters at each iteration, both figures show the results after 20 iterations. Left:  $k=2$ . Right:  $k=3$ .



**Figure 6.32:** Cost of k-Means for LIS patient 11 on day 2, where the x-axis represents the number of clusters and the y-axis represents the cost.

The elbow method in Figure 6.32 shows the cost of k-Means for patient 11 on the day two in different clusters. It is clear to see that the cost decreases rapidly as k increases from 1 to 3, and then reaches an elbow where the cost equals 0.3025, after which the distortion decreases very slowly. Since the cost at this point is at the elbow of this curve, k equals 3 is the correct number of clusters.

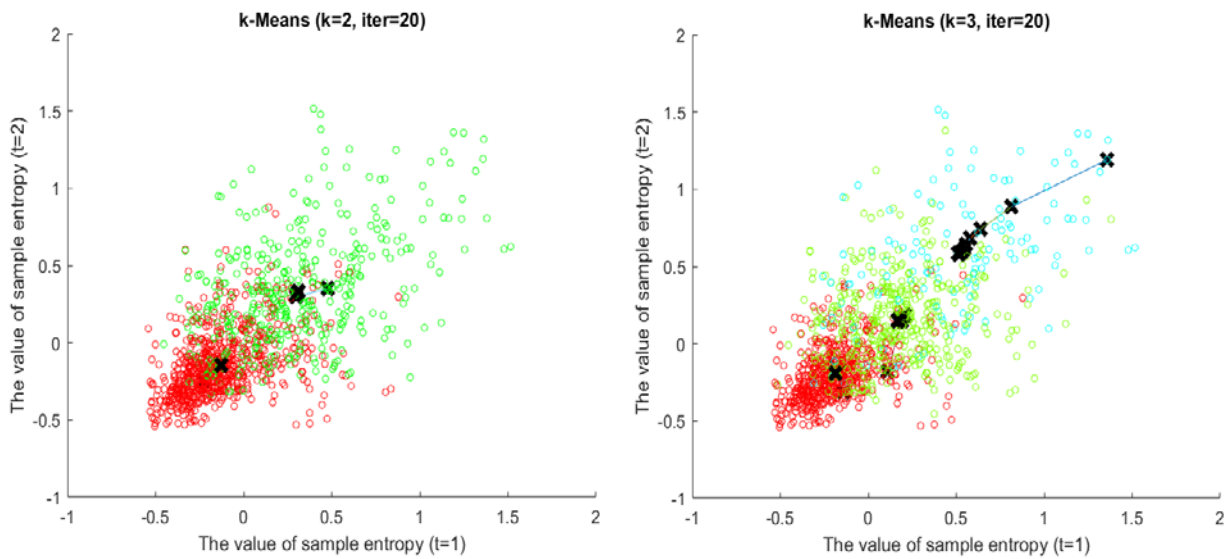
Except for the two clusters of spelling experimental periods and rest periods that we already know. The third cluster, based on the original sample entropy results in Figure 6.18, presumed that the rest period was distinguished into several clusters due to the process of slowly increasing and then decreasing sample entropy values during the rest period of the two experimental periods. Even in the result with the lower cost of k=4, the clusters of the spelling experimental period (red) were not separated into two clusters, but the resting period was divided into three clusters, which shows that the brain activity of the patients was quite consistent when the spelling experiment was performed.

The sample entropy value after mean normalization and feature scaling was approximately less than 0 for the spelling experimental periods of patient 11 on day two, consistent with the clustering result for this patient on another day, but different from patient 13, probably due to individual differences between patients. The clustering number of 3 is generally consistent with the DBSCAN results in Figure 6.42.

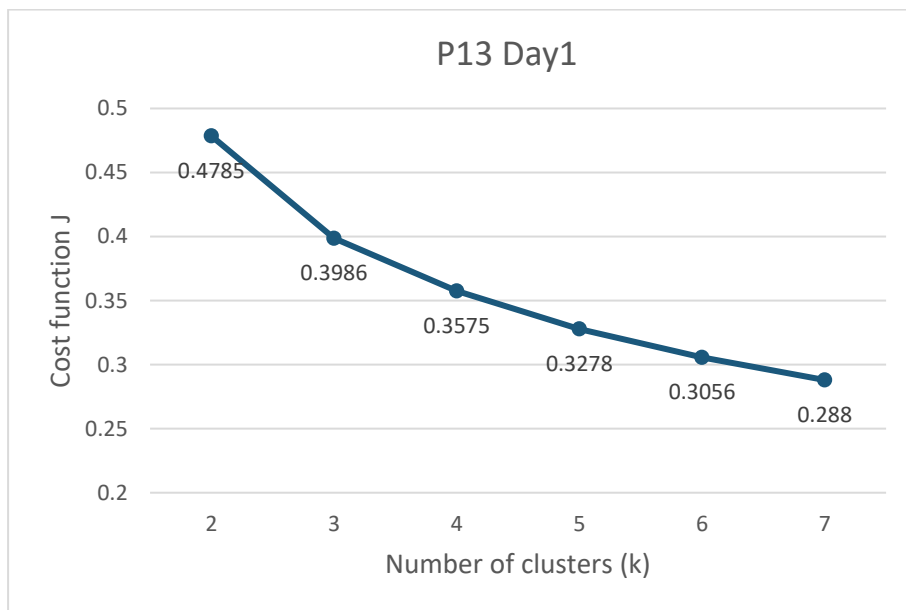
### **LIS patient 13 on day 1**

Figure 6.33 shows the k-Means results for patient 13 on day one, including 1070 1-minute time series, half of which are from the spelling experimental period and the other half from the rest period. The data from this day, even with the data from the rest period on another day with less data from the same patient as the basis for data analysis, the sample entropy values after mean normalization and feature scaling from the two periods still overlap, leading to unstable clustering results.

For all k-Means results, we already know that there are at least two clusters for the spelling experimental and resting periods. The elbow method in Figure 6.34 shows the cost of k-Means for patient 13 on the day one in different clusters. Although it is less obvious compared to Figure 6.36, it can still be seen that the cost decreases rapidly as k increases from 1 to 3, and then reaches an elbow where the cost equals 0.3986, after which the distortion decreases slowly. Since the cost at this point is at the bend of this curve, k equals 3 is the appropriate number of clusters.



**Figure 6.33:** The k-Means results for LIS patient 13 (ALSFRS-R=0) on day 1, where the x-axis and y-axis show the sample entropy values after mean normalization and feature scaling at different time points ( $t=1$  vs.  $t=2$ ). The black crosses are the centers of the clusters at each iteration, both figures show the results after 20 iterations. Left:  $k=2$ . Right:  $k=3$ .



**Figure 6.34:** Cost of k-Means for LIS patient 13 on day 1, where the x-axis represents the number of clusters and the y-axis represents the cost.

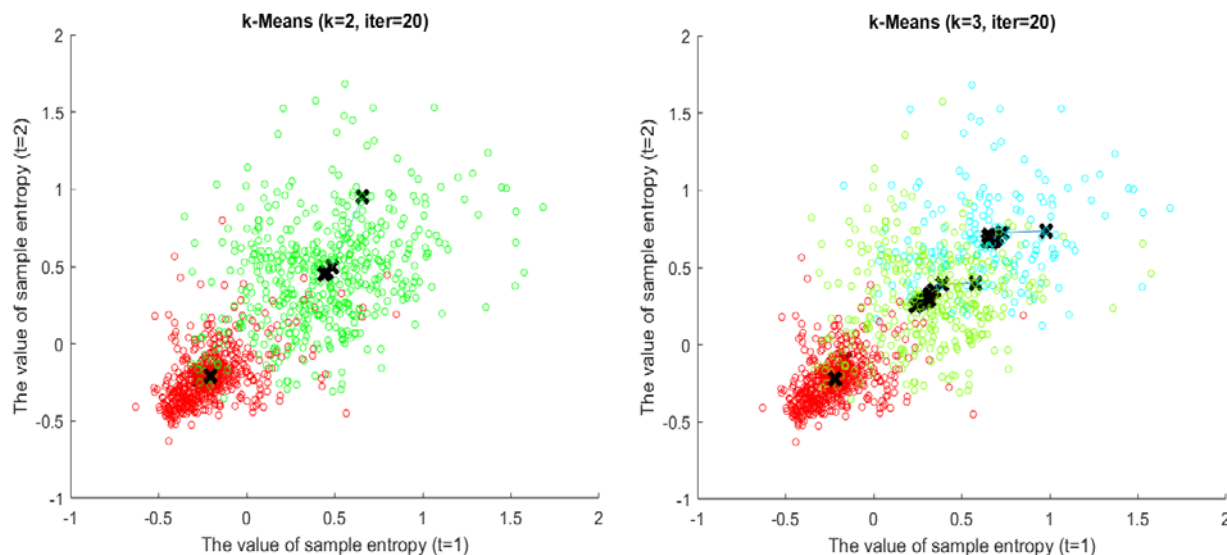
The third cluster, based on the original sample entropy results in Figure 6.19, presumed that the rest period was distinguished into several clusters due to the process of slowly increasing and then decreasing sample entropy values during the rest period of the two experimental periods.



The sample entropy values of the two periods after mean normalization and feature scaling still overlap after data reduction, the distinction of the clusters for patient 13 on the day one is not clear, but compared with the clustering results for this patient on another day, it can be seen that the sample entropy values after mean normalization and feature scaling for the spelling experimental period of this patient are approximately below 0.25. This is different from patient 11 and may be due to individual differences between patients. Compared to the DBSCAN results in Figure 6.44, although the red clusters in both figures are similar for the spelling experimental period in Patient 13 on the day one, the green clusters for K-means are much wider than the blue clusters for rest period of DBSCAN.

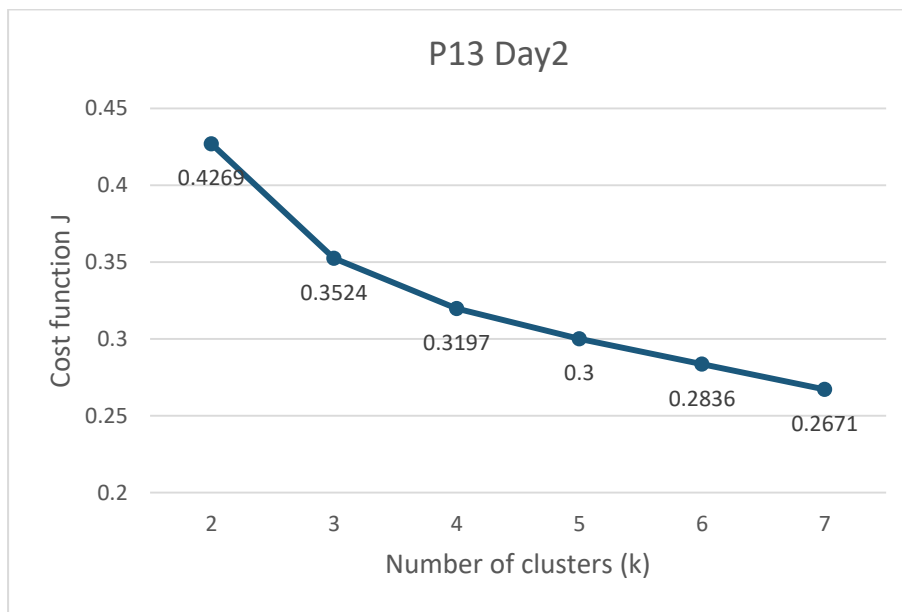
### LIS patient 13 on day 2

Figure 6.35 shows the k-Means results for patient 13 on day two. On this day, the data amount of the rest period with less data was used as the basis, and the same data amount was taken during the spelling experimental period, so that the data amounts of the two periods were equal, including a total of 1068 1-minute time series, half of which are from the spelling experimental period and the other half from the rest period.



**Figure 6.35:** The k-Means results for LIS patient 13 (ALSFRS-R=0) on day 2, where the x-axis and y-axis show the sample entropy values after mean normalization and feature scaling at different time points ( $t=1$  vs.  $t=2$ ). The black crosses are the centers of the clusters at each iteration, both figures show the results after 20 iterations. Left:  $k=2$ . Right:  $k=3$ .

The elbow method in Figure 6.36 shows the cost of k-Means for patient 13 on the day two in different clusters. It is clear to see that the cost decreases rapidly as  $k$  increases from 1 to 3, and then reaches an elbow where the cost equals 0.3524, after which the distortion decreases very slowly. Since the cost at this point is at the bend of this curve,  $k$  equals 3 is the correct number of clusters.



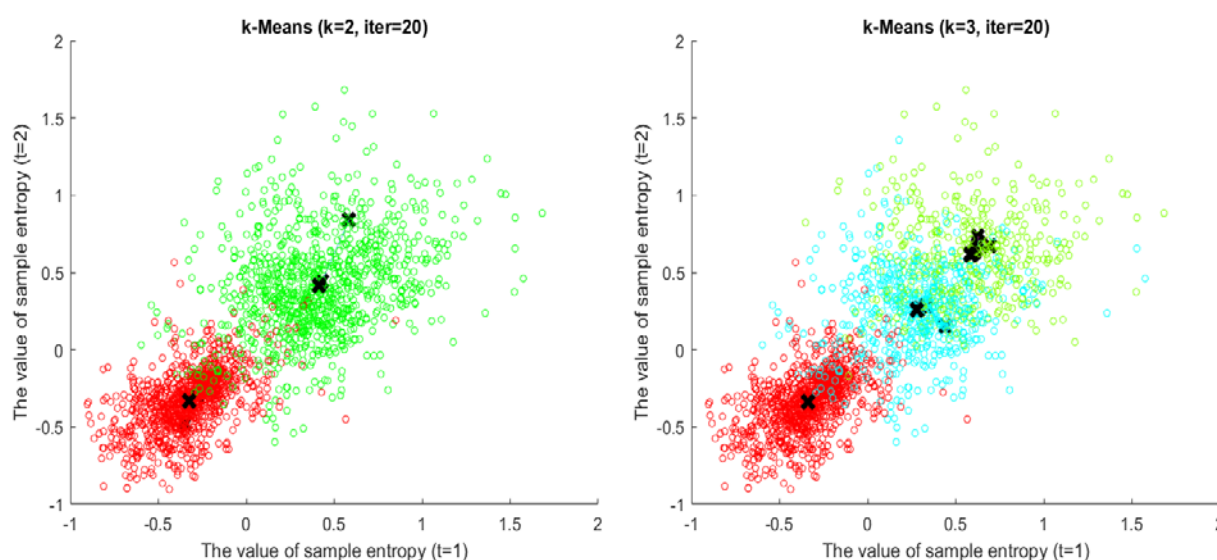
**Figure 6.36:** Cost of k-Means for LIS patient 13 on day 2, where the x-axis represents the number of clusters and the y-axis represents the cost.

Except for the two clusters of spelling experimental periods and rest periods that we already know. The third cluster, based on the original sample entropy results in Figure 6.20, presumed that the rest period was distinguished into several clusters due to the process of slowly decreasing sample entropy values in the first rest period. Even in the result with the lower cost of  $k=4$ , the clusters of the spelling experimental period (red) were not separated into two clusters, but the resting period was divided into three clusters, which shows that the brain activity of the patients was quite consistent when the spelling experiment was performed.

The sample entropy value after mean normalization and feature scaling was approximately less than 0.25 for the spelling experimental periods of patient 13 on day two, consistent with the clustering result for this patient on another day, but different from patient 11, probably due to individual differences between patients. The clustering number of 3 is generally consistent with the DBSCAN results in Figure 6.46.

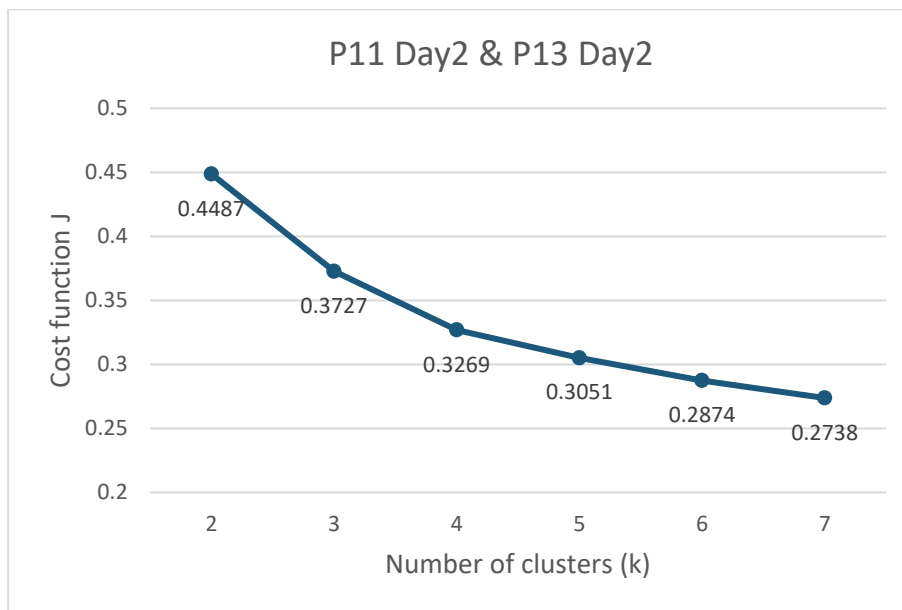
## LIS patient 11&13 on day 2

Figure 6.37 shows the results of combining the data from patients 11 and 13 on the day two as input data for k-Means analysis, which included a total of 1976 1-minute time series, half of which were from the spelling experimental period and the other half from the rest period. The reason for choosing these two days was to take one day for each of the two patients to see if the inclusion of individual differences would still present consistent results with those of a single patient. On the other hand, the amount of data in both days depends on the period with less data, rather than reducing the amount of data, because there is a large overlap between the two periods, so that the sample entropy values after the mean normalization and feature scaling in the experimental and rest periods overlap less, and the problem of unstable clustering results can be avoided as much as possible.



**Figure 6.37:** The k-Means results for LIS patient 11 & 13 (ALSFRS-R=0) on day 2, where the x-axis and y-axis show the sample entropy values after mean normalization and feature scaling at different time points (t=1 vs. t=2). The black crosses are the centers of the clusters at each iteration, both figures show the results after 20 iterations. Left: k=2. Right: k=3.

As we know, the input data included spelling experiments and rest periods for both patients. The elbow method in Figure 6.38 shows the cost of k-Means for patient 11 & 13 on the day two in different clusters. When k increases from 1 to 3, the cost decreases rapidly and then reaches an elbow where the cost equals 0.3727, after which the distortion decreases slowly. Since the cost at this point is at the elbow of this curve, k equals 3 is the correct number of clusters.



**Figure 6.38:** Cost of k-Means for LIS patient 11 & 13 on day 2, where the x-axis represents the number of clusters and the y-axis represents the cost.

The third cluster, based on the original sample entropy results in Figure 6.18 and Figure 6.20, presumed that the rest period was distinguished into several clusters due to the process of slowly increasing and then decreasing sample entropy values during the rest period of the two experimental periods.

The difference with the single-patient results is that the clustering of the spelling experimental period (red) for the result with the lower cost of  $k=4$  is separated into two clusters, which shows the individual difference between the two patients. This is because in the k-Means analysis for a single patient, the sample entropy value after mean normalization and feature scaling for the spelling experimental period was approximately below 0 for patient 11 and below 0.25 for patient 13. But overall, however, the results of the analysis with a cluster number of 3 are generally consistent with the DBSCAN results in Figure 6.48.

### 6.2.2 DBSCAN results

As proposed in section 2.9, this section presents the application of DBSCAN method to the sample entropy results in section 6.1.8, focusing on the clustering analysis during the spelling experimental period and the rest period before and after the experiment. The DBSCAN results are shown in the even numbered figures in Figure 6.40-Figure 6.48, where the x-axis and y-axis show the values of sample entropy after mean normalization and feature scaling.

To increase the amount of data, the 1-minute time series were overlapped with a 10-second moving window, and the overlap also made the data features (maximum, minimum, median, mean, standard deviation, median, and variance) more similar to improve the homogeneity of the input data and reduce outliers. Since the data characteristics are similar for each series ( $t=1,2,3,4,5,6$ ), only the  $t=1$  vs.  $t=2$  figure is shown here.

In the DBSCAN method, the smaller cluster can be considered as noise if the number of the two clusters is significantly different. Due to the different sizes of the two original periods, this work uses the period with the least data as the base, so that the spelling experimental period and the rest period are approximately the same size (Pham et al. 2005).

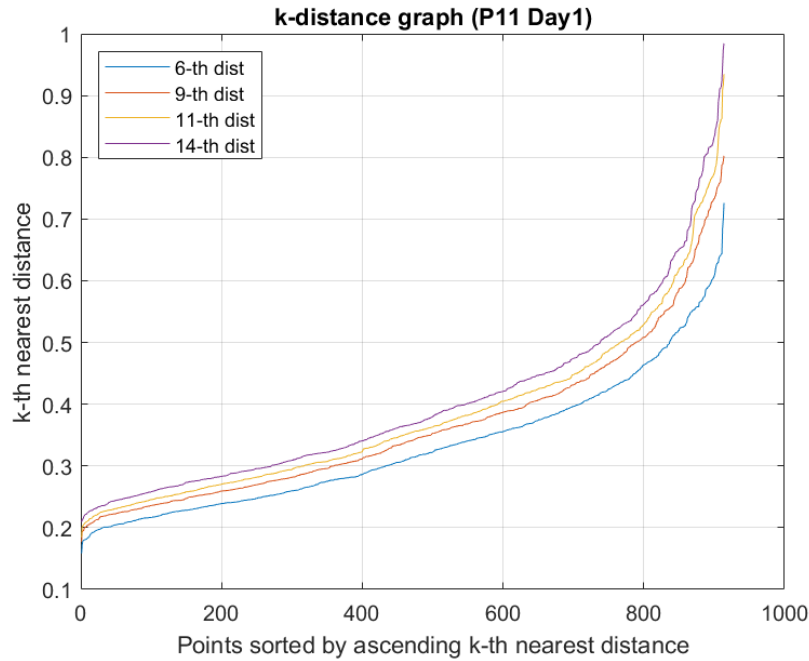
The k-distance graph is used as the basis for parameter selection, as shown in the odd numbered figures in Figure 6.39- Figure 6.47, where the x-axis represents the points sorted by distance and the y-axis represents the epsilon ( $\epsilon$ ) values. The parameter selection is described with reference to section 2.10.

### **LIS patient 11 on day 1**

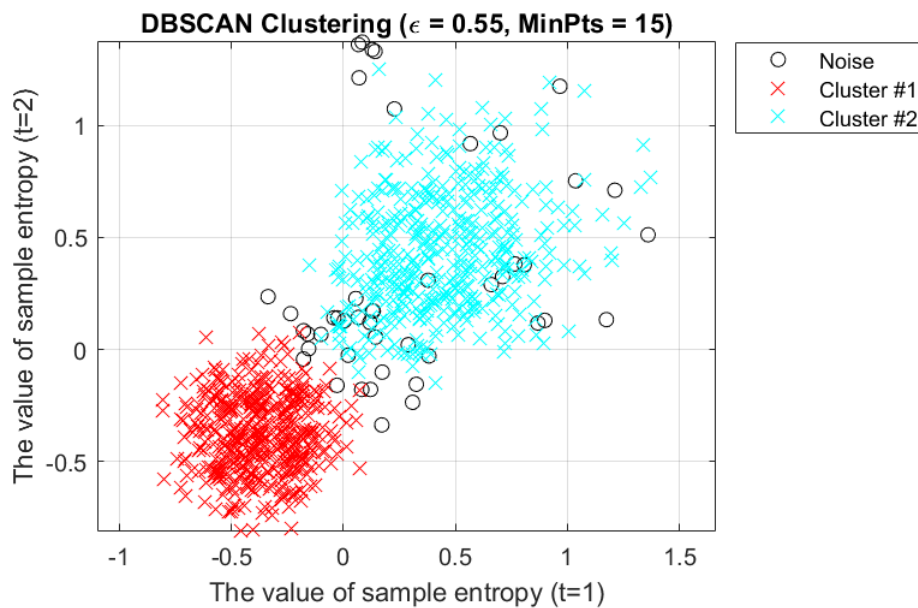
Figure 6.39 shows the k-distance graph for the patient 11 on day one. According to the rule of thumb density threshold  $\minPts \geq D+1$ , and Sander et al. suggested  $\minPts = 2 \times D$  (Sander et al. 1998), here the dimension is 6, so the  $\minPts$  parameter of DBSCAN is set to 7, 10, 12 and 15. Since the clustering is more robust when  $\minPts$  is set to a larger value, and the optimal k-th nearest distance is located at the elbow of this k-distance graph. Therefore, for the resting period and spelling experimental period of patient 11 on day one,  $\minPts$  was set to 15 and  $\epsilon$  was chosen equal to 0.55.

Figure 6.40 shows the DBSCAN results for patient 11 on the day one, including 914 1-minute time series, half of which are from the spelling experimental period and the other half are from the rest period. Here the input data is the same as k-Means, which facilitates the comparison of the subsequent results and also avoids significant differences in the number of the two periods, causing the smaller period to be considered as noise.

According to the parameter selection of k-distance in Figure 6.39, the results of DBSCAN show a total of three clusters, besides the already known spelling experimental period (red crosses) and the rest period (blue crosses), there are also noise (black circles), and the noise is mainly distributed in the part where the two clusters overlap, and in some places far from the center of the rest cluster.



**Figure 6.39:** The k-distance graph for LIS patient 11 on day 1, where the x-axis represents the points sorted by distance and the y-axis represents the epsilon ( $\epsilon$ ) values. Four cluster levels are displayed in blue, red, yellow, and purple when the minPts parameter of DBSCAN is set to 7, 10, 12 and 15, respectively.



**Figure 6.40:** The DBSCAN results for LIS patient 11 (ALSFRS-R=0) on day 1, where the x-axis and y-axis show the sample entropy values after mean normalization and feature scaling at different time points ( $t=1$  vs.  $t=2$ ). All time series are divided into two clusters (red and blue crosses) and noise (black circles).

It can easily be seen in the Figure 6.29 that the DBSCAN cluster distribution is essentially the same as the k-means result ( $k=2$ ). It was found that the sample entropy value

after mean normalization and feature scaling was approximately less than 0 for the spelling experimental period of patient 11 on the day one, which is in agreement with the clustering result of this patient on another day, but unlike the clustering result of patient 13, which is probably caused by the individual differences between the patients, and this result is also consistent with the clustering in the period of spelling experiment of k-means.

### LIS patient 11 on day 2

The k-distance graph for the patient 11 on day two is shown in Figure 6.41. By the rule of thumb density threshold  $\text{minPts} \geq D+1$ , and  $\text{minPts} = 2 \times D$  proposed by Sander et al. (Sander et al. 1998), the dimension here is 6, thus the minPts parameter of DBSCAN is set to 7, 10, 12 and 15. When minPts is set to a larger value, the clustering is more robust, and the optimal k-th nearest distance is located at the elbow of this k-distance graph. This is why minPts was set to 15 and  $\epsilon$  was made equal to 0.52 for the resting period and spelling experimental period of patient 11 on day two.

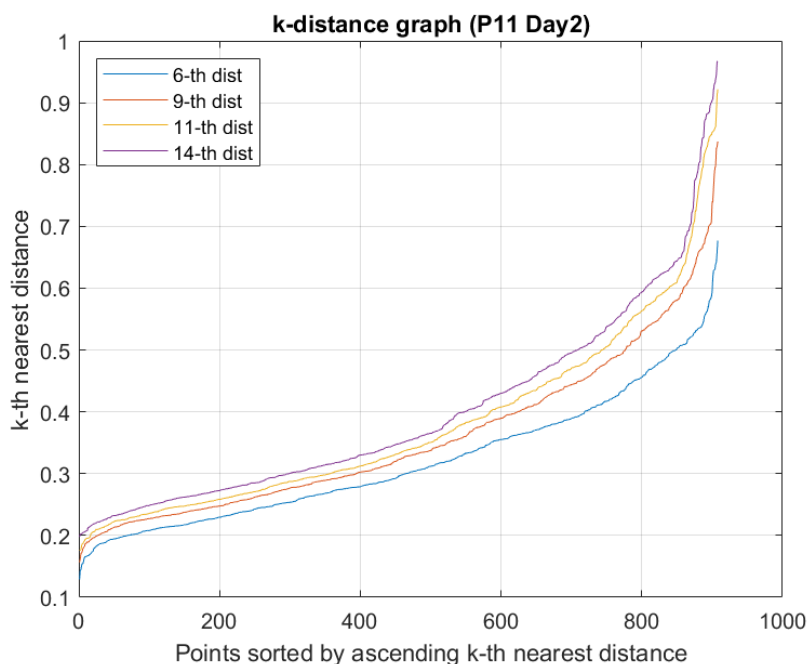


**Figure 6.41:** The k-distance graph for LIS patient 11 on day 2, where the x-axis represents the points sorted by distance and the y-axis represents the epsilon ( $\epsilon$ ) values. Four cluster levels are displayed in blue, red, yellow, and purple when the minPts parameter of DBSCAN is set to 7, 10, 12 and 15, respectively.

The DBSCAN results for patient 11 on the day two are shown in Figure 6.42. The input data here is the same as k-Means and consist of 908 1-minute time series, half of which are from the spelling experimental period and the other half are from the rest period, which

facilitates the comparison of the subsequent results and also avoids significant differences in the number of the two periods, resulting the smaller period to be considered as noise.

Based on the parameter selection of k-distance in Figure 6.41, the results of DBSCAN indicate a total of three clusters, except for the already known spelling experimental period (red crosses) and the rest period (blue crosses), there are also noise (black circles). The noise is mainly distributed in the part where the two clusters overlap and most of the places are far from the center of the rest clusters.

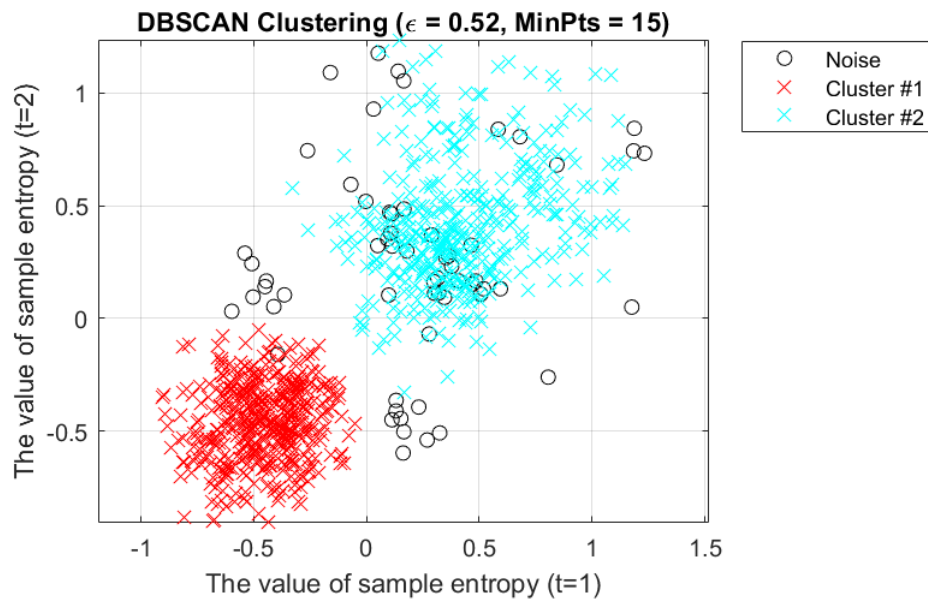


**Figure 6.42:** The DBSCAN results for LIS patient 11 (ALSFRS-R=0) on day 2, where the x-axis and y-axis show the sample entropy values after mean normalization and feature scaling at different time points (t=1 vs. t=2). All time series are divided into two clusters (red and blue crosses) and noise (black circles).

In Figure 6.31, it is easy to see that the DBSCAN cluster distribution essentially matches the k-means result ( $k=2$ ). The red clusters in both figures are the spelling experiment of patient 11 on the day two, whose sample entropy values after mean normalization and feature scaling are approximately below 0. The sample entropy values between 0 and 1.2 are the rest periods, and the noise distribution further away from the center of rest cluster. Overall, the density of DBSCAN was high in the experimental period for patient 11, and there were few noises near the experimental period, which is consistent with the results of k-means ( $k=4$ ), which still did not divide the spelling experimental clusters into two clusters, showing the consistency of brain wave activity when patients participated in the experiment.



### LIS patient 13 on day 1

Figure 6.43 shows the k-distance graph for the patient 13 on day one. According to the rule of thumb  $\text{minPts} \geq D+1$ , and Sander et al. suggested  $\text{minPts} = 2 \times D$  (Sander et al. 1998), here the dimension is 6, so the minPts parameter of DBSCAN is set to 7, 10, 12 and 15. Since the clustering is more robust when minPts is set to a larger value, and the optimal epsilon ( $\epsilon$ ) parameter is located at the elbow of this k-distance graph. Therefore, for the resting period and spelling experimental period of patient 13 on day one, minPts was set to 15 and  $\epsilon$  was chosen equal to 0.37.

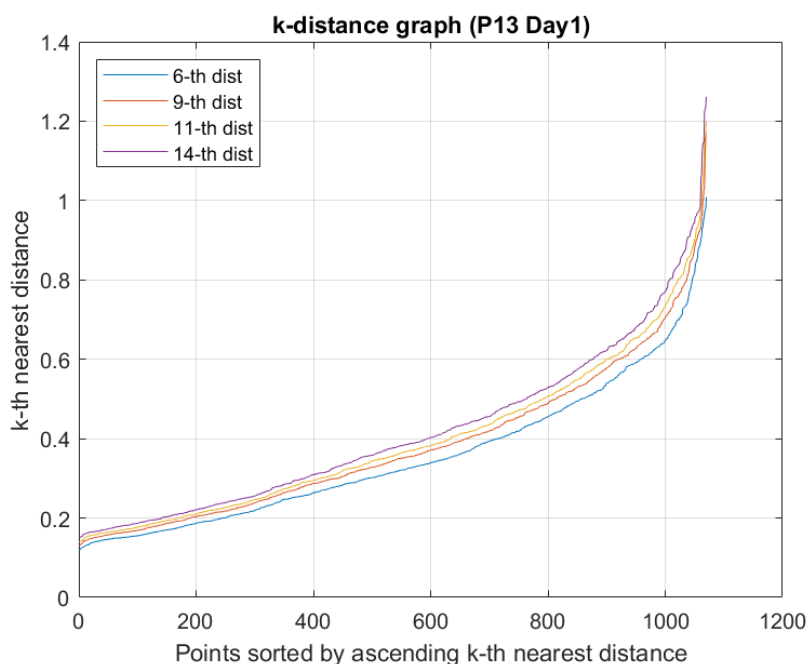


**Figure 6.43:** The k-distance graph for LIS patient 13 on day 1, where the x-axis represents the points sorted by distance and the y-axis represents the epsilon ( $\epsilon$ ) values. Four cluster levels are displayed in blue, red, yellow, and purple when the minPts parameter of DBSCAN is set to 7, 10, 12 and 15, respectively.

Figure 6.44 shows the DBSCAN results for patient 13 on the day one, including 1070 1-minute time series, half of which are from the spelling experimental period and the other half are from the rest period. Here the input data is the same as k-Means, which facilitates the comparison of the subsequent results and also avoids significant differences in the number of the two periods, causing the smaller period to be considered as noise.

According to the parameter selection of k-distance in Figure 6.43, the results of DBSCAN show a total of three clusters, besides the already known spelling experimental period (red crosses) and the rest period (blue crosses), there are also noise (black circles).

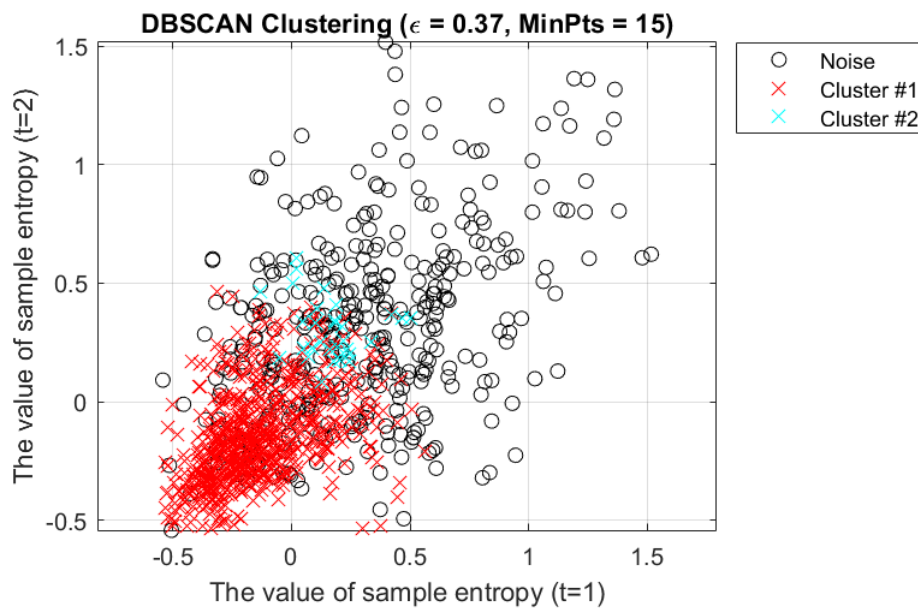


**Figure 6.44:** The DBSCAN results for LIS patient 13 (ALSFRS-R=0) on day 1, where the x-axis and y-axis show the sample entropy values after mean normalization and feature scaling at different time points ( $t=1$  vs.  $t=2$ ). All time series are divided into two clusters (red and blue crosses) and noise (black circles).

It is easily seen in Figure 6.33 that the DBSCAN cluster distribution does not match the k-mean results. The density difference between the spelling experimental period, rest period and noise for patient 13 on the day one was not significant, so the results of the DBSCAN clustering distribution considered the sample entropy values after mean normalization and feature scaling between about 0.25-0.55 as the rest period, while the range of rest periods was larger on other days. As described in section 6.1.8, patient 13 was able to freely spell "I look forward to a vacation" on day two, but the sentences were spelled without meaning on the day one. Based on the original sample entropy results in Figure 6.19, it is presumed that Patient 13 was unable to concentrate due to the process of slowly increasing sample entropy values in the latter part of the experimental periods on this day.

### LIS patient 13 on day 2

The k-distance graph for the patient 13 on day two is shown in Figure 6.45. By the rule of thumb  $\text{minPts} \geq D+1$ , and  $\text{minPts} = 2 \times D$  proposed by Sander et al. (Sander et al. 1998), the dimension here is 6, thus the minPts parameter of DBSCAN is set to 7, 10, 12 and 15. When minPts is set to a larger value, the clustering is more robust, and the optimal epsilon ( $\epsilon$ ) parameter is located at the elbow of this k-distance graph. This is why minPts was set to

15 and  $\epsilon$  was made equal to 0.48 for the resting period and spelling experimental period of patient 13 on day two.

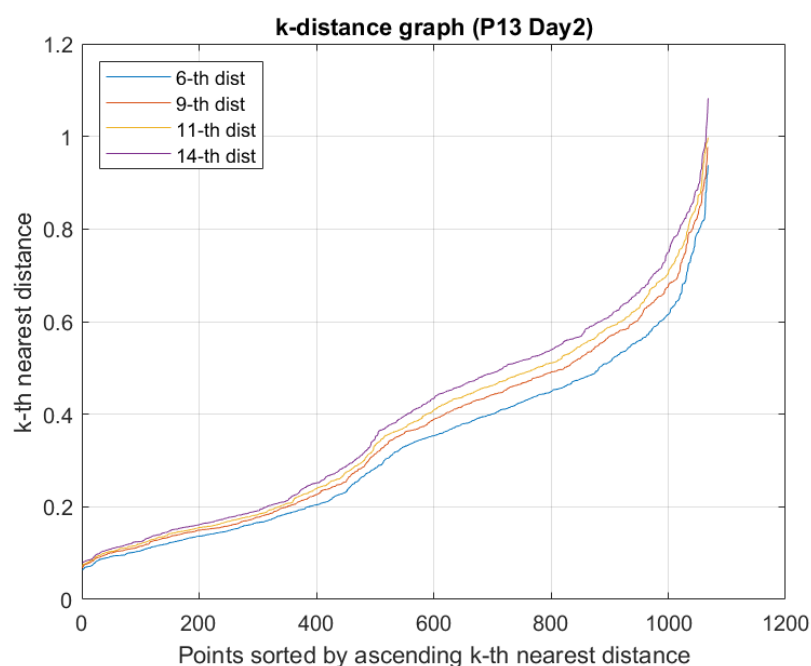


**Figure 6.45:** The k-distance graph for LIS patient 13 on day 2, where the x-axis represents the points sorted by distance and the y-axis represents the epsilon ( $\epsilon$ ) values. Four cluster levels are displayed in blue, red, yellow, and purple when the minPts parameter of DBSCAN is set to 7, 10, 12 and 15, respectively.

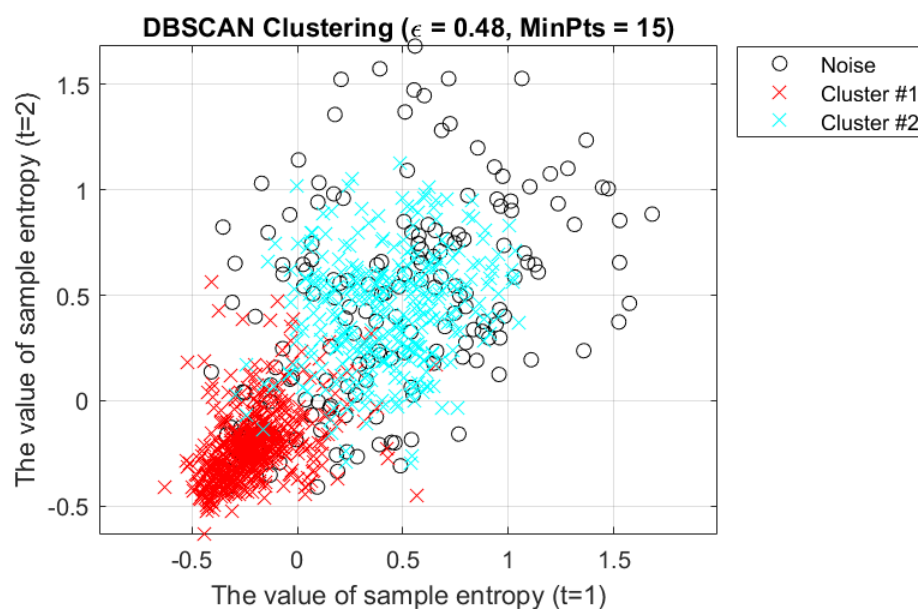


**Figure 6.46:** The DBSCAN results for LIS patient 13 (ALSFRS-R=0) on day 2, where the x-axis and y-axis show the sample entropy values after mean normalization and feature scaling at different time points (t=1 vs. t=2). All time series are divided into two clusters (red and blue crosses) and noise (black circles).

The DBSCAN results for patient 13 on the day two are shown in Figure 6.46. The input data here is the same as k-Means and consist of 1068 1-minute time series, half of which are from the spelling experimental period and the other half are from the rest period, which facilitates the comparison of the subsequent results and also avoids significant differences in the number of the two periods, resulting the smaller period to be considered as noise.

Based on the parameter selection of k-distance in Figure 6.45, the results of DBSCAN indicate a total of three clusters, except for the already known spelling experimental period (red crosses) and the rest period (blue crosses), there are also noise (black circles). The noise is mainly distributed in the part where the two clusters overlap and most of the places are far from the center of the rest clusters.

It can be easily seen in Figure 6.35 that the DBSCAN cluster distribution results are similar to the k-mean results ( $k=3$ ). The red clusters in both figures are the spelling experiment of patient 13 on the day two, whose sample entropy values after mean normalization and feature scaling are approximately below 0.25. The sample entropy values between 0.25 and 1 are the rest periods similar to the green clusters with k-means, and the noise distribution further away from the center of rest cluster resembles the blue clusters for k-means. Overall, the density of DBSCAN was high in the experimental period, and there were few noises were near the experimental period, which is consistent with the results of k-means ( $k=4$ ), which still did not divide the spelling experimental clusters into two clusters, showing the consistency of brain wave activity when patients participated in the experiment.

### **LIS patient 11&13 on day 2**

Figure 6.47 shows the k-distance graph for the patient 11 and 13 on day two. In accordance with the rule of thumb  $\text{minPts} \geq D+1$ , and Sander et al. suggested  $\text{minPts} = 2 \times D$  (Sander et al. 1998), here the dimension is 6, so the minPts parameter of DBSCAN is set to 7, 10, 12 and 15. Since the clustering is more robust when minPts is set to a larger value, and the optimal epsilon ( $\epsilon$ ) parameter is located at the elbow of this k-distance graph. Consequently, minPts was set to 15 and  $\epsilon$  was chosen equal to 0.4 for the resting period and spelling experimental period of patient 11 and 13 on day two,.

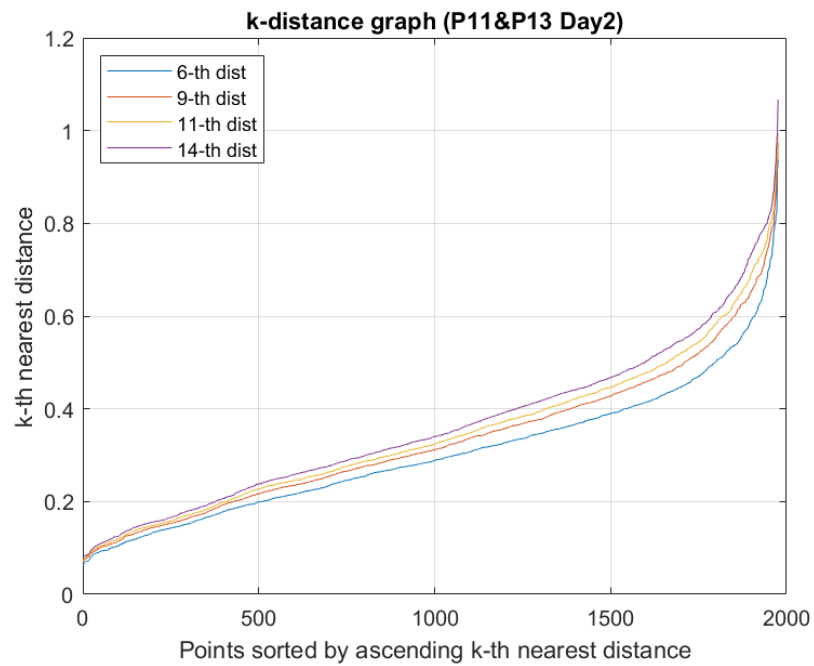


**Figure 6.47:** The k-distance graph for LIS patient 11 & 13 on day 2, where the x-axis represents the points sorted by distance and the y-axis represents the epsilon ( $\epsilon$ ) values. Four cluster levels are displayed in blue, red, yellow, and purple when the minPts parameter of DBSCAN is set to 7, 10, 12 and 15, respectively.

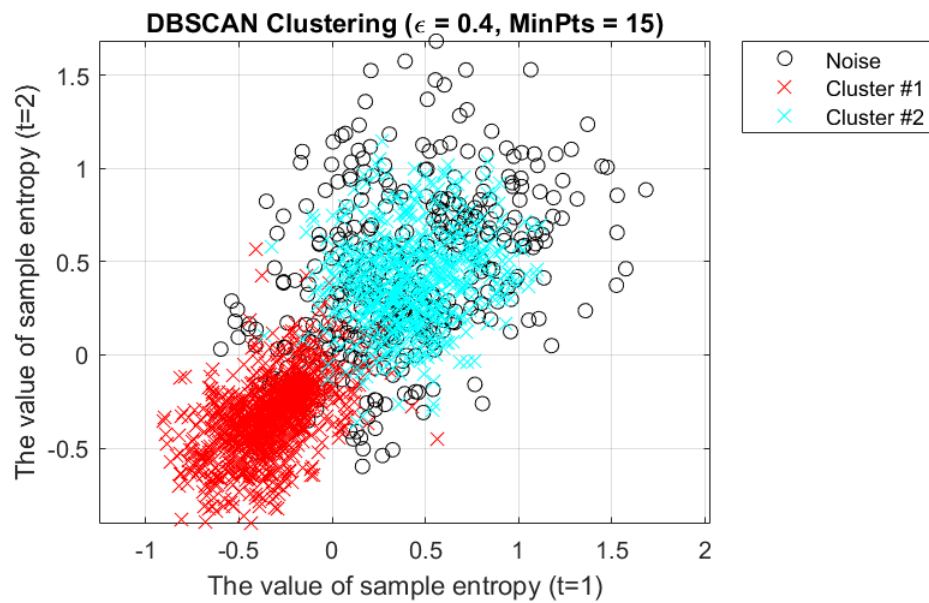


**Figure 6.48:** The DBSCAN results for LIS patient 11 & 13 (ALSFRS-R=0) on day 2, where the x-axis and y-axis show the sample entropy values after mean normalization and feature scaling at different time points (t=1 vs. t=2). All time series are divided into two clusters (red and blue crosses) and noise (black circles).

Figure 6.48 shows the DBSCAN results for patient 11 and 13 on the day two, including 1976 1-minute time series, half of which are from the spelling experimental period and the other half are from the rest period. Here the input data is the same as k-Means, which facilitates the comparison of the subsequent results and also avoids significant differences in the number of the two periods, causing the smaller period to be considered as noise.

According to the parameter selection of k-distance in Figure 6.47, the results of DBSCAN show a total of three clusters, besides the already known spelling experimental period (red crosses) and the rest period (blue crosses), there are also noise (black circles), and the noise is mainly distributed in the part where the two clusters overlap, and in some places far from the center of the rest cluster.

There is an easy observation in Figure 6.37 that the DBSCAN cluster distribution results are similar to the k-mean results ( $k=3$ ). The red clusters in both figures are the spelling experiment of patient 11 and 13 on the day two, whose sample entropy values after mean normalization and feature scaling are approximately below 0.25. The sample entropy values between 0.25 and 1 are the rest periods similar to the blue clusters with k-means, and the noise distribution further away from the center of rest cluster resembles the green clusters for k-means. Overall, the density of DBSCAN was high in the experimental period, and there were few noises near the experimental period.

### 6.2.3 Discussion of machine learning results

In section 6.2, the k-means and DBSCAN methods were applied to the sample entropy results for two days each of two LIS patients, and both clusters of resting and spelling experimental periods were clearly observed for three of these four days.

The data set for each period was selected on the basis of the smallest period of two days' data for the same patient. Patient 11 had more than 450 1-minute time series per period and patient 13 had less than 550 1-minute time series, so that the data for both patients could be combined later with  $500 \pm 50$  1-minute time series per period. First, one is to try to avoid the overlap of sample entropy values after mean normalization and feature scaling in the two periods, which leads to unstable clustering results. Second, it avoids significant differences in the number of the two periods, which leads to the smaller period being considered as noise.

The results of two patients for each of two days were analyzed separately. In the k-means analysis for a single patient, the sample entropy values after mean normalization and feature scaling for the spelling experimental period were approximately below 0 for patient 11 and below 0.25 for patient 13. The DBSCAN results were similar to k-Means results,

---

except that the density of the resting period on day one for patient 13 could not be distinguished from that of the experimental period.

Regarding the number of clusters for a single day of a patient, in addition to the two known clusters of spelling experimental period and resting period, the most suitable number of clusters for k-means according to the results of the elbow method is three, which is probably due to the fact that the sample entropy value of the rest period has a slowly increasing and then decreasing process between the two experimental periods, which separates the rest period into several clusters. The DBSCAN results also showed 3 clusters, besides the already known spelling experimental period and the resting period, there was also noise, the noise was mainly distributed in the part where the two clusters overlapped, and except for patient 13 on the day one, far from the center of the rest period in most places. However, there was almost no noise near the experimental period, which is consistent with the results of k-means, even if the number of clusters was set to four, it still did not divide the spelling experiment cluster into two clusters, indicating the consistency of brainwave activity when patients participated in the experiment.

Finally, in order to see if individual differences had an effect, both k-Means and DBSCAN showed results for 3 clusters when combining two patients for one day each, and the results were consistent with those of a single patient. The sample entropy value after mean normalization and feature scaling of the spelling experimental period was below 0.25 due to the merging of data from patients 11 and 13. And individual differences are also reflected in k-means results, and the spelling experiment clusters were divided into two clusters when the number of clusters was set to 4.

In my opinion, DBSCAN can better find the appropriate number of clusters because an algorithm like k-Means splits the data set at the midpoint of two clusters, so when using the k-Means algorithm, it is important to keep the input data equal for both periods. However, in the case for a single day of a patient with  $k=4$  set in k-Means, the consistency of the patient's consciousness during participation in the experiment is verified, so the k-Means algorithm can be used as a confirmation of the DBSCAN algorithm.

## Chapter 7

# Discussion & Conclusions

*“The brain is the organ of destiny. It holds within its humming mechanism secrets that will determine the future of the human race.”*

*– Wilder Penfield (1891-1976)*

### 7.1 Discussion

The human brain is the most complex organ in the world. As technology becomes more advanced, people understand more and more about every organ of the body, the human brain is still the most unknown part of the human body. Although people have tried to explore and unravel the mystery of the human brain for centuries, our understanding of it is still limited.

CLIS is like being in a prolonged state of muscle relaxant without anesthetic during surgery, or it is like experiencing one in a thousand chance of anesthetic awareness during anesthesia. Both CLIS patients and DOC patients have concerns of band shifts to lower frequencies that are easily recognized as deep sleep states in healthy individuals, as explained in section 3.2. Therefore, in this thesis sample entropy, permutation entropy, and Poincaré plots are used as feature extraction to analyze consciousness from continuously recorded brainwave signals from patients with different clinical states of consciousness.

Not only the time domain methods avoid the problem of lower frequency bands in CLIS and DOC patients, but also these methods have been proposed for monitoring brain waves of patients in surgery (Hayashi et al. 2014; Kreuzer et al. 2014; Wei et al. 2014; Hayashi et al. 2015). An anesthetic procedure can map the entire process from loss of



consciousness to recovery (see Figure 2.1), and there are more anesthesia cases than CLIS patients or DOC patients, so these methods has been well validated in the field of anesthesia, which greatly improves their applicability to CLIS patients. Of course, general anesthesia here refers to healthy people without brain damage. The following lists the patient types and brain signal types applied in this thesis.

- One CLIS patient with invasive ECoG signals
- Four CLIS patients with non-invasive EEG signals
- Two LIS patients (ALSFRS-R=0) with non-invasive EEG signals
- Two MCS patients with non-invasive EEG signals
- Four UWS patients with non-invasive EEG signals

The CLIS patient GR with the invasive ECoG signal is the only CLIS patient dataset I know of with such "ground truth" and it has an 88% accuracy response rate (Wu et al. 2020). Four CLIS patients B, F, G, and W show similar results not only by sample entropy but also by Poincaré plots analysis, which are consistent with the observations in (Chaudhary et al. 2017). It indicates that the results of both analytical methods could be correct. Two LIS patients 11 and 13 with the remaining eye movements as the "ground truth" of consciousness were again able to demonstrate the feasibility of the sample entropy method for LIS patients based on the logical sentences they could spell. In six DOC patients, sample entropy showed an increase in patient brain activity for reported events during the experiment.

These above results applied to various types of patients, different types of brain signals and across different time scales (including sleep), demonstrate the feasibility of these methods in CLIS patient, where sample entropy showed good resolution for both ECoG signals up to 24 hours a day and EEG signals focused on one or two hours at the time of the experiment. It is also found that permutation entropy can be a reference indicator to monitor whether the patient is in sleep state. In addition, not all patients are responsive to external environmental stimuli, both CLIS and DOC patients have the problem that the more severe the disease, the more fragmented the sleep state (Cologan et al. 2013; Soekadar et al. 2013). If the patient can still measure the complete sleep stages, it means that the patient still has internal brain activity. Finally, k-Means and DBSCAN as the unsupervised learning methods were used for two LIS patients with ALSFRS-R score of 0 to estimate the consciousness threshold for individual participation in the experiment.

All the results in this thesis are multiple channels that presented a consistent tendency, first, it indicates that the patient was fully involved in the experiment, and second, to avoid the compensatory effect of brain damage/brain lesions caused by car accidents or strokes

resulting in the patient's Brodmann area to be different from the general healthy subjects. Although detection of consciousness with these methods may involve only a small number of patients with CLIS and DOC, as Tonin et al. (Tonin et al. 2020) reported that slow spelling speed (ca. 0.5 char/min) is preferred by patients compared to experienced social isolation, these methods have the potential to identify features of the conscious state, which provides rehabilitation or improved communication possibilities for these patients.

Like the Salzburg (Austria) dataset, there is another one that also did sleep analysis from Liège (Belgium). Since the dataset did not contain event notes, the sample entropy results could not be checked against the event notes, so the results were not included in the results chapter, although I found that the value of sample entropy seems to be related to the number of months between the time of data collection and death. Unfortunately, this data set does not record this number of months for all patients who died. Therefore, the following figure shows the analysis for the 6 patients with such records.

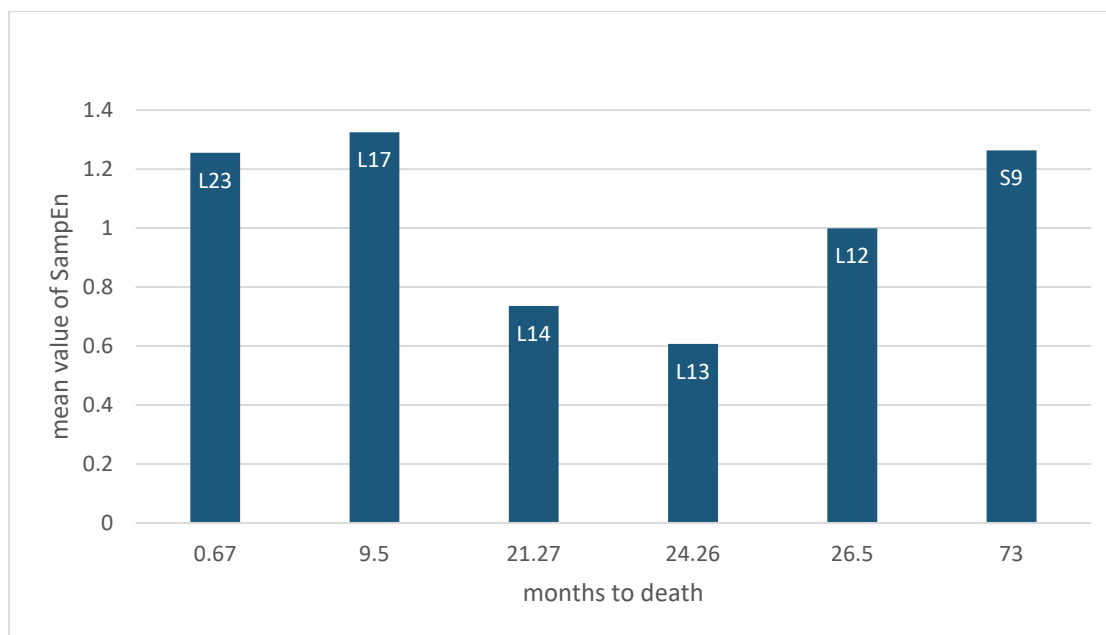


**Figure 7.1:** The average value of sample entropy for 24 h at the time of experiment for 6 patients versus the number of months between experiment and death.

There are five patients from the dataset from Liege, Belgium and one from the dataset from Salzburg, Austria. All these 6 patients are diagnosed as Unresponsive Wakefulness Syndrome (UWS). In Figure 7.1 shows the average value of sample entropy for 24 h, three of the patients had higher sample entropy values when they were more than 6 years and less than 1 year before death, and the other three had lower sample entropy values when they were about 2 years before death.

It seems that the value of sample entropy decreases as the patients get closer to the moment of passing away, but increases steeply within a year before the time of death. I hope that by observing the value of the sample entropy can help doctors to predict the current status of patients. However, due to individual differences and the course of each disease, more information needs to be collected to confirm this claim. For example, the same experiment should be performed with the same patient every month in order to follow the variation of the sample entropy values, etc. Perhaps in the future it can serve as a reference index for physicians when evaluating whether to turn off a patient's life-sustaining equipment.

## **7.2 Conclusions & Future work**

In this thesis, three approaches for detecting the state of consciousness in complete locked-in patients are presented: sample entropy, permutation entropy, and Poincaré plot, implemented not only in intracranial ECoG signals with greater signal-to-noise ratio (SNR) and higher signal amplitude, but also in non-invasive EEG signals widely used in brainwave studies. The portability of EEG signals is a major advantage compared to large instruments such as fMRI. The analysis of time domain signals prevents disease-related reduction of EEG frequency bands in CLIS/LIS or MCS/UWS patients. Different approaches exhibited different healthy interpretations of consciousness. Although each method suggested different time periods for consciousness, all of them were able to identify the time period around the time window of the experiment where consciousness was confirmed by experimenters receiving correct feedback from the CLIS patient during that period. It was also successfully identified that DOC patients were able to recognize stimuli in their surrounding environment and assessed whether the patients experienced periods of consciousness.

During the investigation of consciousness in CLIS patients, my collaborator and I had tried Granger Causality (Hesse et al. 2003; Wang et al. 2007), but when I tried to incorporate it into my processes, I found that Granger Causality was too sensitive to the filter, and the results of consciousness varied greatly when I changed to a different type of filter (Florin et al. 2010). However, Granger Causality is used in EEG signals to find the loss of consciousness (LOC) and recovery of consciousness (ROC) in anesthesia during surgery (Nicolaou et al. 2012; Nicolaou and Georgiou 2014), so it may be an option for future research.

It is worth mentioning that with respect to CLIS/LIS patients, the response rate and the type of questions asked by the experiment answering yes and no questions may be important factors in explaining these results. Therefore, different types of questions and associated feedback can be correlated with each other to obtain further results in the future with reference to the value of sample entropy, where the results based on the sample entropy can be known to serve as an objective reference indicator to avoid making the experimental results dependent on the patient's willingness. Although the results presented in this thesis are currently computed offline, these methods have not yet been implemented in real time. However, due to the short computation time, real-time applications are readily available and several papers have been published on real-time applications of sample entropy, permutation entropy, and Poincaré plots in the field of anesthesia (Hayashi et al. 2014; Kreuzer et al. 2014; Wei et al. 2014; Hayashi et al. 2015).

The final part of this thesis uses unsupervised learning methods k-Means and DBSCAN to obtain a threshold of consciousness for individual participation in the experiment from the feature extraction results for each patient, avoiding different parameter choices in each method and individual patient differences. These methods can be combined with competing methods in the future, as proposed in (Adama et al. 2019; Adama et al. 2022). Moreover, such a hybrid method approach can even be ameliorated by introducing further methods, such as the other unsupervised learning method hierarchical clustering to enhance the analysis of consciousness threshold, or the Silhouette method to distinguish how many clusters of the k-means method. It may significantly advance the solution of the consciousness detection problem in CLIS patients. Once this can also be demonstrated for other CLIS patients with verified periods of consciousness, it can be considered as a step towards reliable consciousness detection and thus a preferred communication option for CLIS patients through a brain–computer interface (BCI). Therefore, we conclude that for the detection of consciousness in CLIS patients, in order to find appropriate communication times, the combination of the presented approaches in a brain–computer interface system increases the probability of correctly detecting the state of consciousness in CLIS patients. Ultimately, the methods and results provided in this thesis can provide an objective reference indicator for family members to communicate with CLIS patients and further enhance the brain stimulation of patients to prolong their lives and improve their quality of life (QOL).

# Appendix A Supplemental Material

## Experimental Protocol

Date: 2008-03-16

Arrive: 14.50  
Heart rate: 98  
Oxygen saturation: 97  
Lying on side: back/left  
Respiration BPM: 15  
Ground: S032  
Reference: G102

Initial eye movement looked much stronger than previous days. I asked him questions (without video):

You feel good today? +

You feel bad today? -

0. Are you happy that I'm here? +

0. Would you prefer to be alone and to watch TV? -

The responses were so strong that I thought a conversation was possible. I turned on the video. The following questions were asked. Someone should check the video to check me.

1. You feel good today? +

1. You feel bad today? -

2. Are you German? +

2. Are you Dutch? -

3. Do you feel pain? -

3. Are you free of pain? +

4. Are you satisfied by the health care at BS (city in Germany)? +

4. Are you unsatisfied by the health care at BS? -

4. Are you unsatisfied by the health care at BS? -

4. Are you satisfied by the health care at BS? +

5. Are you still happy to have decided for the operation? +

5. Are you sorry for having decided to do the operation? -

6. Do you think, you have feedback control over sound? +

6. Do you think the feedback is not controllable? -

7. Are the sounds loud enough for you? +

7. Should we turn the speaker louder? -

7. Should we turn down the speaker?

7. Are the speakers o.k.? +

"We would like to know about your psychological status. We want to know how your mood is."

8. Are you positive regarding the future? +

8. Do you not know exactly what future will bring for you, so, are you neutral for your future? -

8. Are you negative for the future? -

"I will ask you now a question that has to be asked to you some when."

9. Do you wish sometimes, you were dead? -

9. You never wished to be dead? +##

10. Can you enjoy your life under these circumstances? +

10. You don't enjoy your life any more? -
11. Was it a good decision to bring you to BS? +  
11. Do you prefer to go back to Vohenstrauss (his home town)? +&-  
(not clear)  
11. Do you prefer to go back to Vohenstrauss? -
12. Do you want to stay at BS in the future? -  
12. Do you want to stay at BS in the future? -
12. Do you prefer to go into another nursing home? +  
12. Do you prefer to go into another nursing home? +
13. You want to go back to Vohenstrauss in some later period? Do I  
understand you correctly? + (no clear answer)  
13. You want in another nursing home than Vohenstrauss? + (no  
clear answer)

"I have been informed, that our political contacts we have engaged to  
convince the health insurance regarding your care costs will publish a  
report about you in the SPEIGEL (very renown German journal).  
Unfortunately, I don't know more than that, neither about the content  
of the article. I will inform myself to tell you."

14. Shouldn't we go to public with the health insurance? -  
14. Shouldn't we fight we the health insurance? -  
14. Should we fight with the health insurance? -
15. For long term schedule: You want to go to Vohenstrauss? +  
15. For long term schedule: You want to stay at BS? +

"It's not clear to me what you want to say, GR."

16. You don't care where you will be in future? -

"I ask you a different way now."

17. For long term schedule, are you Prefer Vohenstrauss before BS?  
-

"I see a NO in your eyes, is this correct?"  
+ (including corner of the mouth)

(I tried letting him repeat the mouth twitch but it didn't always work.  
Instructed hi to use whatever he could or both).

17. Do you prefer, for long term, to stay at BS before  
Vohenstrauss? -  
17. You want another nursing home than those 2?

You want to spell something?

George then spelled the word "AMBERG"  
This was a long process where I repeatedly double checked (verified  
"correct?" and "wrong?") if I got all letters correct. I also asked him  
for confirmation or declination of the final word "AMBERG". Someone  
should CHECK the video and check me.  
I, then suspected that he wanted to go to Amberg instead of staying in  
BS or going back to Vehenstrauss.

18. You mean, you want to go to Amberg in the future? +  
Did I understood you wrong, that you want to go to Amberg in the  
future? -

VIDEO lost power. We take a break and I type up this conversation.

Time: 17.00  
Heart rate: 94

# Appendix B Sample entropy results

For the CLIS dataset from section 5.2, the top diagram of Figure B.1-Figure B.4 shows the sample entropy results for CLIS patients B and F over two days, the results for the other CLIS patients G and W over two days are presented in section 6.1.7. The figure below shows the trigger marks, those with numbers represent experimental state and those without numbers represent rest state. Between two red vertical lines indicate sessions, each session lasts around 10 minutes. In order to distinguish more clearly the difference between experimental and rest time, in these datasets all sessions in a day are combined in chronological order in the same figure. We assume that the higher the sample entropy value, the higher the relative consciousness of the patient. This interpretation is based on the results shown in (Chaudhary et al. 2017) where during the corresponding time slots (see Figure B.1-Figure B.4 trigger marks), the experimenter received a good number of correct answers, thus indicating the consciousness of the patient.

## CLIS patients B on day 1

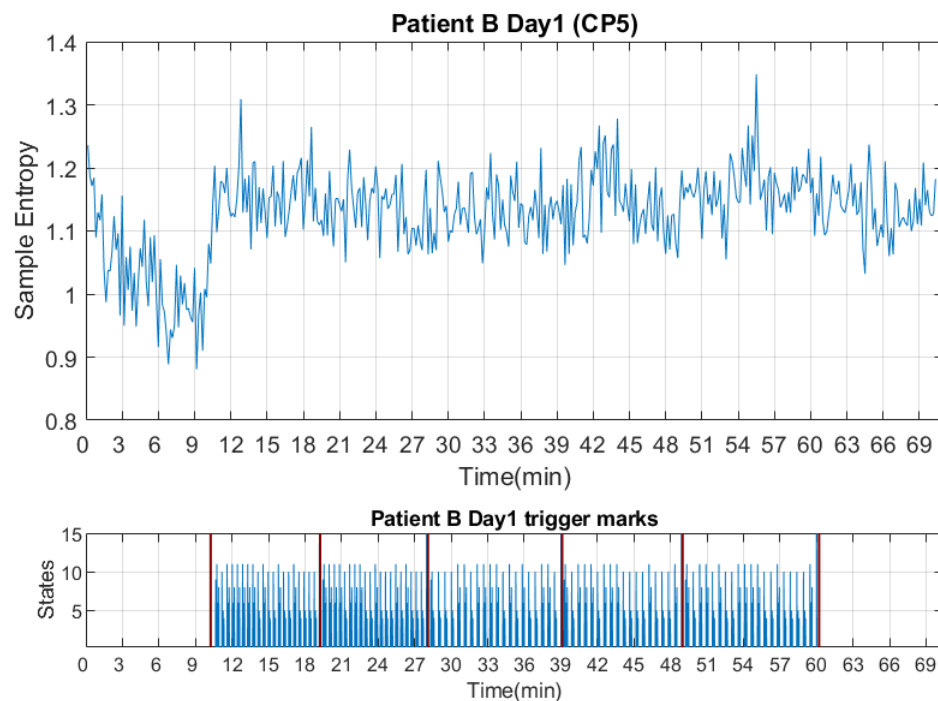


**Figure B.1:** The sample entropy result for CLIS patient B on day 1. Top: the channel CP5 result of the sample entropy. Bottom: The trigger marks for patient B on day 1. The sessions are indicated between two red vertical lines. The periods with numbers are experimental state, and those without numbers are rest state.

For patient B, seven consecutive sessions over 69 min were combined on the day one, as shown in top diagram of Figure B.1. The Figure B.1 below shows that from the second to the sixth sessions are the experimental states, while the first and seventh sessions are resting states. When the experimenter started the auditory experiment in the second session, the value of sample entropy increased accordingly, and at the end of the sixth session, the experimenter stopped the auditory experiment and the value of sample entropy decreased slowly, which clearly shows the difference between experimental and resting state. The sample entropy value was higher at the beginning, probably due to lunch, and the first session was recorded from 12:22 to 12:32. This sample entropy result shows a high similarity to the Poincaré plot result in Figure 6.9.

### CLIS patients B on day 2

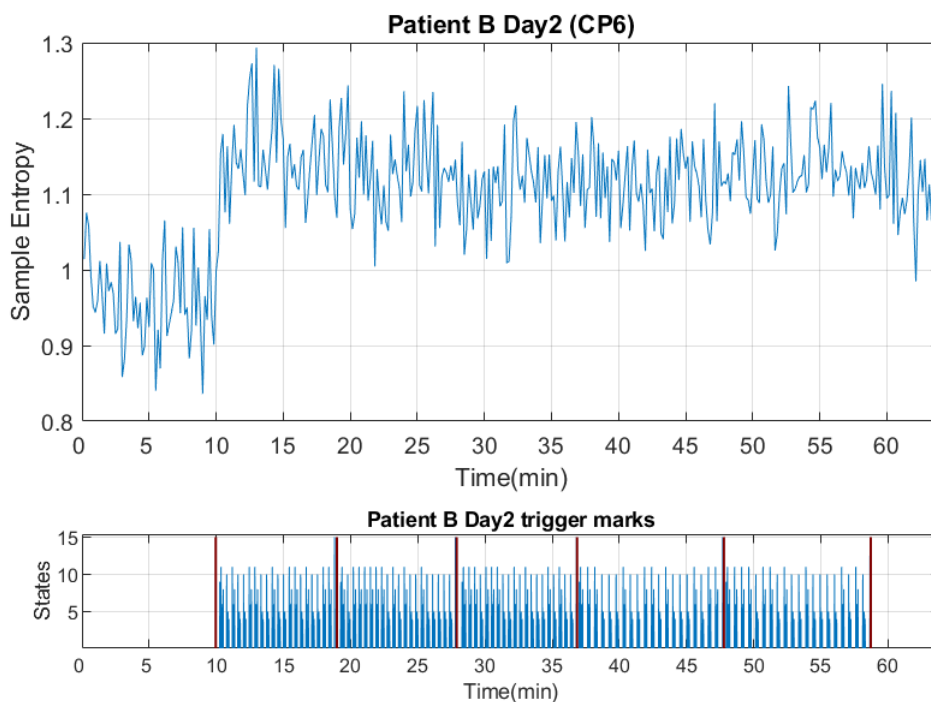


**Figure B.2:** The sample entropy result for CLIS patient B on day 2. Top: the channel CP6 result of the sample entropy. Bottom: The trigger marks for patient B on day 2. The sessions are indicated between two red vertical lines. The periods with numbers are experimental state, and those without numbers are rest state.

Seven consecutive sessions over 64 min were combined on the day two for patient B, as shown in Figure B.2. The Figure B.2 below shows that from the second to the sixth sessions are the experimental states, while the first and seventh sessions are resting states. In the second session, when the experimenter started the auditory experiment, the value of sample entropy rises significantly accordingly, which could be interpreted as a higher level of



consciousness. At the end of the sixth session, the experimenter stopped the auditory experiment and the value of sample entropy slowly declines, which clearly shows the difference between experimental and resting state. Similar trends were observed in the results for patient B in all other channels (FC5, FC1, FC6, CP5, CP1, CP6, AF3, AF4). This sample entropy result also shows a high similarity to the Poincaré plot result in Figure 6.10.

### CLIS patients F on day 1

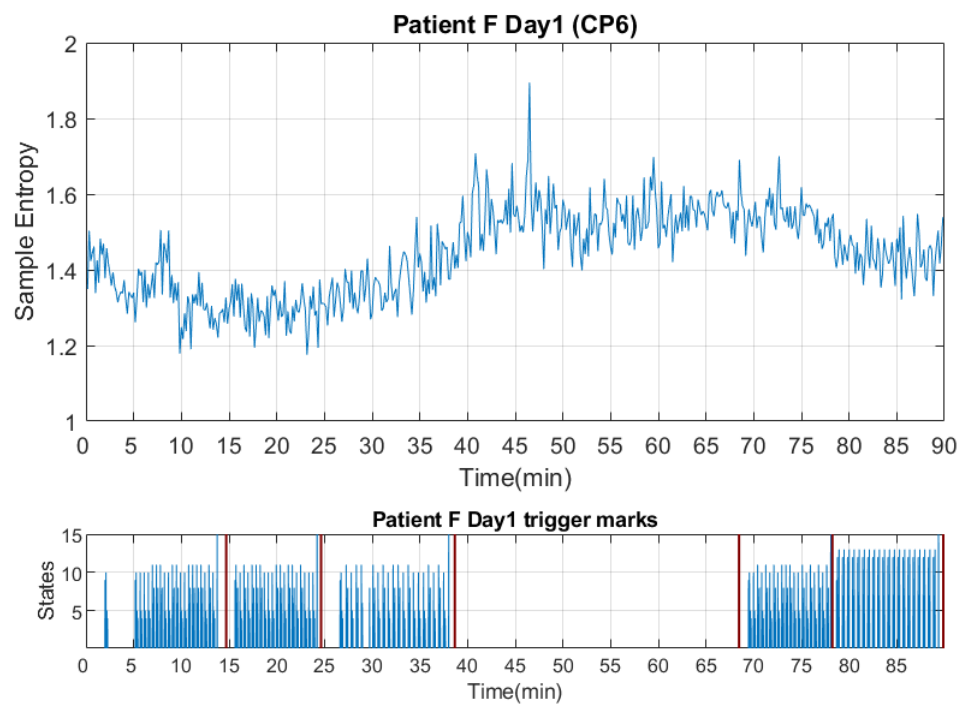


**Figure B.3:** The sample entropy result for CLIS patient F on day 1. Top: the channel CP6 result of the sample entropy. Bottom: The trigger marks for patient F on day 1. The sessions are indicated between two red vertical lines. The periods with numbers are experimental state, and those without numbers are rest state.

Six consecutive sessions over 90 minutes were combined on the day one for Patient F, as shown in the top diagram of Figure B.3, who generally performed less well than Patient B. The Figure B.3 below shows that that only the fourth section is a resting state, while all other sections are experimental states. Before the beginning of the fourth session, when the experimenter stopped the auditory experiment, the sample entropy value increased slowly accordingly, and when the experimenter restarted the auditory experiment towards the end of this session, the sample entropy value decreased slowly again, which still clearly showed the difference between the experimental and resting states. It presents the contrary result to patient B, but compared to the Poincaré plot results in Figure 6.11, these two different methods present consistent results. The trend of symmetrically positioned electrodes (CP5

vs. CP6, FC5 vs. FC6) is similar, whereas not symmetrical positioned electrodes differ. So, depending on the area over which the electrode is placed (e.g., over the Broca area or the Wernicke area), the task-related signal must be different and thus will indicate different corresponding aspects and show different trends on the related electrodes. We speculate that the level of consciousness depends on how difficult the questions were. Perhaps the questions asked by the investigators can promote the patients' thinking?

### CLIS patients F on day 2

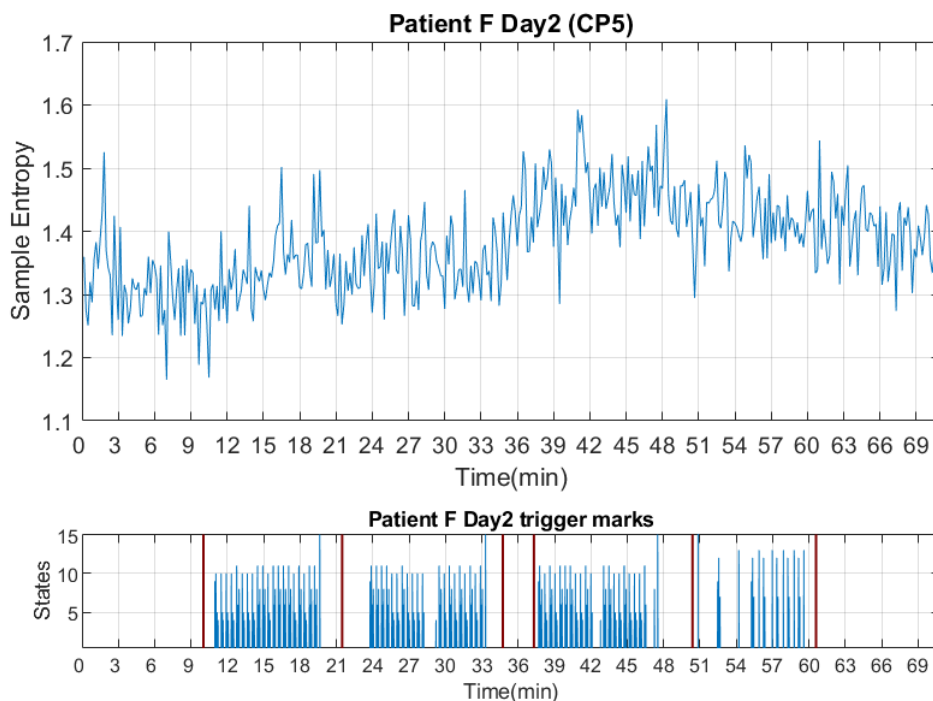


**Figure B.4:** The sample entropy result for CLIS patient F on day 2. Top: the channel CP5 result of the sample entropy. Bottom: The trigger marks for patient F on day 2. The sessions are indicated between two red vertical lines. The periods with numbers are experimental state, and those without numbers are rest state.

For patient F, seven consecutive sessions over 70 min were combined on the day two, as shown in top diagram of Figure B.4. The Figure B.4 below shows that the second, third, fifth, and sixth sessions are the experimental states, while the first, fourth, and seventh sessions are resting states. When the experimenter started the auditory experiment in the second session, the value of sample entropy slowly increased accordingly, and at the end of the sixth session, the experimenter stopped the auditory experiment and the value of sample entropy slowly decreased. The fourth session seemed to be too short that the brain activity of patient F remained active for around the experimental periods. The correct response rate is around 70% by functional near-infrared spectroscopy (fNIRS) and support vector machine

(SVM) to ensure that patients are awake (Chaudhary et al. 2017). There is a similar result between channel CP5 and the other channels (FC5, FC1, FC6) for patient F on day two, and compared to the Poincaré plot results in Figure 6.12, these two different methods show consistent results.

It is speculated that patient F allowed her mind to wander when she was not in the experimental time period, resulting in more brain activity during the rest time period than during the experimental time period. This patient showed the same phenomenon as the LIS patient during the spelling experiment, and the sample entropy results of the LIS patient during the spelling experiment are presented later in section 6.1.8.

# Appendix C Poincaré plot results

For the CLIS dataset from section 5.2, the top diagram of Figure C.1-Figure C.4 shows the Poincaré plot results for CLIS patients G and W over two days, the results for the other CLIS patients B and F over two days are presented in section 6.1.6. The figure below shows the trigger marks, those with numbers represent experimental state and those without numbers represent rest state. Between two red vertical lines indicate sessions, each session lasts around 10 minutes. To more clearly distinguish the difference between experimental and rest time, in these datasets all sessions in a day are combined in chronological order in the same figure. We assume that the higher the Poincaré plot value, the higher the relative consciousness of the patient. This interpretation is based on the results shown in (Chaudhary et al. 2017) where during the corresponding time slots (see Figure C.1-Figure C.4 trigger marks), the experimenter received a good number of correct answers, thus indicating the consciousness of the patient.

## CLIS patients G on day 1

In Figure C.1, five consecutive sessions over 74 minutes were combined for Patient G on the day one. In the second session, the value of Poincaré plot increased accordingly as the experimenter continued with the auditory experiment. However, in the third, fourth, and fifth sessions, the value of Poincaré plot increased when the experimenter stopped the auditory experiment. Patient G was presumed to be more focused at the beginning of the experiment on this day, and gradually decreased as he became more skilled. Biederman et al. (Biederman and Vessel 2006) describe why people like new stimuli and that repeated stimuli weaken the brain's response. It may help us to explain this phenomenon. This Poincaré plot result shows a high similarity to the sample entropy result in Figure 6.13.

Consequently, patient G was able to let her mind wander when she was not in the experimental time period, resulting in higher brain activity during the rest period after the second session. This patient showed the same phenomena as the LIS patients during the spelling experiment, the Poincaré plot results of LIS patients during the spelling experiment are presented later in section 6.1.8.

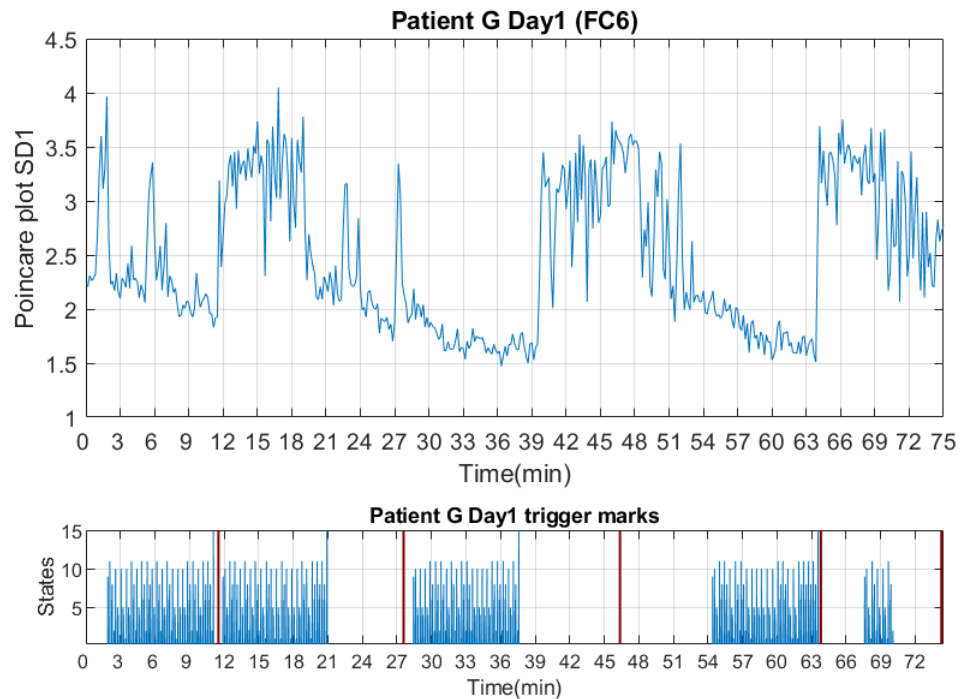


**Figure C.1:** The SD1 result of Poincaré plot for CLIS patient G on day 1. Top: the channel FC6 result of the Poincaré plot. Bottom: The trigger marks for patient G on day 1. The sessions are indicated between two red vertical lines. The periods with numbers are experimental state, and those without numbers are rest state.

Remember, in this thesis we focus on all cases in which significant index changes occurred at the beginning and at the end of the experiment, and overall, the patients responded accordingly to the external stimuli.

## CLIS patients G on day 2

Five consecutive sessions over 56 minutes were combined on the day one for Patient G, as shown in the top diagram of Figure C.2. The Figure C.2 below shows the time window between 0 and 45 min are the experimental states. The period after 45th min is the resting state. During the experimental state, where the Poincaré plot values undergo a slow increase and then decrease. In the rest period, there was a peak at about 48<sup>th</sup> minute, and usually the investigators would keep quiet during the rest period. We asked the experimenters and they replied that there was no record of possible effects causing this peak. Of course, it is not excluded that this patient does some thinking in her own mind after answering the questions asked by the investigators. Similar trends were observed in the results for patient G in all other channels (FC4, FC5, FC3, FC6, Cz). This Poincaré plot result also shows a high similarity to the sample entropy result in Figure 6.14.

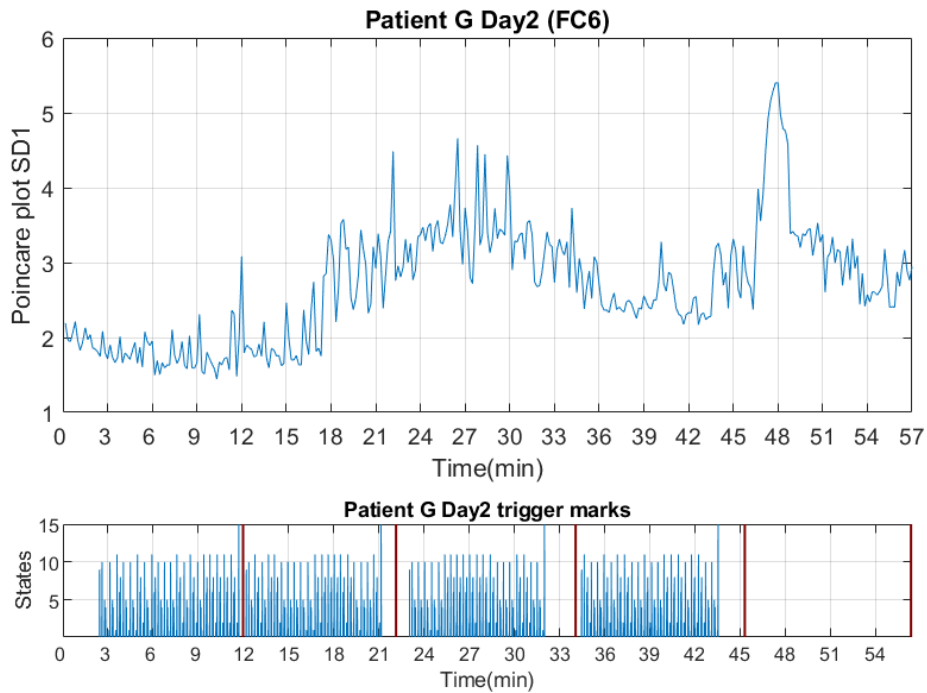


**Figure C.2:** The SD1 result of Poincaré plot for CLIS patient G on day 2. Top: the channel FC6 result of the Poincaré plot. Bottom: The trigger marks for patient G on day 2. The sessions are indicated between two red vertical lines. The periods with numbers are experimental state, and those without numbers are rest state.

### CLIS patients W on day 1

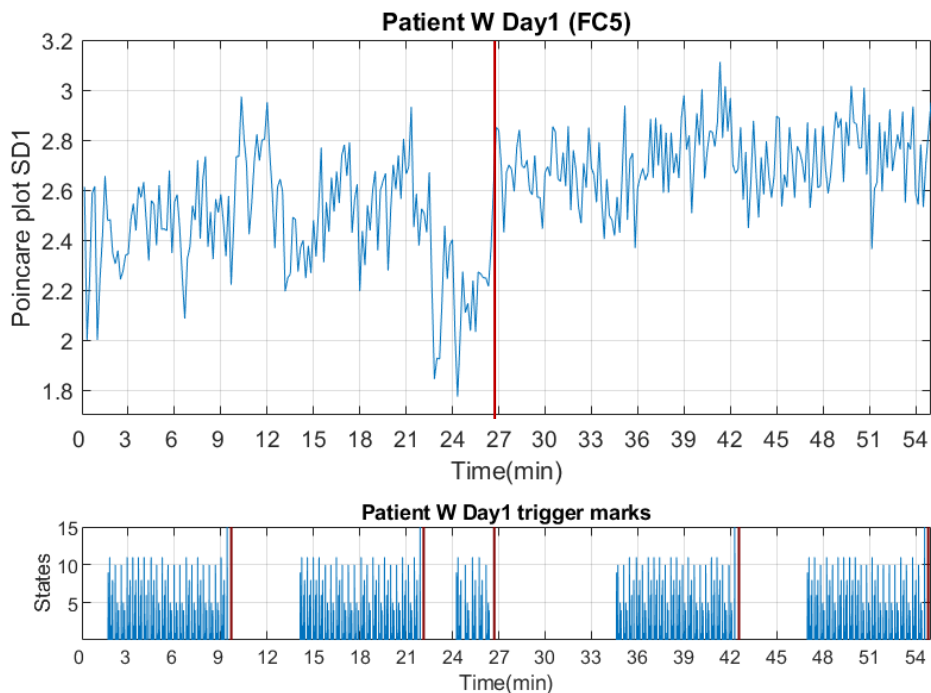


**Figure C.3:** The SD1 result of Poincaré plot for CLIS patient W on day 1. Top: the channel FC5 result of the Poincaré plot. Bottom: The trigger marks for patient W on day 1. The sessions are indicated between two red vertical lines. The periods with numbers are experimental state, and those without numbers are rest state.

Five consecutive sessions over 55 min were combined on the day one for patient W, as shown in Figure C.3, who performed better as patient G in general. The Figure C.3 below shows the time windows between 2-10, 14-22, 35-42, and 47-54 min in which the investigators asked the questions. The time windows from 0 to 2 min, 10-14 min, 27–35 min, and 42-47 min are the rest states. Remark that in most cases the time difference between each session is short, but in this case the data before 27<sup>th</sup> minute was recorded in the morning and the other part in the afternoon. So the baseline is different, but we can still see the difference between experimental and resting period clearly.

The values increase relatively at the 14<sup>th</sup>, 35<sup>th</sup>, and 47<sup>th</sup> minutes. On the contrary, the values decreased relatively at the 12<sup>th</sup>, 22<sup>nd</sup>, and 42<sup>nd</sup> minutes, which is less significant compared to the sample entropy results in Figure 6.15, but still shows the difference between the resting state and the experimental state at the beginning and the end of the questions. In the third session, the number of questions in this session was not 20 as usual. Perhaps the experiment was stopped because of some necessary nursing actions. As described by (Jaramillo-Gonzalez et al. 2021), they put the patients' care and health in the first priority.

## CLIS patients W on day 2

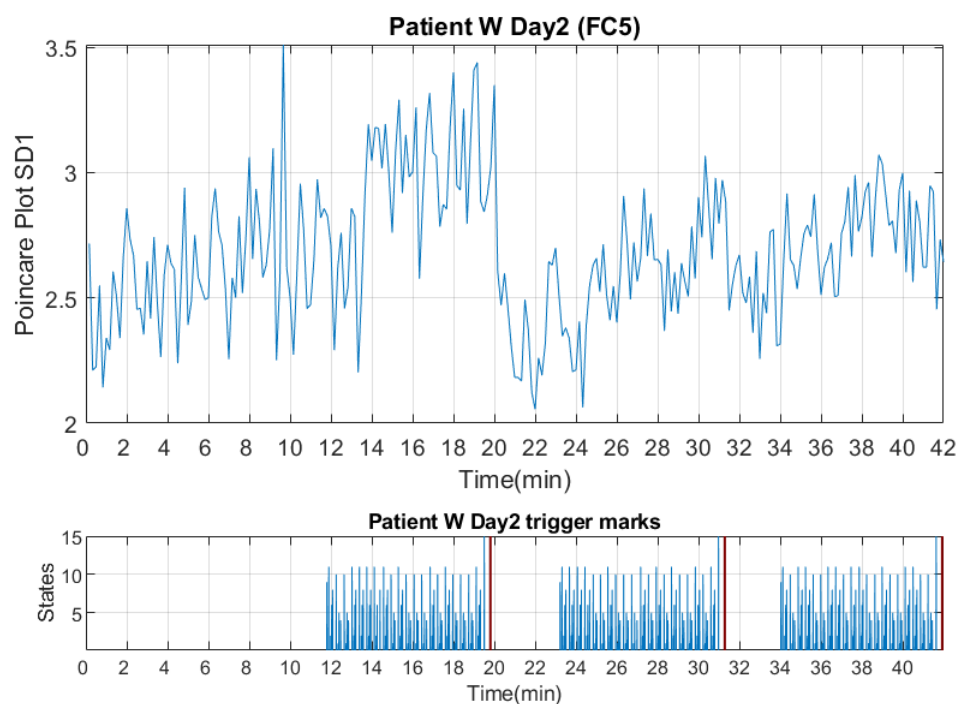


**Figure C.4:** The SD1 result of Poincaré plot for CLIS patient W on day 2. Top: the channel FC5 result of the Poincaré plot. Bottom: The trigger marks for patient W on day 2. The sessions are indicated between two red vertical lines. The periods with numbers are experimental state, and those without numbers are rest state.

For patient W, three consecutive sessions over 42 min were combined on the day two, as shown in Figure C.4. The Figure C.4 below shows the time windows between 12-20, 23-31, and 34-42 min are the experimental states. The time windows from 0 to 12 min, 20-23 min, and 31-34 min are the rest states. The values rise significantly at the 14<sup>th</sup>, 24<sup>th</sup>, and 34<sup>th</sup> minutes. In contrast, the values decline significantly at the 20<sup>th</sup> and 31<sup>st</sup> minutes, which clearly shows the difference between the resting state and the experimental state at the beginning and the end of the questions. Although there are some peaks in the Poincaré plot results, the Poincaré plot results still present similar results to the sample entropy.

There is a similar result between channel FC5 and the other channels (FC1, CP1, CP5) for patient W, all these channels are located in the left hemisphere. Through the medical records we learned that in January 2015, when she completely lost control of her eyes, she tries to twitch the right corner of her mouth to answer yes. As we know, the muscles on the right side of the body are controlled by the left hemisphere, while the muscles on the left side are controlled by the right hemisphere. From the fact that her remaining controllable body muscles are on the right side, we can infer that her left hemisphere is more active.

Although the results of Poincaré plot and sample entropy are similar, Poincaré plot is more sensitive one needs to remove some peaks in order to see the consciousness results. Therefore, the extension results to LIS, MCS, and UWS patients in section 6.1.8 and 6.1.9 are dominated by the sample entropy results in this thesis.



# Bibliography

- Acharya, J. N., A. Hani, J. Cheek, P. Thirumala, and T. N. Tsuchida. 2016. American Clinical Neurophysiology Society Guideline 2: Guidelines for Standard Electrode Position Nomenclature. *Journal of clinical neurophysiology : official publication of the American Electroencephalographic Society* 33(4): 308–311.
- Adama, V. S., S.-J. Wu, N. Nicolaou, and M. Bogdan. 2019. Extendable Hybrid approach to detect conscious states in a CLIS patient using machine learning. *EUROSIM*.
- Adama, S., S.-J. Wu, N. Nicolaou, and M. Bogdan. 2022. Extendable Hybrid Approach to Detect Conscious States in a CLIS Patient Using Machine Learning. *SNE Simulation Notes Europe* 32(1): 37–45.
- Al-Shargie, F. 2019. Assessment of Mental Stress Using EEG and fNIRS Features. *engrXiv*.
- Altenmüller, E. 2003. Focal dystonia: advances in brain imaging and understanding of fine motor control in musicians. *Hand Clinics* 19(3): 523–538.
- Angelakis, E., J. F. Lubar, S. Stathopoulou, and J. Kounios. 2004. Peak alpha frequency: an electroencephalographic measure of cognitive preparedness. *Clinical neurophysiology : official journal of the International Federation of Clinical Neurophysiology* 115(4): 887–897.
- Arsiwalla, X. D., R. Sole, C. Moulin-Frier, I. Herreros, M. Sanchez-Fibla, and P. Verschure. 2017. The Morphospace of Consciousness.
- Azar, A. T., S. A. El-Said, and A. E. Hassanien. 2013. Fuzzy and hard clustering analysis for thyroid disease. *Computer methods and programs in biomedicine* 111(1): 1–16.
- Azari, N. P. and R. J. Seitz. 2000. Brain Plasticity and Recovery from Stroke: What has changed in the brain of a stroke patient who recovers the ability to move a once-disabled limb? *American Scientist* 88(5): 426–431.
- Babiloni, C., F. Pistoia, M. Sarà, F. Vecchio, P. Buffo, M. Conson, P. Onorati, G. Albertini, and P. M. Rossini. 2010. Resting state eyes-closed cortical rhythms in patients with locked-in-syndrome: an EEG study. *Clinical neurophysiology : official journal of the International Federation of Clinical Neurophysiology* 121(11): 1816–1824.
- Babiloni, C., V. Pizzella, C. D. Gratta, A. Ferretti, and G. L. Romani. 2009. Chapter 5 Fundamentals of Electroencefalography, Magnetoencefalography, and Functional Magnetic Resonance Imaging 86: 67–80.
- Ball, T., M. Kern, I. Mutschler, A. Aertsen, and A. Schulze-Bonhage. 2009. Signal quality of simultaneously recorded invasive and non-invasive EEG. *NeuroImage* 46(3): 708–716.
- Bandt, C. and B. Pompe. 2002. Permutation entropy: A Natural Complexity Measure for Time Series. *Physical review letters* 88(17): 174102.
- Barnett, L., A. B. Barrett, and A. K. Seth. 2009. Granger causality and transfer entropy are equivalent for Gaussian variables. *Physical review letters* 103(23): 238701.
- Bauby, J.-D. 1995. *The Diving Bell and the Butterfly*.

- Bensch, M., S. Martens, S. Halder, J. Hill, F. Nijboer, A. Ramos-Murguialday, N. Birbaumer, M. Bogdan, B. Kotchoubey, W. Rosenstiel, B. Schölkopf, and A. Gharabaghi. 2014. Assessing attention and cognitive function in completely locked-in state with event-related brain potentials and epidural electrocorticography. *Journal of neural engineering* 11(2): 26006.
- Berger, H. 1929. Über das Elektrenkephalogramm des Menschen. *Archiv f. Psychiatrie* 87: 527–570.
- Beukelman, D. R. and J. C. Light, eds. 2020. *Augmentative & Alternative Communication: Supporting Children and Adults with Complex Communication Needs*. Ed. 5.
- Biederman, I. and E. A. Vessel. 2006. Perceptual Pleasure and the Brain: A novel theory explains why the brain craves information and seeks it through the senses. *American Scientist* 94: 249–255.
- Birbaumer, N., N. Ghanayim, T. Hinterberger, I. Iversen, B. Kotchoubey, A. Kübler, J. Perelmouter, E. Taub, and H. Flor. 1999. A spelling device for the paralysed. *Nature* 398(6725): 297–298.
- Birbaumer, N., A. R. Murguialday, and L. Cohen. 2008. Brain-computer interface in paralysis. *Current opinion in neurology* 21(6): 634–638.
- Birbaumer, N., F. Piccione, S. Silvoni, and M. Wildgruber. 2012. Ideomotor silence: the case of complete paralysis and brain-computer interfaces (BCI). *Psychological research* 76(2): 183–191.
- Blankertz, B., G. Dornhege, M. Krauledat, K. R. Müller, V. Kunzmann, F. Losch, and G. Curio. 2006. The Berlin brain-computer interface : EEG-based communication without subject training. *IEEE Transactions on Neural Systems and Rehabilitation Engineering* 14(2): 147–152.
- Blume, C., R. Del Giudice, M. Wislowska, J. Lechinger, and M. Schabus. 2015. Across the consciousness continuum-from unresponsive wakefulness to sleep. *Frontiers in human neuroscience* 9: 105.
- Bolaños, J. D., M. Vallverdú, P. Caminal, D. F. Valencia, X. Borrat, P. L. Gambus, and J. F. Valencia. 2016. Assessment of Sedation-Analgesia by means of Poincaré Analysis of the Electroencephalogram. *In Proceedings of the 2016 38th Annual International Conference of the IEEE Engineering in Medicine and Biology Society (EMBC)*: 6425–6428.
- Bruno, M.-A., O. Gosseries, D. Ledoux, R. Hustinx, and S. Laureys. 2011. Assessment of consciousness with electrophysiological and neurological imaging techniques. *Current opinion in critical care* 17(2): 146–151.
- Cantero, J. L., M. Atienza, G. Gomez-Herrero, A. Cruz-Vadell, E. Gil-Neciga, R. Rodriguez-Romero, and D. Garcia-Solis. 2009. Functional integrity of thalamocortical circuits differentiates normal aging from mild cognitive impairment. *Human brain mapping* 30(12): 3944–3957.
- Caria, A., R. Veit, R. Sitaram, M. Lotze, N. Weiskopf, W. Grodd, and N. Birbaumer. 2007. Regulation of anterior insular cortex activity using real-time fMRI. *NeuroImage* 35(3): 1238–1246.
- Casali, A. G., O. Gosseries, M. Rosanova, M. Boly, S. Sarasso, K. R. Casali, S. Casarotto, M.-A. Bruno, S. Laureys, G. Tononi, and M. Massimini. 2013. A Theoretically Based Index of Consciousness Independent of Sensory Processing and Behavior. *Science translational medicine* 5(198): 198ra105.

- Cedarbaum, J. M., N. Stambler, E. Malta, C. Fuller, D. Hilt, B. Thurmond, A. Nakanishi, and BDNF ALS Study Group. 1999. The ALSFRS-R: a revised ALS functional rating scale that incorporates assessments of respiratory function. *Journal of the Neurological Sciences* 169: 13–21.
- Chaudhary, U., N. Birbaumer, and A. Ramos-Murguialday. 2016. Brain-computer interfaces for communication and rehabilitation. *Nature reviews. Neurology* 12(9): 513–525.
- Chaudhary, U., I. Vlachos, J. B. Zimmermann, A. Espinosa, A. Tonin, A. Jaramillo-Gonzalez, M. Khalili-Ardali, H. Topka, J. Lehmeberg, G. M. Friehs, A. Woodtli, J. P. Donoghue, and N. Birbaumer. 2020. Verbal Communication using Intracortical Signals in a Completely Locked In-Patient 16.
- Chaudhary, U., B. Xia, S. Silvoni, L. G. Cohen, and N. Birbaumer. 2017. Brain-Computer Interface-Based Communication in the Completely Locked-In State. *PLoS biology* 15(1): e1002593.
- Chiò, A., G. Logroscino, B. J. Traynor, J. Collins, J. C. Simeone, L. A. Goldstein, and L. A. White. 2013. Global epidemiology of amyotrophic lateral sclerosis: a systematic review of the published literature. *Neuroepidemiology* 41(2): 118–130.
- Cipresso, P., L. Carelli, F. Solca, D. Meazzi, P. Meriggi, B. Poletti, D. Lulé, A. C. Ludolph, V. Silani, and G. Riva. 2012. The use of P300-based BCIs in amyotrophic lateral sclerosis: from augmentative and alternative communication to cognitive assessment. *Brain and behavior* 2(4): 479–498.
- Cologan, V., X. Drouot, S. Parapatics, A. Delorme, G. Gruber, G. Moonen, and S. Laureys. 2013. Sleep in the unresponsive wakefulness syndrome and minimally conscious state. *Journal of neurotrauma* 30(5): 339–346.
- Costa, M., A. L. Goldberger, and C.-K. Peng. 2002. Multiscale Entropy Analysis of Complex Physiologic Time Series. *Physical review letters* 89(6): 68102.
- Costa, M., A. L. Goldberger, and C.-K. Peng. 2005. Multiscale entropy analysis of biological signals. *Physical review. E* 71: 21906.
- Courtiol, J., D. Perdakis, S. Petkoski, V. Müller, R. Huys, R. Sleimen-Malkoun, and V. K. Jirsa. 2016. The multiscale entropy: Guidelines for use and interpretation in brain signal analysis. *Journal of neuroscience methods* 273: 175–190.
- Coyle, S., T. Ward, C. Markham, and G. McDarby. 2004. On the suitability of near-infrared (NIR) systems for next-generation brain-computer interfaces. *Physiological measurement* 25(4): 815–822.
- Coyle, S. M., T. E. Ward, and C. M. Markham. 2007. Brain-computer interface using a simplified functional near-infrared spectroscopy system. *Journal of neural engineering* 4(3): 219–226.
- Cruse, D., M. M. Monti, and A. M. Owen. 2011. Neuroimaging in disorders of consciousness: contributions to diagnosis and prognosis. *Future Neurology* 6(2): 291–299.
- Del Giudice, R., C. Blume, M. Wislowska, J. Lechinger, D. P. J. Heib, G. Pichler, J. Donis, G. Michitsch, M.-T. Gnjezda, M. Chinchilla, C. Machado, and M. Schabus. 2016. Can self-relevant stimuli help assessing patients with disorders of consciousness? *Consciousness and cognition* 44: 51–60.
- Diambra, L., J. C. Bastos de Figueiredo, and C. P. Malta. 1999. Epileptic activity recognition in EEG recording: Phys A 273: 495–505.

- Dvey-Aharon, Z., N. Fogelson, A. Peled, and N. Intrator. 2015. Schizophrenia detection and classification by advanced analysis of EEG recordings using a single electrode approach. *PLoS one* 10(4): e0123033.
- Ester, M., H.-P. Kriegel, J. Sander, and X. Xu. 1996. A Density-Based Algorithm for Discovering Clusters in Large Spatial Databases with Noise. *Proceedings of the Second International Conference on Knowledge Discovery and Data Mining (KDD-96)*: 226–231.
- Felgoise, S. H., V. Zaccheo, J. Duff, and Z. Simmons. 2016. Verbal communication impacts quality of life in patients with amyotrophic lateral sclerosis. *Amyotrophic lateral sclerosis & frontotemporal degeneration* 17(3-4): 179–183.
- Fellinger, R., W. Klimesch, C. Schnakers, F. Perrin, R. Freunberger, W. Gruber, S. Laureys, and M. Schabus. 2011. Cognitive processes in disorders of consciousness as revealed by EEG time-frequency analyses. *Clinical neurophysiology : official journal of the International Federation of Clinical Neurophysiology* 122(11): 2177–2184.
- Florin, E., J. Gross, J. Pfeifer, G. R. Fink, and L. Timmermann. 2010. The effect of filtering on Granger causality based multivariate causality measures. *NeuroImage* 50(2): 577–588.
- Furdea, A., C. A. Ruf, S. Halder, D. de Massari, M. Bogdan, W. Rosenstiel, T. Matuz, and N. Birbaumer. 2012. A new (semantic) reflexive brain-computer interface: in search for a suitable classifier. *Journal of neuroscience methods* 203(1): 233–240.
- Gallegos-Ayala, G., A. Furdea, K. Takano, C. A. Ruf, H. Flor, and N. Birbaumer. 2014. Brain communication in a completely locked-in patient using bedside near-infrared spectroscopy. *Neurology* 82(21): 1930–1932.
- Giacino, J. T., S. Ashwal, N. Childs, R. Cranford, B. Jennett, D. I. Katz, J. P. Kelly, J. H. Rosenberg, J. Whyte, R. D. Zafonte, and N. D. Zasler. 2002. The minimally conscious state: definition and diagnostic criteria. *Neurology* 58(3): 349–353.
- Giacino, J. T., K. Kalmar, and J. Whyte. 2004. The JFK Coma Recovery Scale-Revised: measurement characteristics and diagnostic utility. *Archives of physical medicine and rehabilitation* 85(12): 2020–2029.
- Giacino, J. T., D. I. Katz, N. D. Schiff, J. Whyte, E. J. Ashman, S. Ashwal, R. Barbano, F. M. Hammond, S. Laureys, G. S. F. Ling, R. Nakase-Richardson, R. T. Seel, S. Yablon, T. S. D. Getchius, G. S. Gronseth, and M. J. Armstrong. 2018. Practice Guideline Update Recommendations Summary: Disorders of Consciousness: Report of the Guideline Development, Dissemination, and Implementation Subcommittee of the American Academy of Neurology; the American Congress of Rehabilitation Medicine; and the National Institute on Disability, Independent Living, and Rehabilitation Research. *Archives of physical medicine and rehabilitation* 99(9): 1699–1709.
- Golińska, A. K. 2013. Poincaré Plots in Analysis of Selected Biomedical Signals. *Studies in Logic, Grammar and Rhetoric* 35(1): 117–127.
- Graimann, B., B. Allison, and G. Pfurtscheller. 2010. Brain–Computer Interfaces: A Gentle Introduction. *Springer* 113: 1–27.
- Grandy, T. H., M. Werkle-Bergner, C. Chicherio, F. Schmiedek, M. Lövdén, and U. Lindenberger. 2013. Peak individual alpha frequency qualifies as a stable neurophysiological trait marker in healthy younger and older adults. *Psychophysiology* 50(6): 570–582.

- Grodd, W., E. Hülsmann, M. Lotze, D. Wildgruber, and M. Erb. 2001. Sensorimotor mapping of the human cerebellum: fMRI evidence of somatotopic organization. *Human brain mapping* 13(2): 55–73.
- Güneş, S., K. Polat, and Ş. Yosunkaya. 2010. Efficient sleep stage recognition system based on EEG signal using k-means clustering based feature weighting. *Expert Systems with Applications* 37(12): 7922–7928.
- Guy, V., M.-H. Soriani, M. Bruno, T. Papadopoulo, C. Desnuelle, and M. Clerc. 2018. Brain computer interface with the P300 speller: Usability for disabled people with amyotrophic lateral sclerosis. *Annals of Physical and Rehabilitation Medicine* 61(1): 5–11.
- Han, C.-H., Y.-W. Kim, D. Y. Kim, S. H. Kim, Z. Nenadic, and C.-H. Im. 2019. Electroencephalography-based endogenous brain-computer interface for online communication with a completely locked-in patient. *Journal of neuroengineering and rehabilitation* 16(1): 18.
- Hardiman, O., A. Al-Chalabi, C. Brayne, E. Beghi, L. H. van den Berg, A. Chio, S. Martin, G. Logroscino, and J. Rooney. 2017. The changing picture of amyotrophic lateral sclerosis: lessons from European registers. *Journal of neurology, neurosurgery, and psychiatry* 88(7): 557–563.
- Hardiman, O., A. Al-Chalabi, A. Chio, E. M. Corr, G. Logroscino, W. Robberecht, P. J. Shaw, Z. Simmons, and L. H. van den Berg. 2017. Amyotrophic lateral sclerosis. *Nature reviews. Disease primers* 3: 17071.
- Hayashi, H. and E. A. Oppenheimer. 2003. ALS patients on TPPV: totally locked-in state, neurologic findings and ethical implications. *Neurology* 61(1): 135–137.
- Hayashi, K., N. Mukai, and T. Sawa. 2015. Poincaré analysis of the electroencephalogram during sevoflurane anesthesia. *Clinical Neurophysiology* 126: 404–411.
- Hayashi, K., T. Yamada, and T. Sawa. 2014. Comparative study of Poincaré plot analysis using short electroencephalogram signals during anaesthesia with spectral edge frequency 95 and bispectral index. *Anaesthesia* 70(3): 310–317.
- Henriques, T. S., S. Mariani, A. Burykin, F. Rodrigues, T. F. Silva, and A. L. Goldberger. 2015. Multiscale Poincaré plots for visualizing the structure of heartbeat time series. *BMC medical informatics and decision making* 16(17).
- Hesse, W., E. Möller, M. Arnold, and B. Schack. 2003. The use of time-variant EEG Granger causality for inspecting directed interdependencies of neural assemblies. *Journal of neuroscience methods* 124(1): 27–44.
- Hill, N. J., D. Gupta, P. Brunner, A. Gunduz, M. A. Adamo, A. Ritaccio, and G. Schalk. 2012. Recording human electrocorticographic (ECoG) signals for neuroscientific research and real-time functional cortical mapping. *Journal of visualized experiments : JoVE* (64).
- Hochberg, L. R., M. D. Serruya, G. M. Friehs, J. A. Mukand, M. Saleh, A. H. Caplan, A. Branner, D. Chen, R. D. Penn, and J. P. Donoghue. 2006. Neuronal ensemble control of prosthetic devices by a human with tetraplegia. *Nature* 442(7099): 164–171.
- Hohmann, M. R., T. Fomina, V. Jayaram, T. Emde, J. Just, M. Synofzik, B. Schölkopf, L. Schöls, and M. Grosse-Wentrup. 2018. Case series: Slowing alpha rhythm in late-stage ALS patients. *Clinical neurophysiology : official journal of the International Federation of Clinical Neurophysiology* 129(2): 406–408.

- Horki, P., D. S. Klobassa, C. Pokorny, and G. R. Müller-Putz. 2015. Evaluation of healthy EEG responses for spelling through listener-assisted scanning. *IEEE journal of biomedical and health informatics* 19(1): 29–36.
- Hwang, H.-J., S. Kim, S. Choi, and C.-H. Im. 2013. EEG-Based Brain-Computer Interfaces: A Thorough Literature Survey. *International Journal of Human-Computer Interaction* 29(12): 814–826.
- Hwang, H.-J., K. Kwon, and C.-H. Im. 2009. Neurofeedback-based motor imagery training for brain-computer interface (BCI). *Journal of neuroscience methods* 179(1): 150–156.
- Jaramillo-Gonzalez, A., S. Wu, A. Tonin, A. Rana, M. K. Ardali, N. Birbaumer, and U. Chaudhary. 2021. A dataset of EEG and EOG from an auditory EOG-based communication system for patients in locked-in state. *Scientific data* 8(1): 8.
- Jennett, B. and F. Plum. 1972. Persistent vegetative state after brain damage: a syndrome in search of a name. *The Lancet*: 734–737.
- Jurcak, V., D. Tsuzuki, and I. Dan. 2007. 10/20, 10/10, and 10/5 systems revisited: their validity as relative head-surface-based positioning systems. *NeuroImage* 34(4): 1600–1611.
- Klimesch, W. 1999. EEG alpha and theta oscillations reflect cognitive and memory performance: a review and analysis. *Brain Research Reviews* 29: 169–195.
- Kodinariya, T. M. and P. R. Makwana. 2013. Review on determining number of Cluster in K-Means Clustering. *International Journal of Advance Research in Computer Science and Management Studies* 1(6): 90–95.
- Kögel, J., R. J. Jox, and O. Friedrich. 2020. What is it like to use a BCI? - insights from an interview study with brain-computer interface users. *BMC medical ethics* 21(1): 2.
- Kotchoubey, B., S. Lang, S. Winter, and N. Birbaumer. 2003. Cognitive processing in completely paralyzed patients with amyotrophic lateral sclerosis. *European Journal of Neurology* 10(5): 551–558.
- Kreuzer, M., E. F. Kochs, G. Schneider, and D. Jordan. 2014. Non-stationarity of EEG during wakefulness and anaesthesia: Advantages of EEG permutation entropy monitoring. *Journal of clinical monitoring and computing* 28(6): 573–580.
- Kübler, A. and N. Birbaumer. 2008. Brain-computer interfaces and communication in paralysis: extinction of goal directed thinking in completely paralysed patients? *Clinical neurophysiology : official journal of the International Federation of Clinical Neurophysiology* 119(11): 2658–2666.
- Kübler, A. and B. Kotchoubey. 2007. Brain-computer interfaces in the continuum of consciousness. *Current opinion in neurology* 20(6): 643–649.
- Kuntzelman, K., L. J. Rhodes, L. N. Harrington, and V. Miskovic. 2018. A practical comparison of algorithms for the measurement of multiscale entropy in neural time series data. *Brain and cognition* 123: 126–135.
- Landsness, E., M.-A. Bruno, Q. Noirhomme, B. Riedner, O. Gosseries, C. Schnakers, M. Massimini, S. Laureys, G. Tononi, and M. Boly. 2011. Electrophysiological correlates of behavioural changes in vigilance in vegetative state and minimally conscious state. *Brain : a journal of neurology* 134(Pt 8): 2222–2232.

- Laureys, S. 2005. The neural correlate of (un)awareness: lessons from the vegetative state. *Trends in cognitive sciences* 9(12): 556–559.
- Laureys, S., G. G. Celesia, F. Cohadon, J. Lavrijsen, J. León-Carrión, W. G. Sannita, L. Szabon, E. Schmutzhard, K. R. von Wild, A. Zeman, and G. Dolce. 2010. Unresponsive wakefulness syndrome: a new name for the vegetative state or apallic syndrome. *BMC medicine* 8: 68.
- Laureys, S., A. M. Owen, and N. D. Schiff. 2004. Brain function in coma, vegetative state, and related disorders. *The Lancet Neurology* 3(9): 537–546.
- Lechinger, J., K. Bothe, G. Pichler, G. Michitsch, J. Donis, W. Klimesch, and M. Schabus. 2013. CRS-R score in disorders of consciousness is strongly related to spectral EEG at rest. *Journal of Neurology* 260(9): 2348–2356.
- Lee, R. G. and P. van Donkelaar. 1995. Mechanisms underlying functional recovery following stroke. *The Canadian journal of neurological sciences. Le journal canadien des sciences neurologiques* 22(4): 257–263.
- Lesenfants, D., D. Habbal, C. Chatelle, A. Soddu, S. Laureys, and Q. Noirhomme. 2018. Toward an Attention-Based Diagnostic Tool for Patients With Locked-in Syndrome. *Clinical EEG and neuroscience* 49(2): 122–135.
- Leuthardt, E. C., G. Schalk, J. Roland, A. Rouse, and D. W. Moran. 2009. Evolution of brain-computer interfaces: going beyond classic motor physiology. *Neurosurgical focus* 27(1): E4.
- Leuthardt, E. C., G. Schalk, J. R. Wolpaw, J. G. Ojemann, and D. W. Moran. 2004. A brain-computer interface using electrocorticographic signals in humans. *Journal of neural engineering* 1(2): 63–71.
- Lim, J.-H., Y.-W. Kim, J.-H. Lee, K.-O. An, H.-J. Hwang, H.-S. Cha, C.-H. Han, and C.-H. Im. 2017. An emergency call system for patients in locked-in state using an SSVEP-based brain switch. *Psychophysiology* 54(11): 1632–1643.
- Lo Coco, D., P. Mattaliano, R. Spataro, A. Mattaliano, and V. La Bella. 2011. Sleep-wake disturbances in patients with amyotrophic lateral sclerosis. *Journal of neurology, neurosurgery, and psychiatry* 82(8): 839–842.
- Luauté, J., D. Morlet, and J. Mattout. 2015. BCI in patients with disorders of consciousness: Clinical perspectives. *Annals of Physical and Rehabilitation Medicine* 58: 29–34.
- Markand, O. N. 1976. Electroencephalogram in “locked-in” syndrome. *Electroencephalography and Clinical Neurophysiology* 401: 529–534.
- Martens, S., M. Bensch, S. Halder, J. Hill, F. Nijboer, A. Ramos-Murguialday, B. Schoelkopf, N. Birbaumer, and A. Gharabaghi. 2014. Epidural electrocorticography for monitoring of arousal in locked-in state. *Frontiers in human neuroscience* 8: 861.
- Maruyama, Y., N. Yoshimura, A. Rana, A. Malekshahi, A. Tonin, A. Jaramillo-Gonzalez, N. Birbaumer, and U. Chaudhary. 2021. Electroencephalography of completely locked-in state patients with amyotrophic lateral sclerosis. *Neuroscience research* 162: 45–51.
- McFarland, D. J. and J. R. Wolpaw. 2017. EEG-Based Brain-Computer Interfaces. *Current opinion in biomedical engineering* 4: 194–200.

- Monti, M. M., A. Vanhaudenhuyse, M. R. Coleman, M. Boly, J. D. Pickard, L. Tshibanda, A. M. Owen, and S. Laureys. 2010. Willful modulation of brain activity in disorders of consciousness. *The New England journal of medicine* 362(7): 579–589.
- Müller-Putz, G. R., V. Kaiser, T. Solis-Escalante, and G. Pfurtscheller. 2010. Fast set-up asynchronous brain-switch based on detection of foot motor imagery in 1-channel EEG. *Medical & biological engineering & computing* 48(3): 229–233.
- Nicolaou, N. and J. Georgiou. 2014. Neural network-based classification of anesthesia/awareness using Granger causality features. *Clinical EEG and neuroscience* 45(2): 77–88.
- Nicolaou, N., S. Hourris, P. Alexandrou, and J. Georgiou. 2012. EEG-based automatic classification of 'awake' versus 'anesthetized' state in general anesthesia using Granger causality. *PloS one* 7(3): e33869.
- Nicolas-Alonso, L. F. and J. Gomez-Gil. 2012. Brain computer interfaces, a review. *Sensors (Basel, Switzerland)* 12(2): 1211–1279.
- Nijboer, F., A. Furdea, I. Gunst, J. Mellinger, D. J. McFarland, N. Birbaumer, and A. Kübler. 2008. An auditory brain-computer interface (BCI). *Journal of neuroscience methods* 167(1): 43–50.
- Okahara, Y., K. Takano, M. Nagao, K. Kondo, Y. Iwadate, N. Birbaumer, and K. Kansaku. 2018. Long-term use of a neural prosthesis in progressive paralysis. *Scientific reports* 8(1): 16787.
- Oostenveld, R. and P. Praamstra. 2001. The five percent electrode system for high-resolution EEG and ERP measurements. *Clinical Neurophysiology* 112(4): 713–719.
- Owen, A. M. and M. R. Coleman. 2007. Functional MRI in disorders of consciousness: advantages and limitations. *Current opinion in neurology* 20(6): 632–637.
- Owen, A. M. and M. R. Coleman. 2008. Detecting awareness in the vegetative state. *Annals of the New York Academy of Sciences* 1129: 130–138.
- Owen, A. M., M. R. Coleman, M. Boly, M. H. Davis, S. Laureys, D. Jolles, and J. D. Pickard. 2007. Response to Comments on "Detecting Awareness in the Vegetative State". *Science* 315(5816): 1221.
- Owen, A. M., M. R. Coleman, M. Boly, M. H. Davis, S. Laureys, and J. D. Pickard. 2006. Detecting Awareness in the Vegetative State. *Science (New York, N.Y.)* 313(5792): 1402.
- Owen, A. M., N. D. Schiff, and S. Laureys. 2009. A new era of coma and consciousness science. *Progress in Brain Research* 177: 399–411.
- Penfield, W. and E. Boldrey. 1937. Somatic motor and sensory representation in the cerebral cortex of man as studied by electrical stimulation. *Brain: A Journal of Neurology* 60(4): 389–443.
- Pham, D. T., S. S. Dimov, and C. D. Nguyen. 2005. Selection of K in K -means clustering. *Proceedings of the Institution of Mechanical Engineers, Part C: Journal of Mechanical Engineering Science* 219(1): 103–119.
- Piarulli, A., M. Bergamasco, A. Thibaut, V. Cologan, O. Gosseries, and S. Laureys. 2016. EEG ultradian rhythmicity differences in disorders of consciousness during wakefulness. *Journal of Neurology* 263(9): 1746–1760.



- Pincus, S. M. 1991. Approximate entropy: A complexity measure for biological time series data. *In Proceedings of the 1991 IEEE Seventeenth Annual Northeast Bioengineering Conference*: 35–36.
- Pincus, S. M. and A. L. Goldberger. 1994. Physiological time-series analysis: What does regularity quantify?: *Am J Physiol Heart Circ Physiol* 266: H1643–H1656.
- Pioreckýa, M., J. Štrobl, and V. Krajčaa. 2019. Automatic EEG classification using density based algorithms DBSCAN and DENCLUE. *Acta Polytechnica* 59(5): 498–509.
- Plum, F. and J. B. Posner, eds. 1982. *The diagnosis of stupor and coma*. Ed. 3. Oxford university press.
- Ramos-Murguialday, A. R., J. Hill, M. Bensch, S. Martens, S. Halder, F. Nijboer, B. Schoelkopf, N. Birbaumer, and A. Gharabaghi. 2011. Transition from the locked in to the completely locked-in state: A physiological analysis. *Clinical neurophysiology: official journal of the International Federation of Clinical Neurophysiology* 122(5): 925–933.
- Rehman, S. U., S. Asghar, S. Fong, and S. Sarasvady. 2014. DBSCAN: Past, present and future. *The Fifth International Conference on the Applications of Digital Information and Web Technologies (ICADIWT 2014)*: 232–238.
- Renton, A. E., A. Chiò, and B. J. Traynor. 2014. State of play in amyotrophic lateral sclerosis genetics. *Nature neuroscience* 17(1): 17–23.
- Richman, J. S. and J. R. Moorman. 2000. Physiological time-series analysis using approximate entropy and sample entropy. *American journal of physiology. Heart and circulatory physiology* 278(6): H2039–H2049.
- Riedl, M., A. Müller, and N. Wessel. 2013. Practical considerations of permutation entropy. *The European Physical Journal Special Topics* 222(2): 249–262.
- Ruf, C. A., D. de Massari, A. Furdea, T. Matuz, C. Fioravanti, L. van der Heiden, S. Halder, and N. Birbaumer. 2013. Semantic classical conditioning and brain-computer interface control: encoding of affirmative and negative thinking. *Frontiers in neuroscience* 7: 23.
- Sander, J., M. Ester, H.-P. Kriegel, and X. Xu. 1998. Density-Based Clustering in Spatial Databases: The Algorithm GDBSCAN and Its Applications. *Data Mining and Knowledge Discovery* 2(2): 169–194.
- Schalk, G. and E. C. Leuthardt. 2011. Brain-computer interfaces using electrocorticographic signals. *IEEE reviews in biomedical engineering* 4: 140–154.
- Schiff, N. D., D. Rodriguez-Moreno, A. Kamal, K. H. S. Kim, J. T. Giacino, F. Plum, and J. Hirsch. 2005. fMRI reveals large-scale network activation in minimally conscious patients. *Neurology* 64(3): 514–523.
- Schnakers, C., S. Majerus, S. Goldman, M. Boly, P. van Eeckhout, S. Gay, F. Pellas, V. Bartsch, P. Peigneux, G. Moonen, and S. Laureys. 2008. Cognitive function in the locked-in syndrome. *Journal of Neurology* 255(3): 323–330.
- Schubert, E., J. Sander, M. Ester, H. P. Kriegel, and X. Xu. 2017. DBSCAN Revisited, Revisited. *ACM Transactions on Database Systems* 42(3): 1–21.

- Schwender, D., M. Dauser, S. Mulzer, S. Klasing, U. Finsterer, and K. Peter. 1996. Spectral edge frequency of the electroencephalogram to monitor "depth" of anaesthesia with isoflurane or propofol. *British journal of anaesthesia* 77(2): 179–184.
- Secco, A., A. Tonin, A. Rana, A. Jaramillo-Gonzalez, M. Khalili-Ardali, N. Birbaumer, and U. Chaudhary. 2020. EEG power spectral density in locked-in and completely locked-in state patients: a longitudinal study. *Cognitive Neurodynamics* 121(2): 1816.
- Sharbrough, F., G.-E. Chatrian, R. P. Lesser, H. Lüders, M. Nuwer, and T. W. Picton. 1991. American Electroencephalographic Society Guidelines for Standard Electrode Position Nomenclature. *Journal of Clinical Neurophysiology* 8(2): 200–202.
- Sitt, J. D., J.-R. King, I. El Karoui, B. Rohaut, F. Faugeras, A. Gramfort, L. Cohen, M. Sigman, S. Dehaene, and L. Naccache. 2014. Large scale screening of neural signatures of consciousness in patients in a vegetative or minimally conscious state. *Brain : a journal of neurology* 137(Pt 8): 2258–2270.
- Soekadar, S. R., J. Born, N. Birbaumer, M. Bensch, S. Halder, A. R. Murguialday, A. Gharabaghi, F. Nijboer, B. Schölkopf, and S. Martens. 2013. Fragmentation of Slow Wave Sleep after Onset of Complete Locked-In State. *Journal of clinical sleep medicine : JCSM : official publication of the American Academy of Sleep Medicine* 9(9): 951–953.
- Spüler, M. 2019. Questioning the evidence for BCI-based communication in the complete locked-in state. *PLoS biology* 17(4): e2004750.
- Stender, J., O. Gosseries, M.-A. Bruno, V. Charland-Verville, A. Vanhauzenhuysse, A. Demertzi, C. Chatelle, M. Thonnard, A. Thibaut, L. Heine, A. Soddu, M. Boly, C. Schnakers, A. Gjedde, and S. Laureys. 2014. Diagnostic precision of PET imaging and functional MRI in disorders of consciousness: a clinical validation study. *The Lancet* 384(9942): 514–522.
- Teasdale, G. and B. Jennett. 1974. Assessment of Coma and impaired Consciousness: A Practical Scale. *The Lancet* 304(7872): 81–84.
- Teplan, M. 2002. Fundamentals of EEG measurement. *Measurement science review* 2: 1–11.
- The Multi-Society Task Force on PVS. 1994. Medical Aspects of the Persistent Vegetative State. *The New England journal of medicine* 330(21): 1499–1508.
- The PLOS Biology Editors. 2019. Retraction: Brain-Computer Interface-Based Communication in the Completely Locked-In State. *PLoS biology* 17(12): e3000607.
- Tonin, A., A. Jaramillo-Gonzalez, A. Rana, M. Khalili-Ardali, N. Birbaumer, and U. Chaudhary. 2020. Auditory Electrooculogram-based Communication System for ALS Patients in Transition from Locked-in to Complete Locked-in State. *Scientific reports* 10(1): 8452.
- van Gerven, M., J. Farquhar, R. Schaefer, R. Vlek, J. Geuze, A. Nijholt, N. Ramsey, P. Haselager, L. Vuurpijl, S. Gielen, and P. Desain. 2009. The brain-computer interface cycle. *Journal of neural engineering* 6(4): 41001.
- Vanhauzenhuysse, A., V. Charland-Verville, A. Thibaut, C. Chatelle, J.-F. L. Tshibanda, A. Maudoux, M.-E. Faymonville, S. Laureys, and O. Gosseries. 2018. Conscious While Being Considered in an Unresponsive Wakefulness Syndrome for 20 Years. *Frontiers in neurology* 9: 671.
- Vidaurre, C. and B. Blankertz. 2010. Towards a cure for BCI illiteracy. *Brain topography* 23(2): 194–198.

- Wang, X., Y. Chen, S. L. Bressler, and M. Ding. 2007. Granger Causality between multiple interdependent neurobiological time series: blockwise versus pairwise methods. *International Journal of Neural Systems* 17: 71–78.
- Ware, V. S. and H. N. Bharathi. 2013. Study of Density based Algorithms. *International Journal of Computer Applications* 69(26): 1–4.
- Wei, Q., Y. Li, S.-Z. Fan, Q. Liu, M. F. Abbod, C.-W. Lu, T.-Y. Lin, K.-K. Jen, S.-J. Wu, and J.-S. Shieh. 2014. A critical care monitoring system for depth of anaesthesia analysis based on entropy analysis and physiological information database. *Australasian physical & engineering sciences in medicine* 37(3): 591–605.
- Weiskopf, N., K. Mathiak, S. W. Bock, F. Scharnowski, R. Veit, W. Grodd, R. Goebel, and N. Birbaumer. 2004. Principles of a brain-computer interface (BCI) based on real-time functional magnetic resonance imaging (fMRI). *IEEE transactions on bio-medical engineering* 51(6): 966–970.
- Wielek, T., J. Lechinger, M. Wislowska, C. Blume, P. Ott, S. Wegenkittl, R. Del Giudice, D. P. J. Heib, H. A. Mayer, S. Laureys, G. Pichler, and M. Schabus. 2018. Sleep in patients with disorders of consciousness characterized by means of machine learning. *PLoS one* 13(1): e0190458.
- Wislowska, M., R. Del Giudice, J. Lechinger, T. Wielek, D. P. J. Heib, A. Pitiot, G. Pichler, G. Michitsch, J. Donis, and M. Schabus. 2017. Night and day variations of sleep in patients with disorders of consciousness. *Scientific reports* 7(1): 266.
- Working Party of the Royal College of Physicians. 2003. The vegetative state: guidance on diagnosis and management. *Clinical medicine (London, England)* 3(3): 249–254.
- Wu, S.-J. and M. Bogdan. 2020. Application of Sample Entropy to Analyze Consciousness in CLIS Patients. *Springer* 176: 521–531.
- Wu, S.-J., N.-T. Chen, and K.-K. Jen. 2014. Application of Improving Sample Entropy to Measure the Depth of Anesthesia. In *Proceedings of the International Conference on Advanced Manufacturing (ICAM)*.
- Wu, S.-J., N.-T. Chen, K.-K. Jen, and S.-Z. Fan. 2015. Analysis of the Level of Consciousness with Sample Entropy: a comparative study with Bispectral Index study with Bispectral Index. *European Journal of Anaesthesiology* 32: 11.
- Wu, S.-J., N. Nicolaou, and M. Bogdan. 2020. Consciousness Detection in a Complete Locked-in Syndrome Patient through Multiscale Approach Analysis. *Entropy (Basel, Switzerland)* 22(12).
- Yeragani, V. K., R. Pohl, M. Mallavarapu, and R. Balon. 2003. Approximate entropy of symptoms of mood: An effective technique to quantify regularity of mood. *Bipolar Disord* 5: 279–286.
- Zeman, A. 2003. What is consciousness and what does it mean for the persistent vegetative state? *Advances in Clinical Neuroscience and Rehabilitation* 3(3): 12–14.
- Zeman, A. and J. A. Coebergh. 2013. The nature of consciousness. *Handbook of clinical neurology* 118: 373–407.

# Bibliographic Details

Wu, Shang-Ju

Analysis of the consciousness with complete locked-in syndrome patients

Universität Leipzig, Fakultät für Mathematik und Informatik, Dissertation, 2021.

# Selbständigkeitserklärung

Hiermit erkläre ich, die vorliegende Dissertation selbständig und ohne unzulässige fremde Hilfe angefertigt zu haben. Ich habe keine anderen als die angeführten Quellen und Hilfsmittel benutzt und sämtliche Textstellen, die wörtlich oder sinngemäß aus veröffentlichten oder unveröffentlichten Schriften entnommen wurden, und alle Angaben, die auf mündlichen Auskünften beruhen, als solche kenntlich gemacht. Ebenfalls sind alle von anderen Personen bereitgestellten Materialien oder erbrachten Dienstleistungen als solche gekennzeichnet.

Leipzig, den 03.12.2021

Shang-Ju Wu